THE NORMAL CANINE HEART : ANATOMICAL CRITERIA FOR THE STUDY OF REAL -TIME ULTRASONOGRAPHY AND DOPPLER ECHOCARDIOGRAPHY.

A thesis submitted to the faculty of Veterinary Medicine,
University of Glasgow.

For the Degree of Master of Science (Vet. Sci.)
by
Calum Paterson.

Department of Veterinary Anatomy,
University of Glasgow,
October, 1990.

ProQuest LLC.
789 East Eisenhower Parkway
P.O. Box 1346
Ann Arbor, MI 48106 – 1346

CONTENTS

ACKNOWLEDGMENTS.

I wish to express my sincere gratitude to my supervisor Professor J.S.Boyd for his continual guidance and constructive criticism throughout the period of this study.

I am also most grateful for the support extended by Professor N.G.Wright, Head of the Department of Veterinary Anatomy, University of Glasgow.

I wish to express my thanks to Mr. J. Ndungu, for his patience, help and advice with the Doppler ultrasound scans.

Help extended by the Welcome Institute and the Department of Veterinary Medicine in the provision of animals is greatly appreciated.

The author also acknowledges the help of Dr. M. Bain and Mr E. Lowson for their help with the Apple Macintosh computers.

I am most grateful to Mr. A. May, for his patience and expertise in the Department of Photography.

I should like to express my love to my wife Jean,and children Julie and Michael for their never ending support and encouragement throughout this study.

Finally, I wish to dedicate this Thesis to the memory of my parents Angus and Margaret Paterson, for their continuous love and guidance which I shall forever warmly remember.

DECLARATION.

I declare, that the work carried out in this thesis, was carried out by me personally.

CALUM PATERSON.

SUMMARY.

The present work has two main objectives, firstly, to establish acriterion that enables the successful, real - time imaging of the canine heart, and secondly, to carry out a Doppler ultrasound study of the bloodflow signatures that occurr across the various heart valves.

The historical development of ultrasound, (Chapter 1) describes the early applications of the technique in relation to shipping as a navigational aid, and also to industry where it is employed to detect flaws in metals. The scientific review in the same chapter, establishes the uptake of ultrasound as a tool for echocardiography in the early 1950's, but only in the M - mode format. It is not until the 1980's that the real - time echocardiography of the dog heart is studied in any detail. To date, the only reports of Doppler echocardiography in the dog are those describing cardiac abnormalities. The normal ultrasonic anatomy of the heart combined with the Doppler bloodflow patterns through the heart valves has not been fully explained.

The practical physics of ultrasound is described in Chapter 2, and provides information on the acoustic physics and principles of the ultrasonic images. The common artifacts encountered in an ultrasonic examination, such as reverberation and absorption, are discussed along with basic information about various types of transducers and ultrasound scanners employed in all aspects of ultrasonic investigations.

In Chapter 3, a detailed description of Doppler ultrasound is explained. This includes the description of the principles of Doppler ultrasound, the Doppler spectrum, and the differing types of bloodflow encountered during a Doppler echocardiographic examination. The various modes of Doppler ultrasound (pulse - wave and continuous wave) are also described to allow a comprehensive understanding of the subject.

The procedures and disciplines, along with the equipment employed in the study are outlined in Chapter 4. The importance of the scanner adjustment via the depth, gain and power controls are identified along with the selection of the proper transducer frequencies required for the different scanning planes.

Images of the dog heart are recorded in four positional planes; the right and left parasternal, subcostal and suprasternal. The positioning of the transducer and the anatomical structures to be found in these imaging planes are identified.

In Chapter 5, the images of the heart recorded are displayed in both colour and black and white prints, with the anatomical structures annotated. The echocardiographs are displayed in all the imaging planes using a combination of real - time and M - mode ultrasound, along with pulsed wave and continuous wave Doppler.

The results of the present work are explained in Chapter 6. They include a detailed description of the anatomical structures that are found during the various scans. The bloodflow velocities of the various heart valves (mitral, tricuspid, aortic and pulmonary) are measured as well as the left ventricular function of the heart.

List of Figures. Page.

LIST OF ABBREVIATIONS.

LVOT : Left ventricular outflow tract.
MV : Mitral valve
AV : Aortic valve
PV : Pulmonary valve
TV : Tricuspid valve
AO : Aorta
RV : Right ventricle
RA : Right atrium
LA : Left atrium
LV : Left ventricle
PM : Papillary muscle
IVS : Interventricular septum
2D : Two - dimensional
PW : Pulsed wave
CW : Continuous wave
PA : Pulmonary artery

CHAPTER 1.

INTRODUCTION AND REVIEW OF LITERATURE.

1: 1. GENERAL INTRODUCTION.

The use of real - time ultrasonography is a relatively new technique in the field of Veterinary Medicine, even so popularity in its use has been increasing over the last decade. Many factors have led to this popularity, none more evident than ultrasounds safe, non - invasive properties with regard to the body tissue. The relative ease of ultrasonographic examination along with instant receiving of results make it a powerful diagnostic tool for the veterinary physician.

The principles of ultrasound application in animals has been well documented (Rantanen and Ewing III, 1981) as has its use in the field of echocardiology. (Thomas, 1984) However, the development of pulse - wave Doppler (PW) ultrasound which allowed the examination of the heart in real - time along with the recording of bloodflow velocities through the heart valves and vessels, opened a new dimension to echocardiography. The employment of this technique was isolated to human echocardiography until 1985 when it was used for the first time to study heart diseases in the domestic animals. (Hagio and Otsuka, 1985)

The configuration of the dog chest by nature is different from that of the human and therefore direct comparison and transfer of techniques was not applicable. The present work was undertaken to set up a criterion which would permit the evaluation of the optimum viewing windows with real - time echocardiography in the normal dog heart. This allowed the study of the internal cardiac anatomy and also the bloodflow velocities across the various heart valves with PW.

The further development of PW to include colour flow mapping capabilities has taken the technique to another level, where bloodflow velocities are displayed as a spectrum of colour. The use of colour flow Doppler was incorporated in this study to show the complete range of techniques now available in the field of echocardiography.

1: 2. HISTORICAL REVIEW AND DEVELOPMENT.

The discovery of piezo - electrical properties of certain crystals in 1880 (Curie and Curie, 1880) was responsible for the development of diagnostic ultrasonography as we know it today. It is this property that permits the conversion of electrical current into ultrasound waves with the subsequent conversion of the mechanical energy of the echoes into electrical current.

Apparatuses to detect submerged objects and potential hazards by fog - bound ships, based on ultrasonic waves were first patented in 1912 (Richardson, 1912a,Richardson, 1912b) and further development of this concept led to the invention of a device as an aid to shipping for sounding the ocean depth.(Langevin, 1924). The arrival of World War II led to the improvement of Langevin's system in the form of SONAR (Sound Navigation and Ranging) in which sound waves were used to detect submarines.(Shirley, Blackwell, Cusick, Farman and Vicary, 1978). The use of ultrasound was adopted in industry to detect flaws in metals. (Sokolov, 1935).

The use of ultrasound as a diagnostic aid was proposed towards the end of the Second World War as the technology progressed (Dussik, 1942), and in 1947 "hyperphonograms" of the head were produced. (Dussik, Dussik and Wyt, 1947). In the same year, ultrasound was reported as a diagnostic aid in obstretics (King, 1973), and later was used to identify gallstones and foreign bodies by the acoustic shadows which they produced. (Ludwig and Struthers, 1949). The first recorded study of the heart using ultrasound techniques was in 1954 (Edler and Hertz, 1954a, Edler, 1955), and the following year it was used to demonstrate the eye.(Henry, Mundt and Hughes, 1956).

The application of ultrasound in animals formed the basis of a technique for the assessment of carcass quality by the measurement of back fat.(Temple, Stonaker, Howery, Posukany and Hazelus, 1956, Hazel and Kline, 1959). This procedure was carried out at the Colorado State University using A - mode ultrasound.

The first compound water bath scanner was described in 1958 (Howry,1958). Imaging was made possible by the total submersion of the subject in a tank of water to achieve acoustic contact and the submerged transducer was moved in a circle around the subject. It's use was therefore limited to experimental situations. (Shirley, Blackwell, Cusik, Farman and Vicary, 1978). Subsequent refinement of the technique in Glasgow led to the production of the first contact scanner (Brown, 1960), this was an important advancement in that a transducer could now be placed directly onto a patient without the use of a water bath. This apparatus was used by the gynaecologists to distinguish between cystic and solid lesions in the female reproductive tract using the full urinary bladder to create an acoustic window. (Donald and Brown, 1961).

The early ultrasonographic units utilised analogue conversion systems (Wells and Ross, 1969). Analysis of small echoes arising within organs to produce an image had originally been proposed in 1950 (Wild, 1950), but it was not until the application of a digital computer system that this was achieved successfully. (Kossof, Fry and Eggleton, 1971. Milan, 1972). This innovation led to the development of grey - scale imaging in the early 1970's (Shirley and others , 1978). The many amplitudes of echoes were represented by the levels of grey - scale, and these signals were stored in a scan converter and then displayed on a television monitor. This gave the present form of two - dimensional ultrasonographic imaging.

Further major improvements followed; the development of sector scanning (Northeved,Holm and Gammalgaard, 1971), and real - time systems (Griffith and Henry, 1973), allowed the operator to observe movements as they occurred. Reports of imaging of the breast (Kossof, 1974) and thyroid gland (Crocker, McLaughlin, Kossof and Jellins, 1974) marked the beginning of the clinical application of grey - scale technology and the successful demonstration of the anatomy and pathology of the liver (Taylor, Carpenter, Hill and McCready, 1976), stimulated interest which led to the widespread adoption of the technique in many fields of medicine and revolutionised non - invasive imaging.

Although the use of ultrasound for imaging the heart rapidly advanced through M - mode and two - dimensional echocardiography, the interest of the medical community did not develop concurrently. The first medical Doppler instrument was built in Japan in 1955 (Nimura, 1983), and following this Doppler instruments were developed in the late 1950's and early 1960's that measured mean or average bloodflow velocity. (Franklin, Schlegel and Rushmer, 1961; Stegall,Rushmer and Baker, 1966; Rushmer, Baker, Johnson and Strandness, 1967). Further development resulted in pulsed Doppler systems for medical use, that were able to examine the direction of flow and localise qualitative disturbances of flow in selected areas of the heart. (McLeod. 1967; Wells, 1969). During the same period, others were in the progress of developing continuous wave Doppler ultrasound for medical examinations, (Light, 1969; Kalmanson, Veyrat, Derai and Chiche, 1972).

By 1980, the main accomplishments of pulse and continuous wave Doppler echocardiography were in the investigation of patterns of bloodflow in the heart and great vessels. (Tajik, and others, 1978). What standard echocardiographic methods were for visualisation of cardiac anatomy, Doppler was for the assessment of bloodflow through the heart. However, Doppler echocardiology could not keep pace with its ultrasound imaging counter parts. Worldwide applications of M - mode and two - dimensional echocardiography soared, whereas Doppler had its support among only a few determined individuals who saw its potential.

Today however, there is a great deal of excitement concerning the clinical application of Doppler ultrasound. Much of this can be attributed to the work of Hatle and Angelsen, who made Doppler readily understandable to physicians and applicable to clinical care of patients. (Hatle and Angelsen, 1985).

The final development of Doppler techniques of the 1980's is that of Color Flow Mapping. (Walton, Underwood and Hunter, 1989). In this technique, simultaneous Doppler shifts are measured across an arc and the resulting velocities are displayed in colour on top of a standard M - mode or two -

dimensional image. This allows bloodflow jets through stenotic or regurgitant valves or across septal defects to be readily identified and their severity defined. The continuing development of Doppler ultrasound ensures it as a powerful, non - invasive tool for the future.

1 : 3. SCIENTIFIC REVIEW.

During the past twenty years, ultrasonography, the technique of imaging soft tissue structures using pulsed, reflected, high frequency sound has become an important diagnostic tool. Its abilities to distinguish between fluid filled and soft tissue (unlike conventional radiography) to define spatial relationships between structures and to detect and quantitate cardiac disorders, have made it a particularly valuable tool in cardiovascular diagnosis (Feigenbaum, H. and others, 1967., Feigenbaum, H. 1981).

The first recorded study of the heart using echocardiographic techniques was carried out using M - mode ultrasound (Edler and Hertz, 1954b). This allowed the motion of the mitral valve and posterior ventricular wall to be observed by the use of an ultrasonic reflectoscope. The clinical application of M - mode echocardiography expanded over the following twenty- five years and the technique was regarded as an essential diagnostic tool in the evaluation of patients with a variety of cardiac disorders (Kotler, and others, 1980). The advantages of M - mode echocardiography included the ability to provide accurate reliable and reproducible information at no risk to the patient and at a relatively low cost. Of all the non - invasive techniques available, M - mode echocardiography is the most useful in obtaining quantitative measurements of heart chamber size and wall thickness.

The possibility of producing two - dimensional pictures of the internal structures of the human heart in situ by the ultrasound pulse - echo method was investigated in the mid 1960's (Ashberg, 1967). This system involved the operation of an ultrasound optical mirror system to produce pictures of a high resolution. These pictures were obtained at a rate of seven frames per second, which was fast enough for the movements of internal structures of the heart but had the disadvantage of the picture being created relatively slowly which sometimes led to the distortion of the image , therefore instantaneous and continuous pictures could not be achieved. The following year led to the development of the sector scanner, (Somer, 1968) which consisted of a twenty - one element array that allowed sound pulses to be transmitted in every

direction within a sector of 90^{o} at a repetition rate of thirty scans per second. Both these developments were used to ascertain the viability of ultrasound scanners in echocardiology, so that by the mid 1970's real - time ultrasound had been made available and the use of ultrasound echocardiography became accelerated.

The validity of structure identification for cross - sectional echocardiography was investigated by visualising catheter echoes and also echoes produced after selective chamber injections of indocyanine green dye (Sahn and others, 1974). This study confirmed the accuracy of real - time cross - sectional echo localisation of cardiac chambers and validated the positions used routinely for the assessment of congenital and acquired cardiac disease in pediatric patients. The development of a sector scanner that produced real - time, two - dimensional echocardiograms, led to further investigation to determine whether visualisation of the great arteries at their origin would provide diagnostically useful information in patients with cyantonic congenital heart disease (Henry and others, 1975). The findings proved favourable and resulted in further investigation throughout the remainder of the decade.

Real - time, wide angle, two - dimensional echocardiography was an exciting development and opened a new era in non - invasive cardiological investigation. Detailed anatomic and functional information provided by this technique had hitherto been unavailable either with standard M - mode echocardiography or with invasive angiographic techniques (Tajik, and others, 1978), and the development of a phased array ultrasound system further enhanced the ability to steer the ultrasound beam through structures under investigation (Kisslo and others, 1976).

The details of three - dimensional cardiac anatomy were complex and structure recognition proved difficult in tomograms produced in two - dimensional ultrasonic sector scanners. Cardiac anatomy is familiar to all physicians and veterinary surgeons due both to memories of gross anatomy classes and ongoing practical analysis of the pathophysiology of cardiac disease. Nevertheless, to optimally obtain and understand the newly available

ultrasonic images of the heart, even cardiologists performing angiographic examinations regularly found it necessary to relearn the details of three - dimensional cardiac anatomy. In trying to recognise cardiac structures in cross - sectional images, standard anatomical textbooks were found to be unsatisfactory or cumbersome for easy understanding (Popp and others, 1979). The ultrasonic imaging planes used to achieve these structures were many and contrasting, so it came about that a Echocardiography Committee on Nomenclature and Standards was set up in the United States of America to establish imaging planes and transducer orientation during the performance of a two -dimensional study (Henry and others, 1980). These imaging planes will be described in greater detail in Chapter 4.

The newer real - time , two - dimensional imaging systems were capable of extraordinarily rapid image formation times, offering the viewer a remarkable appreciation of the heart in motion. Although M - mode techniques were extremely valuable in assessing left ventricular function, its major disadvantage was that it provided a limited "ice - pick", one - dimensional view of the heart (Kotler and others, 1980). The entire left ventricular cavity, apex of the left ventricle and all leaflets of the tricuspid valve, could not be readily evaluated with M - mode techniques. In addition, intracardiac structures were displayed in an unfamiliar format that bears little resemblance to cardiac anatomy. Spatial orientation of intracardiac structures was not readily appreciated with M - mode echocardiography (e.g. motion of the entire left ventricle could not be visualised) and by providing spatial orientation, two - dimensional echocardiography allowed both lateral and axial distances to be appreciated.

The availability of two - dimensional echocardiography in its various formats, (B - mode, sector and phased array) led to an upsurge in cardiac research. However, two - dimensional techniques resulted in new pitfalls in ultrasonic diagnosis related to instrument artifacts as well as performance and interpretation of the examination (Park and others,1981). The spurious appearance of cardiac masses because of these ultrasound artifacts represented a particularly prominent problem that had to be avoided in daily practice (DeMaria and others,1980).

In Veterinary Medicine, ultrasound was still in its developmental stages in the early 1980's although echocardiographic studies of the dog had been carried out prior to this for the measurement of ventricular dimensions (Mashiro and others, 1976) and also normal and abnormal valvular functions (Dennis and others, 1978). Experimental ultrasonic studies in clinically normal dogs , cats, swine and horses were shown to have marked similarities with that of human echocardiograms (Pipers and Hamlin, 1977, Pipers, Muir and Hamlin, 1978, Pipers, Reef and others,1979) and so the use of ultrasonic echocardiography in Veterinary Medicine was studied in more detail. Likewise as in human echocardiography, the principles of ultrasound application in animals had to be studied so as to set up a discipline for ultrasound examination (Rantanen and Ewing III, 1981). The results from clinical investigations proved successful and provided diagnostic information which in many cases had not been possible using other clinical testing methods and also became an exciting new area in the veterinary teaching programme (Miller and Wingfield, 1981).

Work carried out at the Ohio State University Veterinary Teaching Hospital found echocardiography useful in the evaluation of animals with cardiovascular diseases (Pipers, Rings and Hull, 1978, Bonagura, 1981). Several techniques had been used to estimate left ventricular dimensions experimentally in the dog but they were all invasive approaches. Hawthorne used a variable resistance gauge to estimate changes in the left ventricular circumference (Hawthorne, 1961). Subsequently, ultrasound transducers placed epicardially, were used to estimate left ventricular function and transverse diameter (Rushmer and others, 1954; and Stegall and others, 1967). This technique was developed with ultrasound transducers placed endocardially to obtain more accurate measurements of left ventricular function (Horwitz, and others, 1968).

Although surface echocardiography had been accomplished in dogs (Stefan and Bing, 1972), the technique proved difficult due to the configuration of the canine chest. Echocardiograms had also been obtained by holding an echo transducer on the surface of the heart (Kerber and Abboud, 1973.), but this technique could not be used in a long - term experimental model. The design

of a reflected ultrasound transducer that could be sutured on to the heart, allowed tracings of better quality , and made it possible to obtain both short - term , open chest measurements, and long - term measurements in the closed chest, concious animal (Myerowitz, and others, 1974).

A reliable non - invasive method to monitor changes in left ventricular volumes in the dog which would facilitate the study of physiological and pharmacological interventions and also provide a means of following the effects of induced cardiac damage was the next field for investigation. This was achieved by the development of a surface echocardiographic technique that allowed the measurement of the left ventricular dimension in the concious dog (Mashiro, and others, 1976, and Gooding, and others, 1986). Surface transducers applied to the chest were commonly used for echocardiography; however, this was sometimes prevented by the obstructive pulmonary disease, gross obesity or an extremely large or deformed chest (Frazin, and others, 1976). The development of an oesophageal echocardiographic technique to complement the transcutaneous was described, (Dennis, and others, 1978) and proved useful in assessing normal and abnormal valvular function in Beagle dogs.

Cardiovascular disease in dogs has an estimated prevalence of approximately 10% (Detweiler and Patterson, 1965). This substantial incedence provoked numerous investigations leading to advancements in medical and surgical management of cardiovascular disorders. Although previous studies had dealt with the dog, (Dennis and others, 1978, Mashiro, and others, 1976) there had been little clinical material demonstrating the usefulness of echocardiography in particular cardiovascular disorders. A study was therefore carried out by means of M - mode echocardiography, to detect echocardiographic features of pericardial effusion in dogs (Bonagura and Pipers, 1981). This condition, pericardial effusion, caused the separation of the ventricular epicardial and parietal pericardial surfaces and was displayed as a anechoic (black) line between the surfaces. The findings were similar to these reported for pericardial effusion in man, and suggested that echocardiography could be valuable for evaluating dogs with naturally occurring pericardial disease.

The recognition of M - mode echocardiography as an non - invasive diagnostic aid became more prevelant over the following years as many researchers recorded their findings in numerous reports. Its use in diagnosing valvular defects in dogs (Pipers, and others, 1981, Wingfield, and others, 1982, Wingfield, and others, 1983, and Jacobs, and others, 1983) and comparative domestic animals, (Bonagura and Pipers, 1983a) was widely accepted. The technique also proved successful in diagnosing cardiac lesions (Bonagura and Pipers, 1983b), severe congestive heart failure in the dog, (Kittleson, and others, 1984, Wingfield and Boon, 1987) and congestive cardiomyopathy, (Calvert and Brown, 1986.) a condition primarily affecting the myocardium.

Up until the early 1980's, the cardiac applications of ultrasonography in Veterinary Medicine had been confined to unidimensional M - mode techniques, although experimental two - dimensional, real - time echocardiography (2DE) had been reported (Franklin, and others, 1977, Gueret, and others. 1980). Neither documentation of technique, normal echocardiographic appearance,nor clinical reports of its applications in dogs , had been investigated. Research carried out at the University of California, U.S.A. on dogs (Thomas, 1984) and at the Veterinary Hospital of Hokkaido University in Japan on domestic animals (Yamaga and Too, 1984), found indications that 2DE was extremely valuable in cardiac examination and its uses could eventually be as broad as those in human patients.

For 2DE to become clinically useful, normal values for heart chamber and also wall dimensions as well as normal indices for myocardial function in the normal dog, were needed. With 2DE, an infinite number of tomographic planes were employed to interrogate the heart, and a standardisation of these planes in each of the domestic animals was required to facilitate collaboration and comparison amongst establishments. A study was conducted with clinically normal concious dogs to define tomographic planes for cross - sectional echocardiographic examination of the normal canine heart (O'Grady, and others, 1986), and to compare these with previously described imaging planes (Salcedo, and others, 1979, Wyatt, and others, 1979, Gueret, and others,1980,

and Haendchen, and others, 1982) to establish normal chamber and wall dimensions.

Satisfactory quantitative echocardiograms were obtained by using consistent sites of transducer placements and by identifying internal structures. O'Grady and his colleagues (1986) concluded from their findings that cross - sectional echocardiography allowed repeatable assessment of cardiac anatomy and that it would prove useful for identification and quantification of heart disease in the dog.

Neither standard nor cross - sectional echocardiography however dealt with blood flow. Conventional M - mode echocardiography could not visualise blood flow directly and could only detect abnormalities of flow when they were of sufficient magnitude to produce obvious alterations in cardiac structure and function, as in the case of aortic insufficiency (Baker, and others, 1977). The arrival of Doppler ultrasound was to be a revolutionary tool in the field of echocardiography.

As described in the Historical Review, Doppler instruments that measured mean or average blood flow were developed in the mid 1960's. (Stegall, Rushmer and Baker, 1966.). These studies used continuous wave systems for use in peripheral vascular investigations. However, continuous wave Doppler devices were not readily applicable to cardiac diagnosis because by their nature, they detected motion or blood flow occurring at any and all points along the path of the soundbeam.

The study of various cardiac disorders , (e.g. aortic stenosis and insufficiency, mitral and tricuspid regurgitation.) was achieved by the development of a Pulsed Doppler System (Baker, and others, 1977). This was in effect a combination of the continuous wave Doppler and a conventional pulsed echo system, which enabled bursts of ultrasound at very high frequencies, to be transmitted into the heart and allowed the measurement of velocity and direction of blood flow. This technique was advanced with Doppler systems being combined with two - dimensional echocardiography, which allowed a

visual two - dimensional picture of the vessels being scanned enabling greater accuracy of the Doppler beam placement (Miyatake, and others, 1980, Miyatake, and others,1982).

So far however, the real - time measurement of blood flow had been possible only at a single point in the cardiac chamber. To assess the whole aspect of the intra- cardiac blood flow, Doppler investigation had to be performed point by point in the cardiac chamber. Such a system was developed that imaged with a wide - angled, phased array transducer that simultaneously gave 2DE and Doppler images. Each cross - section of the heart was composed of 32 beam directions, and in each of these beams 8 ultrasound pulses were transmitted (Bommer and Miller, 1982.). Research using this format allowed the clear demonstration of mitral inflow and aortic ejection, and also a regurgitant jet from the valve orifices was dynamically visualised allowing the concurrence that the new technique greatly improved the diagnostic efficiency of ultrasound (Miyatake, and others,1984.).

The development of Doppler Color Flow Mapping was the next advancement in echocardiography. Here the Doppler signal was written into a digital scan converter, and supplied to a color converter. The color converter assigned colors based on direction and variance of detected frequency shifts. Flow towards the transducer was coded as red, whereas blue designated flow away from the transducer. The degree of variance (or turbulence) was also calculated and coded as the amount of green mixed with red or blue. The velocity was recorded also and was proportional to the brightness of each color and displayed in seven gradations. The color coding therefore facilitated demonstration of three aspects of intra - cardiac flow ; direction, velocity and turbulence.

Two - dimensional Doppler ultrasound now offered for the first time, non - invasive, real - time, two -dimensional imaging of simultaneous intra - cardiac morphology and flow. It provided haemodynamic information regarding the severity of regurgitation and to some extent, stenotic lesions by the real - time display of the regurgitant or stenotic jet, as well as shunt size in patients with

intra - cardiac communications (Switzer and Navin, 1985.). The advancement of Doppler technology led to further studies into the pulsed Doppler regurgitant flow patterns of normal valves. (Kostucki, and others,1986).

Little information had been made available in the clinical use of Doppler echocardiography in Veterinary medicine although these modalities were employed on preliminary studies (Hagio and Otsuka, 1985, Pipers, Reef and Wilson, 1985). Pulsed Doppler echocardiography in normal dogs and calves was carried out along with three cases of valvular regurgitation in the dog (Hagio and Otsuka, 1987.) and from these studies it was found that pulsed Doppler echocardiography was a very useful technique for the detection and estimation of the severity of valvular regurgitation in domestic animals.

In Veterinary cardiology however, research in this field has just begun and further study on the usefulness and limitations of this modality is required.

CHAPTER 2.

PRINCIPLES AND INTRODUCTION OF ULTRASONIC IMAGING.

2:1. PRACTICAL PHYSICS OF ULTRASOUND.

There is no field of medical imaging that is more dependant upon the skill of the machine operator than ultrasound scanning.
An operator's first encounter with a scanner is that of great enthusiasm closely followed by confusion and general bewilderment, as they gaze at the images swirling and pulsating on the screen before them. It is therefore essential that a basic understanding of the physics of ultrasound is established. This does not mean however that a knowledge of ultrasound computer electronics is required but the principles of sound propagation and interaction with body tissues should be known. A knowledge of the cross sectional anatomy of the organ being examined is also recommended before any proper study can be undertaken.

As stated in the previous chapter, diagnostic ultrasound originates from crystals that have *"piezoelectric "* properties. The term *"piezo"* is derived from the Greek word meaning *"pressure "*, hence the the term pressure electric. When piezo electric crystals are deformed by pressure, electricity is produced and conversely, when an electrical current is applied to them, the crystals expand and contract producing sound waves.

This is the process by which ultrasound is generated and received by the transducer. The expansion and contraction of the crystals can be compared to that of a drumskin being struck, where the expansion of the skin causes compression of the neighbouring air molecules and the following contraction causes refraction of the same molecules. (fig. 2:1) The sound waves of the drum will continue to travel getting progressively weaker. However, if a barrier such as a wall is reached before the sound waves are too weak, they are reflected back at the same frequency and speed (in this case, the speed of sound, 741 m.p.h.) back to the ear producing the vibration of the eardrum. This vibration is in turn interpreted by the auditory system of the inner ear. (fig. 2:2)
Ultrasound imaging uses this same pulse - echo principle. A short pulse of ultrasound is emitted into the body where it travels through the tissues at a

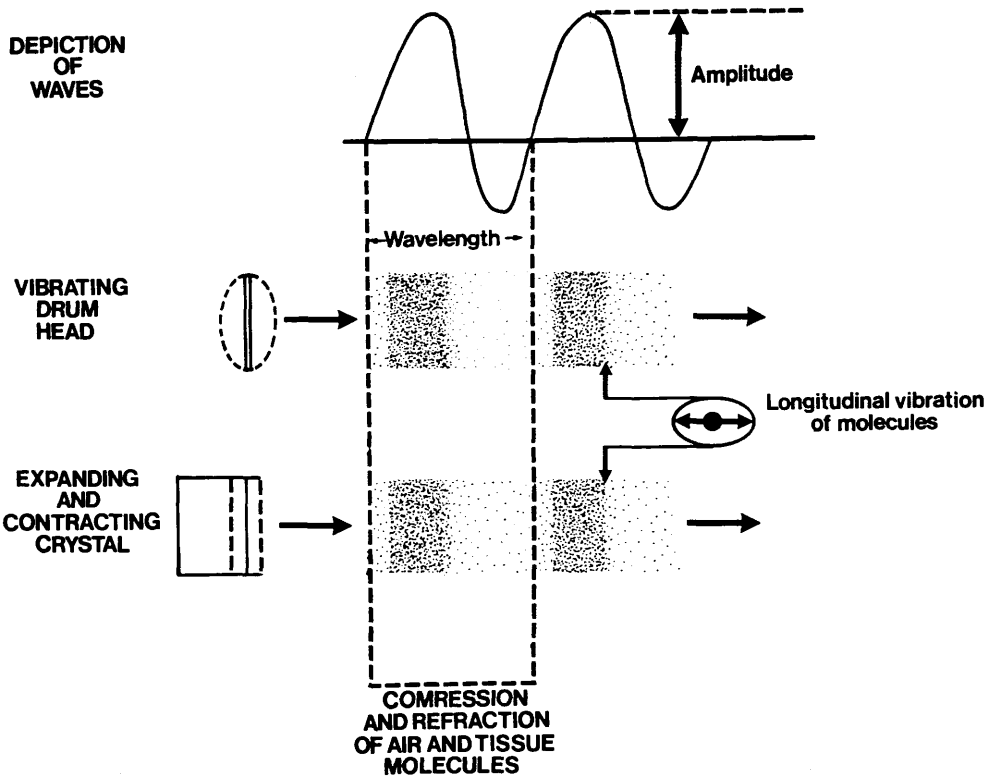

fig. 2 : 1. Comparative propagation or travelling of audible sound waves and ultrasound waves.

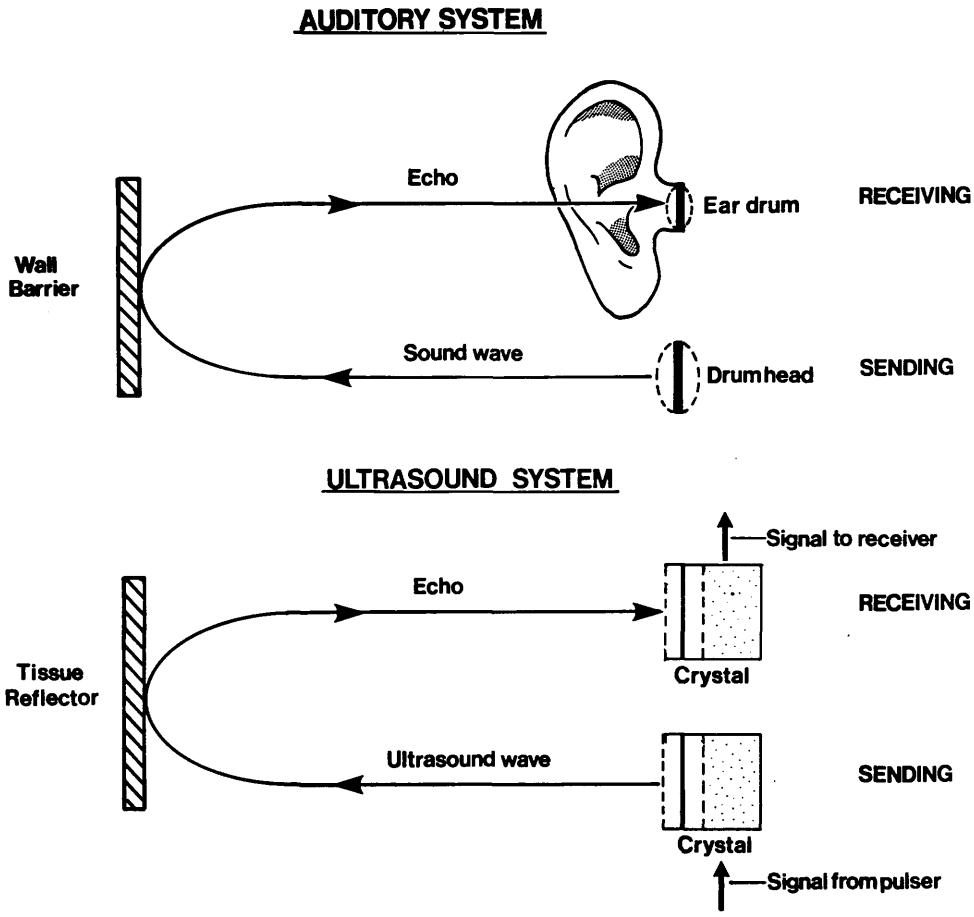

fig. 2 : 2. Comparison of the reception of echoes from audible sound and diagnostic ultrasound.

constant speed, until it encounters a reflecting surface. This causes some of the sound beam to be reflected back towards the source (i.e. the transducer); the force of the returning sound waves compresses and expands the crystal which produces a voltage that is then transmitted to a receiver. (i.e. the scanner). The delay between the formation of the wave and the reception of the echo, allows the calculation of the distance from the crystal to the reflector. This chain of events can be summarised by the following equation ;

$$d = \frac{Vt}{2}$$

where d = distance,
V = velocity,
t = time.

In the case of the drum, the distance travelled by the sound wave can be calculate with a stopwatch to measure the time it takes for the returning echo to reach the ear. However, with the ultrasound scanner, instead of recording the distance as a number it records this figure as a pixel or spike on a television screen or oscilloscope. This spike is proportional to the distance the echo has travelled which enables not only the measurement of distance but a visual picture of it as well.

Although the principle of ultrasonic pulse echo diagnosis is the same as the drum beat echo, there are several practical differences. To understand these differences, we need to know a little about sound.

All sound, be it ultrasound or audible sound is actually a series of repeating pressure waves. It is convenient to think about these waves and illustrate them as sine wave forms. (fig. 2 : 3). Line A shows a single wave or cycle, and as we move along the horizontal axis, which represents time, the pressure starts at zero then rises to a peak before falling back to zero, and continues to a negative before returning to zero. Line B. shows a continuous wave from where a large number of the single waves have been strung together.

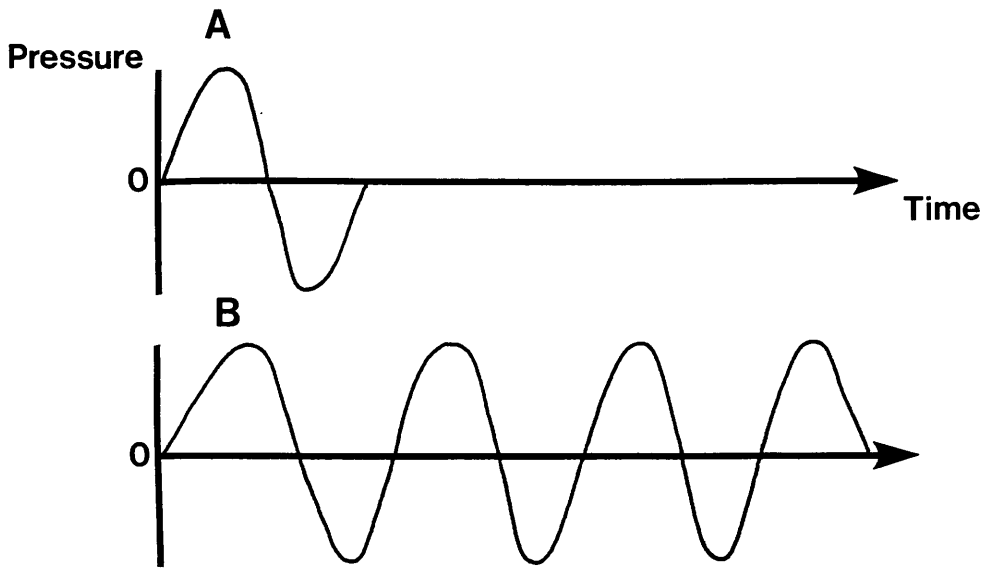

fig. 2 : 3. Diagrammatic representation of sound as a sine wave.

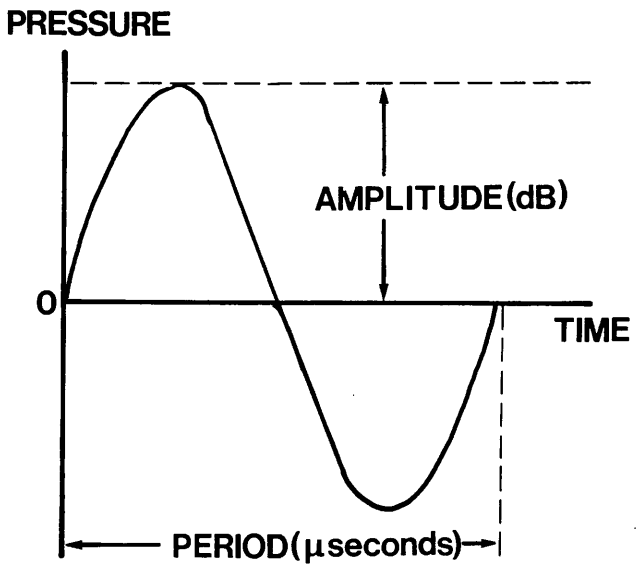

fig. 2 : 4. Common parameters of a sound beam.

The single wave can be compared to an extremely short beep of a car horn, while the continuous wave represents the horn being stuck in the "on" position. This simple waveform is not adequate to fully describe the sound and therefore more information about the wave must be known before it can be predicted how it will behave. This data or parameters of the wave are illustrated. (fig. 2 : 4) The period is the time it takes to complete a single cycle of the wave.

The **amplitude** is the peak pressure or height of the wave and is also a measure of the strength or loudness of the soundwave. A shouted "hello" has a large amplitude while a whispered "hello" has a small amplitude.

The **velocity** is the speed of the wave and this depends on the type of material in which the wave is travelling. For instance, in air, sound travels at 741 miles per hour which is equivalent to 331 meters per second, whereas in the soft tissues of the body, sound travels at 1540 meters per second compared to that of 4080 meters per second for bone and 600 meters per second in lung tissue (due to the air in the tissue.)

The **frequency** is the number of times the wave is repeated per second and this is calculated by dividing the period (the time it takes to complete a single cycle) into 1.

Finally there is **wavelength,** this is the distance the wave travels during a single cycle. The wavelength is calculated by dividing the velocity by the frequency. It can now be seen how ultrasound differs from audible sound. First, and most important is frequency. Audible sound ranges in frequency from 16 to 20,000 cycles per second. A cycle per second is known as a **Hertz** ; a million cycles per / second is called a **MegaHertz** and is abbreviated to **MHz.**
Ultrasound is defined as any sound with a frequency of greater than 20,000 Hertz. In echocardiology, sound frequencies ranging from 1 - 5 MHz are used. The next consideration is velocity; although velocity is independent of frequency and is determined by the medium in which the sound is travelling, there are practical differences. As previously described there is a difference

between audible sound and ultrasound. The wavelengths of audible sound range from 2 - 200 centimetres, while the wavelengths used in B - mode ultrasound range from 0.3 - 1.5 millimetres. The amplitude or power of the ultrasound used for diagnosis is much smaller than that needed to shout "hello", therefore since amplitudes vary so widely and for most purposes we are not concerned with the actual amplitude as with the relationship of one amplitude to another, a different type of measurement of amplitude is used for sound. This measurement is the **decibel** (dB) notation which is based on comparing the amplitudes of two different soundwaves. For example, in describing the virtues of a goalkeeper, it could be said that goalkeeper A can throw a ball twice as far as goalkeeper B or that a lorry weighs ten times as much as a mini. In neither case is it stated the actual number of feet the football is thrown or the number of hundredweight the lorry weighs, but if some concept of how much a mini weighs is understood, then other vehicles can be compared to a mini and at the same time some idea of their actual weight can be surmised. In this way a comparative measurement system can be used as if the figures correspond to some real quantity. Even though it is not really correct to use decibels as if they were some real and absolute measurement of sound, amplitude or power, it is useful and convenient to do so and does not introduce any errors into our understanding. So, the amplitude of ultrasound echoes is often referred to as X number of decibels, the greater the amplitude the greater the echo.

Before the topic of decibels is left, it should be pointed out that this is a logarithmic system ; where a decibel is defined as ;

$$dB = 20 \log \frac{E_2}{E_1}$$

where E2 and E1 are the actual measurements of the amplitudes of two different echoes. Logarithmic scales are used whenever the quantities involved cover very large ranges and this enables widely different numbers to be compared.

2 : 2. INTERACTION OF ULTRASOUND AND BODY TISSUES.

Sound travelling through the air such as the soundwave from a drumskin, has a pretty uncomplicated life. It simply passes through the air until it reaches a reflector (e.g. a wall) and comes rebounding back. The only really noticeable change is that the sound gets weaker as it travels, so the echo is not nearly as loud as the initial drumbeat. When an ultrasonic pulse is sent into the soft tissues of the body however, it undergoes continuous modification.

The most significant change is **Attenuation**. This is described as the progressive weakening of the sound beam as it travels through the tissue. Thus the further through the tissue the sound travels, the weaker it gets. The attenuation of ultrasound is dependent on many factors including wavelength of the sound, the type and density of the tissue and the number and type of echo interfaces in the tissue.

Attenuation measurements have been made for many different human tissues with many different frequencies of ultrasound, and the general rule of thumb is that the average attenuation of an ultrasound beam in human soft tissue is 1dB per centimetre per MHz. This means that an ultrasound beam with a frequency of 1MHz looses 1dB of amplitude for every centimetre it travels. It must be remembered that each echo received has actually travelled twice as far as the distance to the reflecting surface, since it has made a trip to the reflecting surface and back to the source. Therefore, the attenuation is multiplied by 2 to calculate how much an echo from any given depth has been attenuated.
Attenuation of the ultrasound beam occurs primarily through three processes ; **Absorption, Reflection** and **Scattering.** (fig. 2 : 5).

Absorption occurs when energy in the sound beam is captured (or absorbed) by the tissue. It is this process which is the basis for ultrasound diathermy, a common therapeutic use of ultrasound. However, at the low energy levels used in diagnostic ultrasound, the biological effect of absorption is negligeable.

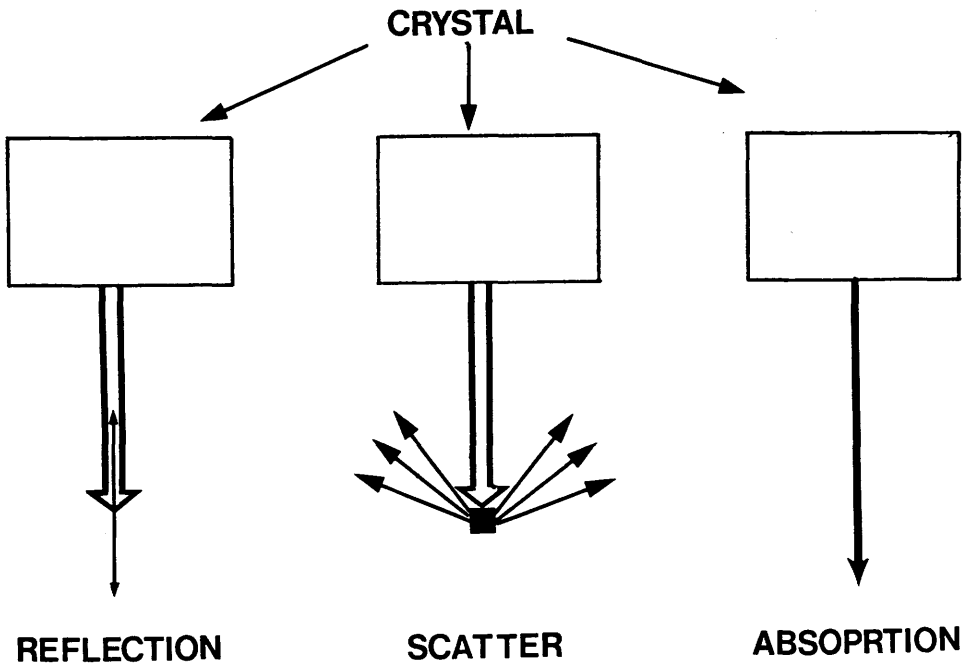

fig. 2 : 5. Conditions of ultrasound beam Attenuation.

Reflection is the redirection of a portion of the ultrasound beam back towards its source; this gives rise to echoes and forms the basis of diagnostic ultrasound scanning. Whenever the sound beam passes from a tissue of one acoustic impedance to a tissue of a different acoustic impedance, a small portion of the beam will be reflected back to the source, while the remainder will continue on.

Scattering occurs when the beam encounters an interface which is irregular and smaller than the soundbeam. As the term suggests, the portion of the beam which interacts with this is "scattered " in all directions. The portion of the beam which is scattered directly backwards will return to the transducer and produce an echo known as non - specular reflection.

REFLECTION AND ECHO PRODUCTION.

Since the process of ultrasonic reflection and echo production is the basis of B - mode scanning, it must be looked at with a little more detail. As previously described, reflection occurs, that is an echo is produced, whenever the ultrasound beam passes from a tissue of one acoustic impedance to a tissue of different acoustic impedance. This is also known as crossing an acoustic interface. An interface occurs whenever two tissues of differing acoustic impedance are in contact with each other. The acoustic impedance of a tissue is the product of the density of the tissue and the speed of sound in the tissue. This can be shown in the following equation ; $Z = p \times c$.

where ; Z = the acoustic impedance
p = the density of tissue
c = the speed of sound in the tissue.

The speed of sound in soft tissue is assumed to be a constant 1540 metres per second, so that the only thing which effects the acoustic impedance is the density of the tissue. It can therefore be assumed that the acoustic impedance is the same as the density of the tissue, so an interface occurs every time

tissues of different density are in contact with each other. When the sound beam crosses an interface, only a small percentage of it is reflected, the remainder continues through the tissues where it can be reflected by other interfaces. The amount of sound reflected at an interface determines how much amplitude the returning echo will have. The amount depends on how great the difference is between the two acoustic impedances which make up the interface. The smaller the difference, the smaller the percentage of the sound reflected; conversely, the larger the difference the larger the portion will be reflected. It would therefore seem logical that large echoes would be desirable, but this is not the case. Ideally only enough of the beam should be reflected to enable the echo to be detected by the scanner, the rest of the beam being available to travel to create further echoes. If too large a portion of the beam is reflected at an interface, there is too little of the sound left to produce echoes from other interfaces deeper in the tissue. This is why ultrasound scanners cannot "see " through gas or bone. The difference in acoustic impedance between soft tissue and gas or bone is very large, so that most of the beam is reflected and none is left to continue deeper. (e.g. soft tissue - bone interface 70% beam reflection, soft tissue - gas interface 90% beam reflection.)

It can be seen from this information that bone and gas are the ultrasonographers " stone wall "; nothing gets through them. No matter how powerful the ultrasound beam, the same percentage will be reflected. This can be compared to shinning a torch at a mirror, no matter how bright the light is you cannot see through the mirror and all you get is glare.

There is another term called Refraction, which is sometimes confused with reflection. Refraction describes what happens to the beam that is not reflected but continues on through the interface. The direction of the beam is changed very slightly and this slight change is referred to as refraction.

SPECULAR AND NON -SPECULAR REFLECTIONS.

Interfaces give rise to two types of reflections, specular and non - specular. (fig. 2 : 6). Specular reflections occur when the interface is larger than the sound beam. These reflections have the property that the angle of the reflection is equal to the angle of incidence. This can be compared to a billiard ball on a snooker table, if the ball is struck against one of the cushions, it will bounce off at the same angle at which it was shot. Likewise, if the ball is shot head on to the cushion, it will come directly back. It is therefore obvious that unless the ultrasound beam strikes a specular reflector head on , the echo will not come back to the transducer but will go angling off into the tissue. Specular echoes are very common in abdominal scanning. The capsule of the kidney and liver, gall bladder,aorta and major blood vessels are all examples of specular reflectors.

Non - specular reflections occur when the interface is smaller than the sound beam. The sound beam from a modern, well focused transducer is approximately 10 millimetres in diameter. therefore interfaces smaller than 10 millimetres will give rise to non - specular reflections. Many small parenchymal tissue echoes fall into this category, such as those arising between cells and small vessels. In contrast to specular echoes, the amplitude of a non - specular echo is independent of the beam angle. The small non - specular interface is always surrounded by the beam and hence there is no such thing as an incident angle as far as the interface is concerned.

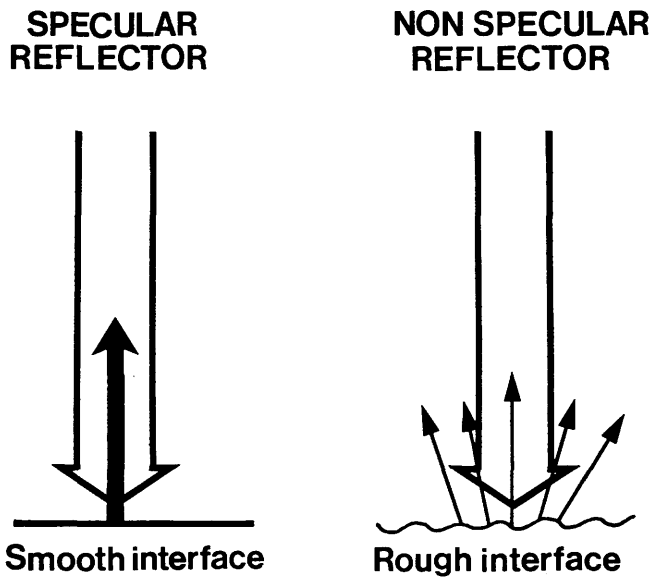

fig. 2 : 6. Specular and Non - Specular Reflections.

2 : 3. RESOLUTION.

Resolution is the ability to separate two closely spaced interfaces. (fig. 2 : 7). Resolution is usually expressed as a distance and as an example we shall take this distance to be 3 millimetres. If the ultrasound system has a resolution of 3 millimetres, it follows that two small interfaces spaced only 3 millimetres apart will appear as two separate echoes in the image. However, if the two interfaces are closer together than this they will appear as a single echo.

Ultrasonic resolution has two components ; Axial and Lateral resolution.
Axial resolution refers to the resolution along the path of the sound beam. This form of resolution is dependant upon many factors, namely the type and quality of the electronics in the scanner and the transducer design and construction but the ultimate limitation is the is the physical constraints of the beam itself.

The beam is actually a series of ultrasonic pulses with each pulse having a small but definite length. A typical gray - scale scanners pulse lasts about 1 micro - second (μ second). The length of the pulse can be calculated by multiplying 1 μ second by the speed of sound (1540 meters per second) to give us a pulse length of 1.54 millimetres. Physical principles state that the resolution can be no better than half the pulse length so the axial resolution of a system with a 1 μ second pulse can be no better than 1.54/2 = 0.77 millimetres. The same principles state that the axial resolution can be no more than one wavelength. The wavelengths of commonly used transducers are ;

2.25 MHz = 0.96 millimetres.
3.5 MHz = 0.68 millimetres.
5.0 MHz = 0.31 millimetres.

As frequency increases so also does resolution, however it is important to notice that the overall resolution is limited not only by the frequency but by the pulse length. The point to remember is that the frequency is only one of the many factors affecting resolution and simply using a higher frequency

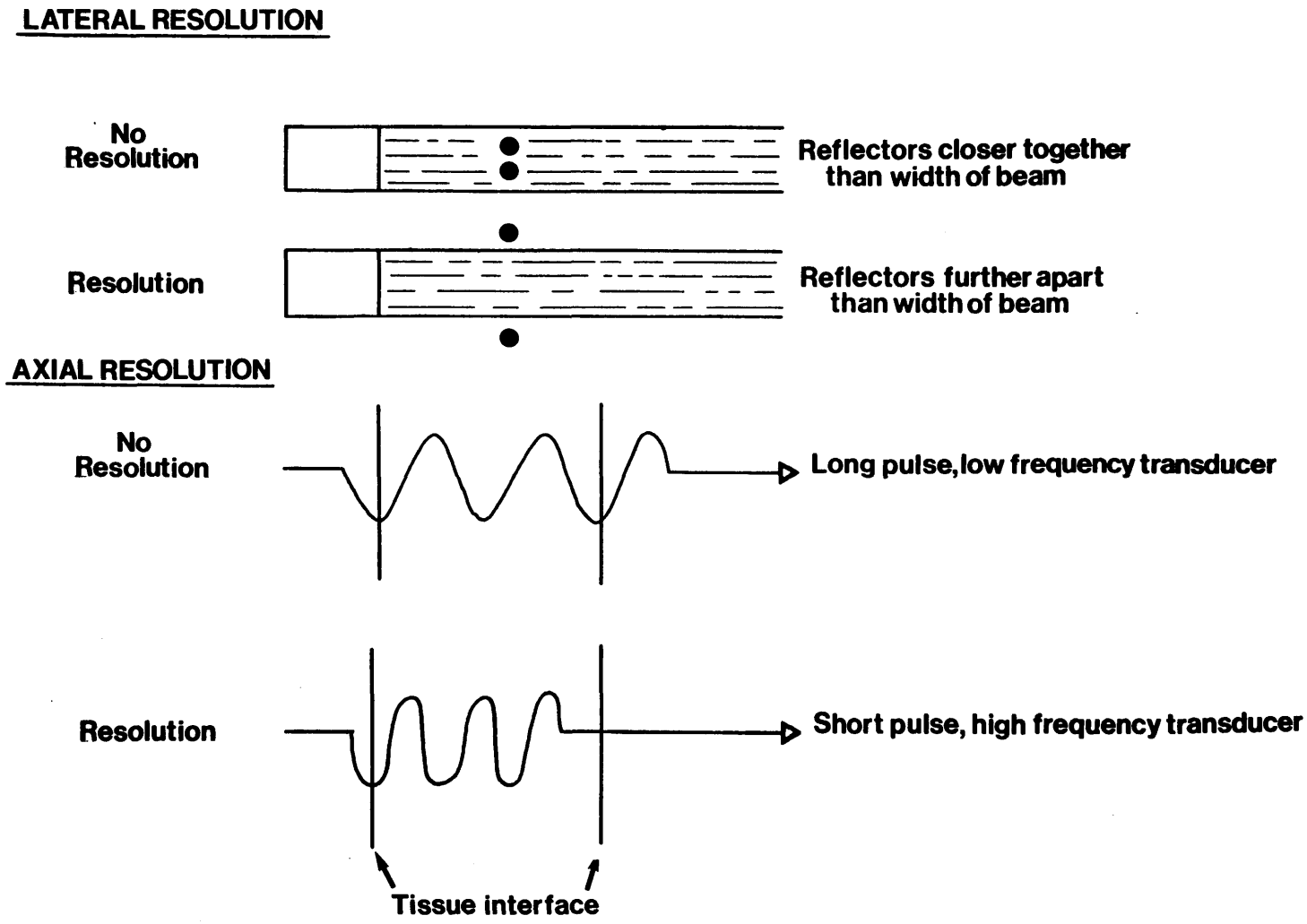

fig. 2 : 7. Axial and Lateral Resolution

transducer does not guarantee that resolution will be improved. Lateral resolution refers to the resolution perpendicular to the axis of the sound beam. Lateral resolution is dependant upon the size or diameter of the ultrasound beam; the smaller the beam, the better the resolution. If two interfaces are closer together than the beam width, then they will both give rise to an echo at the same time and only a single echo will be received by the transducer.

2 : 4. TRANSDUCERS.

The transducer can be best described as the work - horse in ultrasound imaging. When connected to an ultrasound scanner it produces the ultrasound waves and receives the reflections from the interfaces which are then converted into images on the scanner screen. The transducer, if operated normally acts more as a receiver than that of a transmitter (99% receiver, 1% transmitter).

The transducer is composed of several single, basic transducers - the piezo -electric crystal. These crystals act as the transmitter and receiver of the ultrasound waves. The crystals are composed of piezo - electric materials such as quartz, lead zirconate and barium titanate which convert the electric signals into ultrasound waves and vice versa. The piezo - electric material in the transducer is coated with an electrical conductor on two parallel surfaces. If a voltage is applied to the conductor, the piezo - electric crystal will change in thickness by an amount dependant on that of the voltage. Likewise, if the crystal is subjected to a mechanical stress (e.g. from an ultrasound pulse) such that it is deformed. a voltage will appear between the conductors, which is dependant on the strain subjected upon the crystal. An alternating voltage will produce an alternating change of thickness and vice versa. A transducer frequency is therefore determined by the number of times a crystal expands and contracts per second.

Transducers can be classified into two groups ; **focussed or unfocussed**.
The ultrasound beam produced by an unfocussed transducer has two regions; (fig. 2 : 8) the near field (Fresnel Zone) is the section closest to the transducer and is about the same diameter as the transducer. The region beyond the near field is called the far field (Fraunhofer Zone) and it is here that the ultrasound beam becomes divergent. The location of the transition between the near field and the far field depends on the diameter of the transducer in relation to that of the frequency (wave - length). The wide field produced by an unfocussed transducer limits the ability to define small structures, this is referred to as Lateral Resolution (fig. 2 : 7) and is the ability to define two structures at right

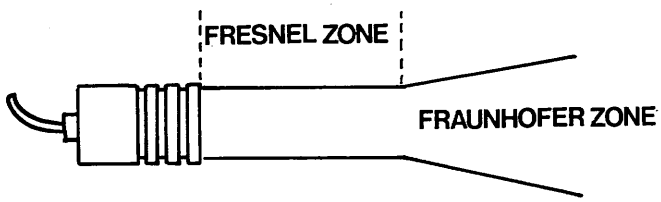

fig. 2 : 8. The two sections of a sound beam from a non - focused transducer.

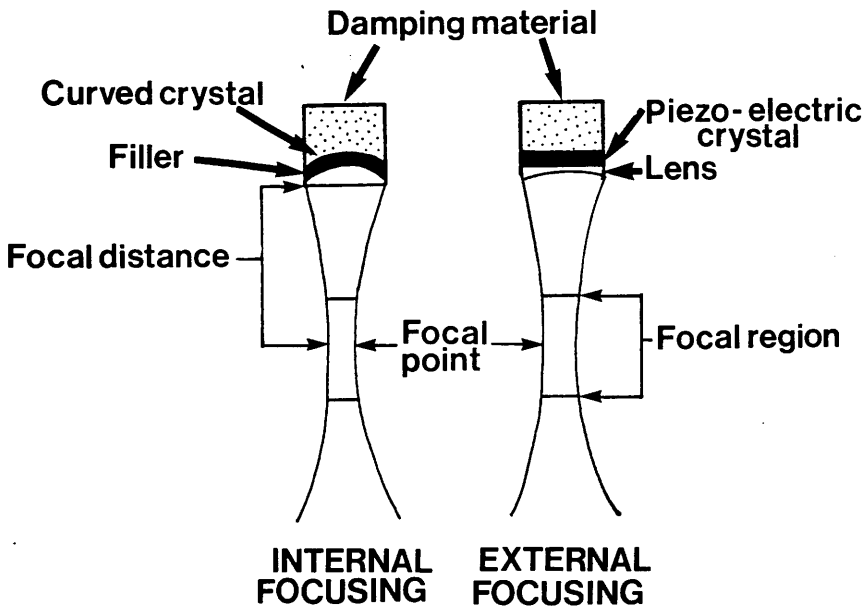

fig. 2 : 9. Internal and External focusing of transducers.

angles to the sound beam separately. The near field beam width can be narrowed to improve lateral resolution by decreasing the diameter of the transducer. Beams can be focussed in the thickness plane to give a better lateral resolution at a given depth. This is achieved by using curved crystals (Internal focusing), or by placing an acoustic lens beneath the crystals (external focusing , fig. 2 : 9).

Focusing narrows a portion of the beam's profile and thereby increases the amplitude of the echoes from certain depths. It is therefore important to select a transducer that is focussed closest to the depth of interest. In transducers with a high frequency, the focal region is closer to the transducer. In the case of a 7.5 MHz transducer, the depth of focus is 20 millimetres and could be used in the examination of ovaries via a rectal probe. A 5 MHz transducer, has a depth of focus of 35 millimetres and is suitable for thoracic and abdominal examinations, whereas a 3.5 MHz transducer, with a 70 millimetre depth of focus, would allow examination of a post - partum uterus or foetus.

2 : 5. ULTRASOUND SCANNERS.

The connection of a transducer to an ultrasound scanner has a series of encoders which spatially orient the returning echoes to display accurately the acoustic interfaces of the tissue on the display screen. There are three main display formats or modes; (fig. 2: 10).

1. Amplitude mode. (A - mode).

A - mode ultrasonic imaging is a one dimensional display of the returning echo amplitude and distance. Each peak represents a returning echo, the height of which is proportional to its amplitude. A - mode has a number of uses in Veterinary Medicine, one of which is dermatological examinations.

2. Brightness mode. (B - mode).

B - mode ultrasound is a two dimensional display of dots. The transducer is moved across the surface of the body and a cross - sectional anatomy is depicted. The position of the dot (depth) on the screen is determined by the time it takes for an echo to return to the transducer. The brightness of the dot is proportional to the amplitude of the returning echoes. This form of ultrasound is most commonly used in medical and veterinary imaging.

3. Time - Motion mode. (TM or M - mode).

M - mode is a one dimensional format displaying dots as in B - mode. The first step in forming this mode is to convert the A - mode information about the echo amplitudes, into a B - mode format. A cursor enables the selection of one line on the B - mode. The B - mode trace as described previously, is continuously updated and the image is moved along that line to be recorded. M - mode is used primarily in echocardiographic studies to measure cardiac wall motion, valve movement and also heart chamber dimensions.

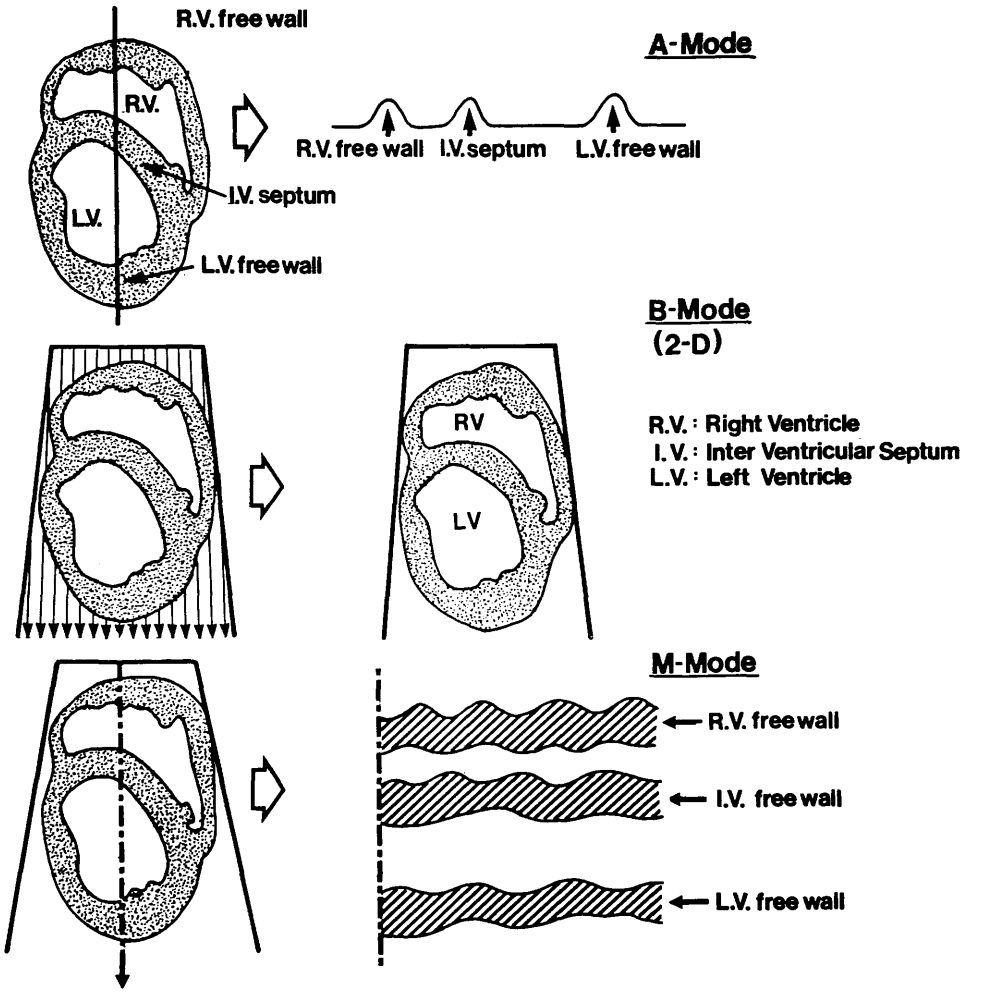

fig. 2 : 10. Diagram of sections through a dog heart illustrating different Mode display.

Unlike A - mode and M - mode, there are two basic types of B - mode scanners, they are ;

A) Static Scanner.

This requires the operator to move the transducer across the part to be imaged to produce the ultrasound image. The image is then displayed and held on the screen during the sweep. This scan can then be studied and if required measured or the image photographed before being removed by the operator to create the next transducer sweep. This form of scanner is seldom used nowadays, and is largely replaced by the real - time scanner.

B) Real - Time Scanner.

Real - time ultrasonic imaging is a form of B - mode used to record moving structures. In real - time, imaging echoes are recorded continuously on a non - storage, cathode - ray display screen, which is analogous to image intensified flouroscopy except that cross - sectional anatomy is displayed. Since new images are produced rapidly many times per second, moving structures such as a heartbeat and foetal movements, can be observed. The transducer head of real - time units is attached by a flexible cable, encoders are housed within the movable head to allow rapid transducer movement from one area to another.

TYPES OF REAL - TIME SCANNERS.

1) Linear Array Scanner / Transducer.

The linear transducer (fig. 2: 11) has piezoelectric crystals arranged in a line along its face, each of which produce soundwaves from one end of the array of crystals to the other. This process is repeated continuously producing a rectangular shaped beam. On the cathode - ray tube, a set of lines corresponding to all the positions of the beam is generated. The reflections received by a group of elements are displayed along the appropriate line and so a rectangular image is formed.

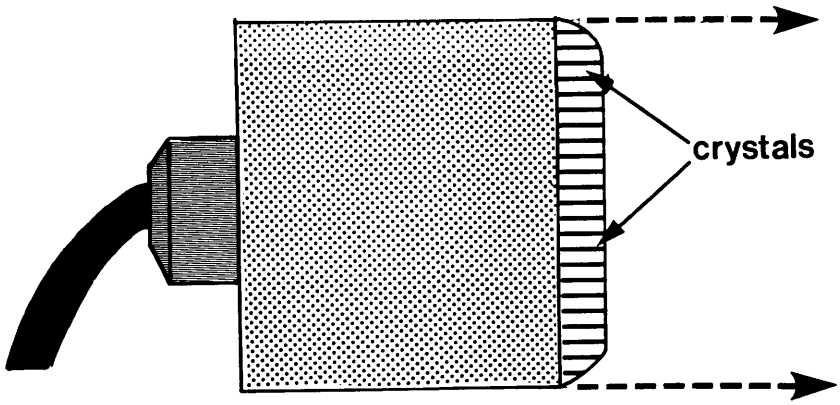

Linear Transducer

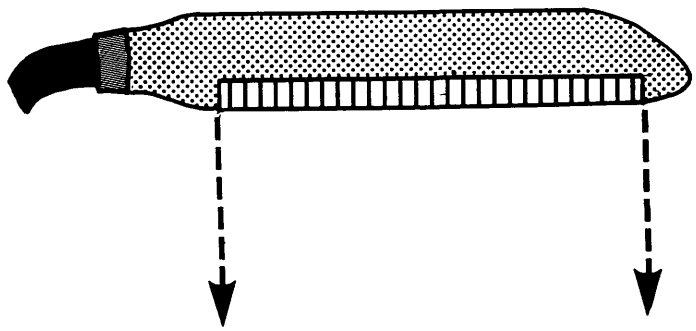

Rectal Linear Transducer

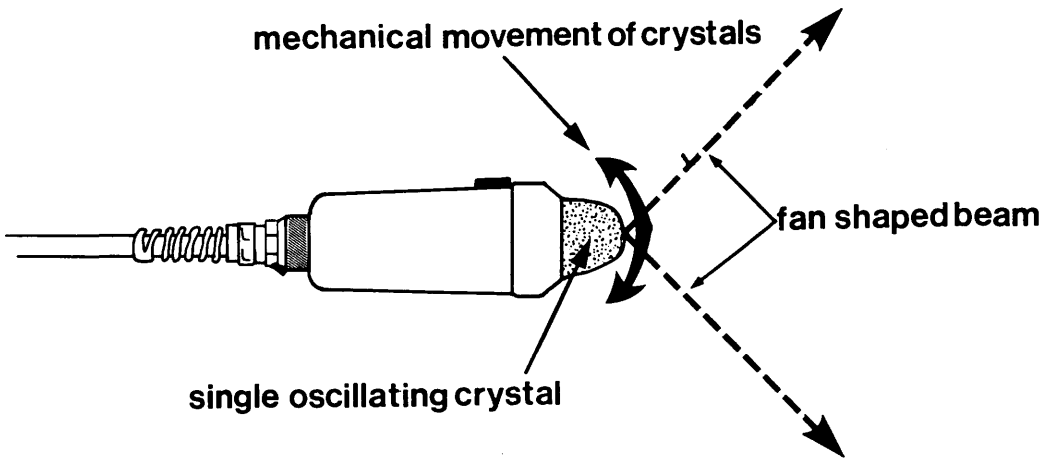

Sector Transducer

fig. 2 : 11. Range of Real - Time Transducers.

Linear array scanners allow superficial structures to be seen and analysis of the anatomical relationships between them. The size of the transducer restricts its use, but is useful in carrying out abdominal scans. Linear transducers also come in the form of rectal probes and allow examination of the ovaries and uterine condition. (e.g. pregnancy diagnosis).

2. Sector Scanner / Transducer.

The sector scanner transducer (fig. 2 : 11) consists of three - four crystals which are mechanically rocked from side to side whilst they are being oscillated. Each crystal is active when it passes an acoustic window in the housing, resulting in a fan - shaped beam. This is displayed as a sector of an arc on the screen, hence the name " sector scanner ". The small size of the transducer allows easy handling and is used for examination of the thoracic and abdominal cavities. The one limitation of this type of scan is that due to the shape of the beam, very superficial structures may not be well visualised.

3. Phased Arrays.

Developments in electronics has made it possible to make the beam from a linear array scanner leave at an angle; furthermore, this angle can be varied. This arrangement can be used to give a radial scan similar to that obtained with the sector transducer. As there are no moving parts involved, higher scanning speeds are possible and complex scan patterns can be carried out. This produces a high quality resolution scan.

2 : 6 ULTRASOUND IMAGE ARTIFACTS.

The ultrasonographer after mastering the fundamental physics of ultrasound and its interaction with tissue is then met with a new frontier, that of ultrasound image artifacts.

An artifact on a B - mode, grey scale, ultrasound image is defined as any dot appearing in the ultrasound image that does not correspond to a real echo in the subject. This definition might be expanded to include an alteration in the ultrasound image which does not portray a representation of actual structures. Like the image itself, an understanding of the artifact production and identification are necessary to avoid or diminish interpretation errors.

Ultrasound artifacts may be produced by various factors; firstly electronic noise or interference. This may be reduced by having the machine adjusted and tuned, whereas outside interference, which may cause severe image distortion, can usually in most cases be corrected by a suppressor. Secondly, echo distortions; these are caused by ultrasound matter interactions and occur more frequently than other artifacts. This artifact group consists of reverberations, shadowing, refractive and reflective zones and through transmission. As well as being artifacts, shadowing, through transmission, refractive and reflective zones also serve as diagnostic ultrasound signs.

Reverberation echoes are the most frequent and troublesome artifacts produced on ultrasound images. Reverberation artifacts are produced by a sound pulse bouncing back and forth between two interfaces. They may be produced by sound waves reflecting between the transducer and tissue interfaces or internally between two reflecting interfaces. Transducer - interface reverberation echoes are produced each time the sound pulse returns to the transducer. The time lapse that occurs between the second, third or fourth returning echoes, places them at a greater depth in the tissue on the recorded image. In the case of the transducer interface reverberation, only the initial recorded echoes are real, other reverberation echoes that appear deeper in

the tissue are multiples of the original echo and succeeding reverberation echoes will be smaller because of attenuation. These types of reverberations are more likely to occur from highly reflective interfaces (e.g. gas and bone) and may appear as parallel lines or " column of echoes ".

Internal structure to structure reverberations, occur when the sound pulse bounces back and forth between two tissue interfaces. This delays the sound pulse from returning to the transducer and the recorded reverberation echoes are deeper in the tissue than the original reflecting interface. This type of reverberation may appear as a mirror image of tissue structures or as diffuse echoes. Diffuse echoes are easily recognised over cystic, anechoic structures or deep to normal structures, but are difficult to recognise over echoic structures.

Shadowing is created by the complete reflection or attenuation of the sound beam. The zone deep to the reflecting or attenuating surface is anechoic; however, light reverberation echoes may appear in the shadowed area. This shadowing artifact may be produced by bone or gas and can impede adequate imaging of deeper structures. Refractive and reflective acoustic shadowing zones may occur distal to margins of a rounded structure containing material of lower acoustic velocity, such as fluid filled cystic structures. The sound penetrating the edge of such a structure may be slightly refracted or reflected producing a linear anechoic zone deep to the cystic structure. These zones are evidence of a cystic, fluid filled structure and should not be mistaken for shadows produced by gas or bone.

Through transmission is caused by a relative lack of sound attenuation. When sound passes through a fluid filled structure, there is less tissue reflectance and attenuation. A bright or densely echoic area is produced immediately deep to the cystic structure because more sound waves are present in this area compared to tissues at the same depth, but not beneath the cyst.

Technical imaging artifacts include off - normal incidence defects, echo displacement and improper time gain compensation (TGC) settings. Off - normal incidence artifacts result in echo omission from a specular reflecting surface, such as an organ border. The borders or interfaces not at or near a 90^{o} angle to the incident of the sound beam may appear incomplete.

Echo displacement may be caused by imaging through or over a rib, or by the movement of the transducer or subject being examined. These movement artifacts appear as straight lines, causing a discontinuity through the image. Sound attenuation or reflection causes the displacement when scanning through a rib, whereas breathing motion is the most common cause of transducer movement when scanning animals.

Lastly there is Time Gain Compensation (TGC) which corrects for echo attenuation with time or distance through tissues. Improperly adjusted TGC will produce an unacceptable image; if the TGC is too high, a densely echoic zone will appear near the skin surface and the deeper echoes will be within an acceptable intensity range. Conversely, if the TGC is too low, acceptable intensity echoes will appear near the transducer but there will be no deep echoes. The TGC must be adjusted while performing the scan to provide an even image.

CHAPTER 3.
DOPPLER ULTRASOUND.

3 : 1. INTRODUCTION TO DOPPLER ULTRASOUND.

As in the case with ultrasonography, before using Doppler echocardiography, certain basic principles must be understood. The physical principles involved in its use have been understood for well over a century, and Doppler itself has been used as a diagnostic tool in echocardiography for over twenty - five years.

The first scientific description of the physical principle commonly termed " the Doppler effect " is credited to Johann Christian Doppler, an Austrian mathematician and physicist who lived during the first half of the nineteenth century. In 1842, Doppler gave a paper before the Royal Bohemian Society of Learning in which he stated that certain properties of wave phenomena (e.g. light or sound) depended on the relative motion of the observer and the wave source. It was however unfortunate that despite his accurate description of the principle, the example he chose to describe this event, that the colour appearance of certain stars was caused by their motion relative to earth, (the blue stars moving towards the earth, the red moving away) was totally wrong. This was due to a misunderstanding of the composition of the electromagnetic wave spectrum of which visible light is a part.

Experimental verification of the Doppler principle was to prove difficult, due to the lack of instrumentation to accurately measure the frequency of light or sound waves, and it was not until 1845 that an experiment was carried out to test the hypothesis. The " measurement instrument " used was that of an observer with the ability to describe the absolute pitch of musical sounds. This ability was used to compare the pitch of a trumpet sounded from several stationary positions with that of a trumpet sounded from the top of a moving railway carriage. (fig. 3 : 1). The observer concluded that the sounds emitted from the various stationary trumpets all had the same pitch, whereas the pitch from the moving trumpet increased as it approached and in contrast decreased as it moved away from him, just as Doppler had predicted. These results were confirmed by several scientists over the preceding years (Fizeau and Russel 1848) and in 1868 the British astronomer, William Higgins demonstrated the validity of Doppler's hypothesis in the realms of light and sound. In this century ,

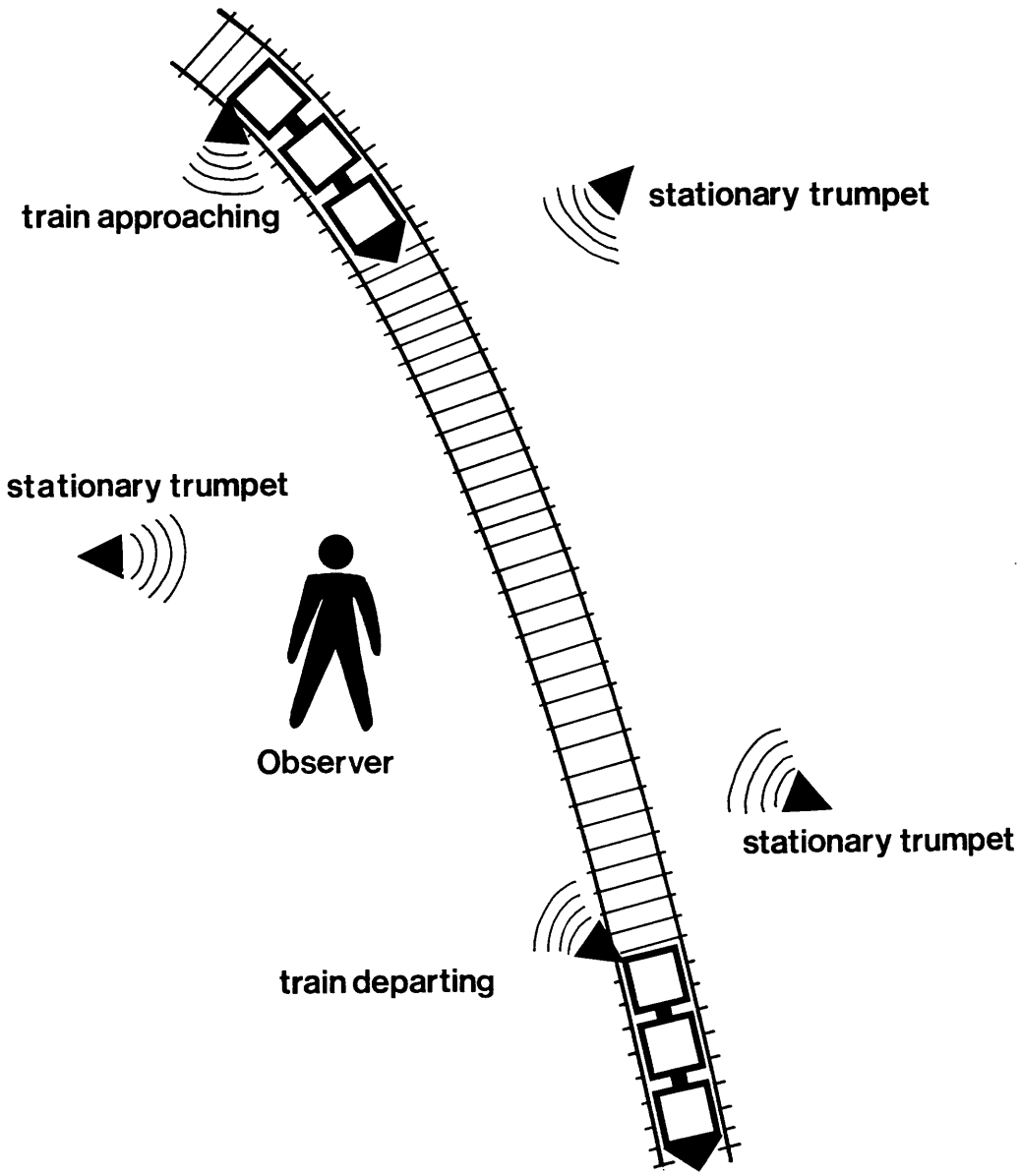

fig. 3 : 1. Schematic recreation of the experiment to prove Doppler hypothesis

the Doppler effect has become a major tool in the science of Astronomy, and the " Big Bang " theory of the origin of the universe is based on observations using the Doppler effect.

3 : 2. THE DOPPLER EFFECT OR DOPPLER SHIFT.

Doppler ultrasound systems operate differently from standard ultrasound imaging systems. In standard echocardiographic imaging, a given pulse of ultrasound is transmitted into the body and then reflected back from the various tissues. Since the speed of sound is known, (1540 meters per second) a standard ultrasound system can measure the time required for the transmitted pulse to travel to a target and then return, and use this information to create an image of the target.

In modern two - dimensional imaging systems, this alternating process is repeated in a variety of directions thousands of times each second. The best ultrasound images are made when the target is as perpendicular to the sound beam as possible. A standard M - mode or B - mode echocardiographic system does not measure the frequency of the transmitted or returning signal; Doppler echocardiology conversely depends on the measurement of relative change in the returning ultrasound frequency when compared to that of the transmitted frequency. (fig. 3 : 2.). The example of the first experimental test of the Doppler principle involving the train, (fig. 3 : 1) highlighted two important features of the Doppler effect. Firstly, the note sounded by all the trumpets, stationary or moving was identical. Secondly, there was an apparent change in the pitch noted by the stationary observer which was caused by the motion of the sound source.

The pitch or note of a sound is a subjective feature that is appreciated by the ear. The corresponding objective that can be measured and quantified is frequency. As described in the previous chapter, frequency is the fundamental characteristic of any wave phenomenon and refers to the number of waves that pass a given point in one second. (fig. 2 : 3). The relationship between pitch and frequency is simple ; the pitch of any given sound is proportional to its

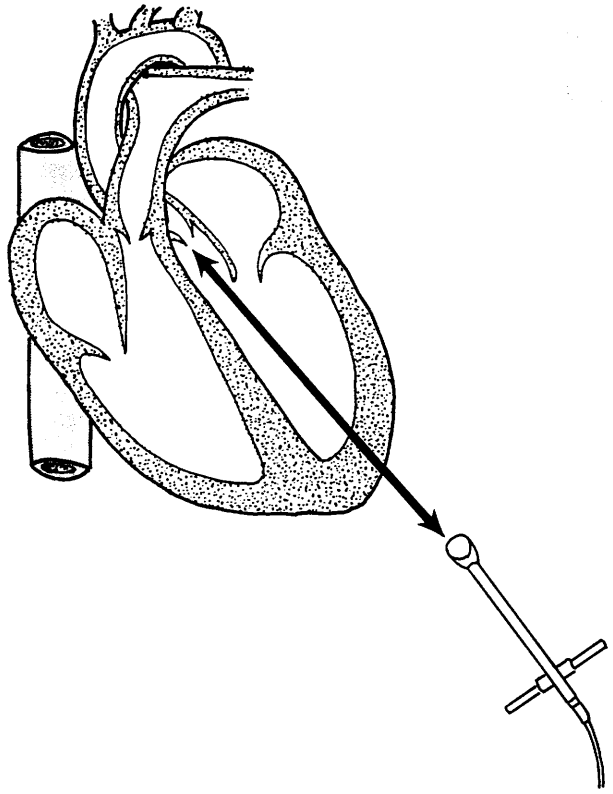

fig. 3 : 2. Ultrasound waves reflected back to the transducer by moving blood cells.

frequency. As sound wave frequency goes up, the pitch gets higher ; likewise, as the frequency goes down the pitch declines. The altering effect of the Doppler shift is more than just an interesting curiosity in that it is a method which is used in many familiar devices that measure the direction and speed of moving objects.

The radar unit used by police to monitor the speed of cars is one such device. The police radar is set up in a position where it can be directed along the line of traffic flow and, when activated, it sends a beam of radar waves of a known , uniform frequency at the oncoming cars. Each time the beam encounters an oncoming car, waves of higher frequency are reflected back to the police unit. The frequency of these returning waves is measured and compared with the transmitted frequency. The magnitude of this Doppler shift is proportional to the speed or velocity of the car that produced it. If the radar beam strikes a stationary car, then the reflected wave will have a frequency identical to the transmitted waves, and no Doppler shift is recorded. However, if a vehicle is moving towards the radar, the return frequency will be higher than the transmitted frequency, and a positive Doppler shift will be noted. Conversely, if the vehicle is moving away from the radar source, the returned frequency will be less than that transmitted and the Doppler shift will be a negative value.

There are important similarities between the example of the police radar and how Doppler systems operate in the body. In both cases, transmitted waves of some type encounter moving objects and are reflected back with altered frequencies. (fig. 3 : 3). The magnitude of the induced frequency change or Doppler shift also allows the velocity of the moving objects to be calculated.This can be done by the following equation ;

$$V = \frac{c\,F}{2Fo\,Cos}$$

where ; V is the Bloodflow velocity, c is the speed of sound in soft tissue (1540 meters per second), F is the Doppler frequency shift, Fo is the transmitting frequency shift, and Cos is the angle between flow velocity vector.

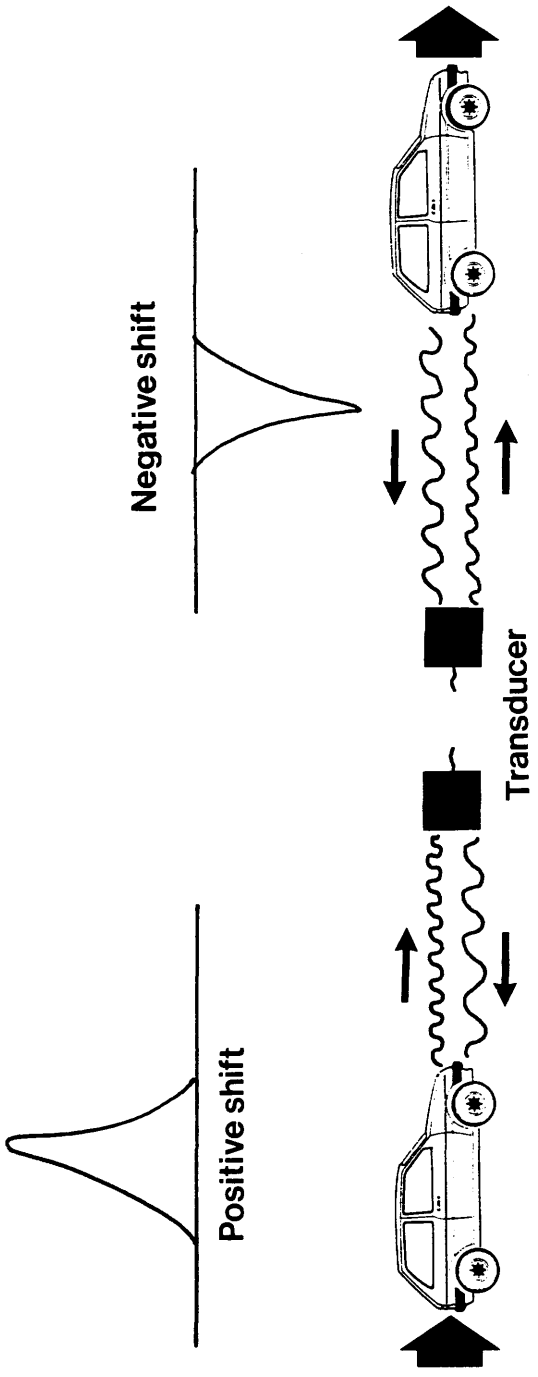

fig. 3 : 3. The Doppler Shift.

One important difference between the radar unit and the Doppler ultrasound is that the radar is used to measure the speed of single objects (e.g. cars), whereas the Doppler ultrasound system measures the speed of millions of objects (e.g. bloodcells) at a time, and therefore is looking at a spectrum of velocities. (fig. 3 : 3).

DIRECTION OF FLOW.

A good example of the ability of Doppler to determine the direction of flow can be shown when a Doppler transducer is held in the suprasternal notch, first being angled towards the ascending aorta, and then towards the right where it encounters the descending aorta. (fig. 3 : 4.). When angled into the ascending aorta, flow is towards the transducer, and the Doppler Shift is positive or upward from the baseline of the display. Conversely, if the transducer is angled into the descending aorta, flow is away from the transducer and the Doppler Shift is negative or downward from the baseline.

Doppler ultrasound systems measure the frequency change between emitted and returned frequencies caused by moving objects. The relationships between the Doppler frequency shift produced by the moving red blood cells and the velocity of the cells is expressed formally in the Doppler equation ;

$$f_2 = \frac{2f_0}{c} v \cos \theta$$

where ; f_2 is the returned frequency, fo is the transmitted frequency, v is the maximal velocity, cos 0 is the angle between beam and velocity, and c is the velocity.

If the transducer is positioned as parallel to the blood flow as possible, then the angle between beam and the velocity is zero degrees and cos θ becomes 1.

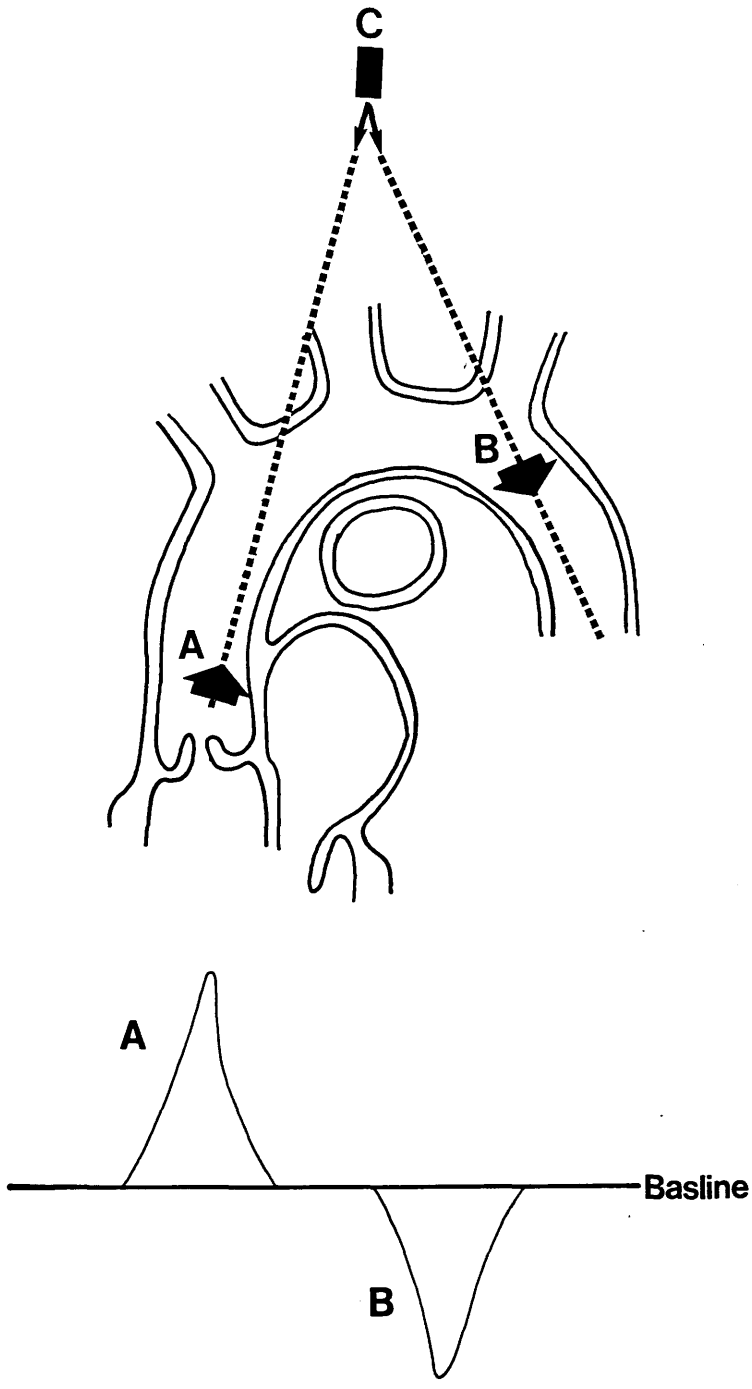

A : Blood flow towards transducer

B : Blood flow away from transducer

C : Transducer

fig. 3 : 4. Direction of blood flow in relation to transducer position.

THE EFFECT OF ANGLE.

The Doppler equation also states that the angle the Doppler beam makes with the lines of flow being evaluated is very important. This angle (θ) is of crucial importance in the calculation of velocities from Doppler Shift data. (fig. 3 : 5). When the ultrasound beam is directed parallel to the blood flow, angle θ is 0 (cosine $\theta = 1$), and the measured velocity on the recording will be true velocity. In contrast , when the ultrasound beam is directed perpendicular to flow, angle θ is 90 (cosine $90 = 0$) and measured velocity will be 0. Therefore, the smaller the angle θ, the closer angle cosine θ is to 1, and the more reliable is the recorded Doppler velocity. A wider angle θ will result in a greater reduction in measured velocity compared with true velocity. Thus, the more parallel to flow the Doppler ultrasound beam is directed, the more faithfully the measured velocity will reflect the true velocity.

For practical purposes, angles of greater than 25°between the ultrasound beam and the blood flow being studied will generally yield clinically unacceptable quantitative estimates of velocity. The best quantitative estimates of flow are therefore achieved when the Doppler signal is as parallel to the flow as possible. This need to be parallel to flow leads to the dependence on some windows for examination that may sacrifice the quality of the two - dimensional image. (fig. 3 : 6.).

The direction of the ultrasound beam through either the mitral or tricuspid orifices from the apical position, gives an excellent Doppler window , but one which may allow significant echocardiographic "drop out" since the imaging beams are parallel to the endocardium.

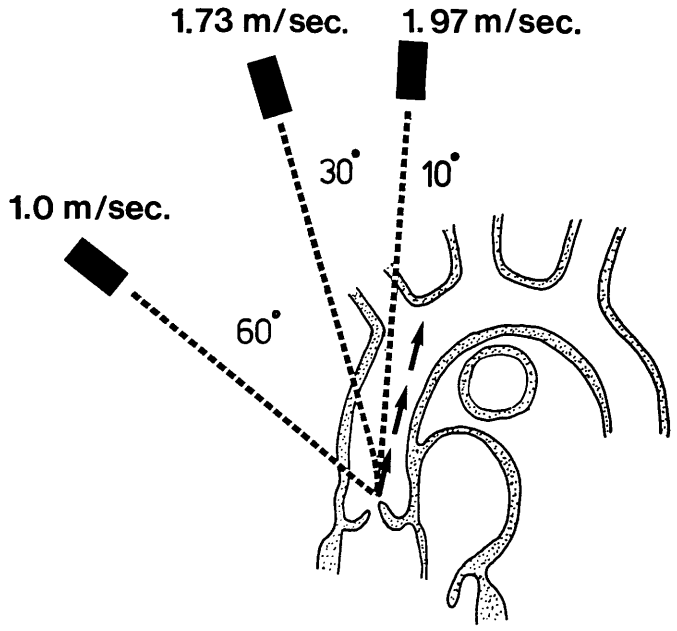

fig. 3 : 5. The effect of beam angle in relation to blood flow velocities.

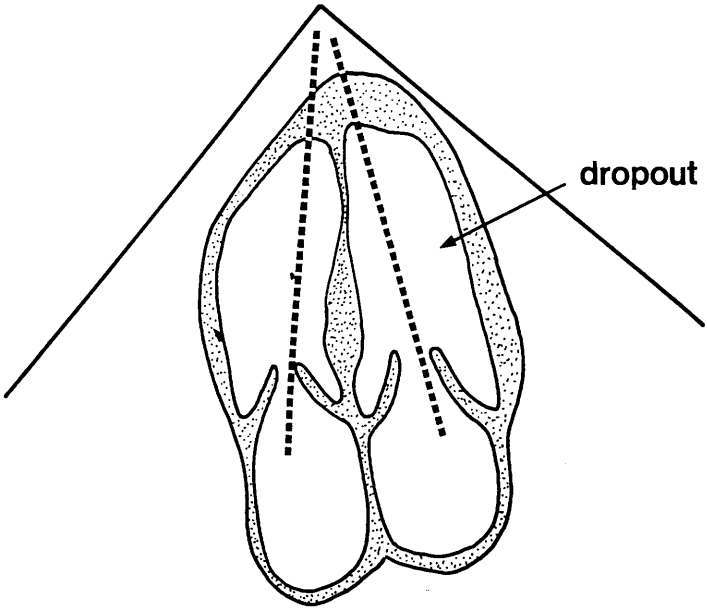

fig. 3 : 6. " Target dropout " due to the imaging beam being parallel to the target

3 : 3. FLOW PATTERNS.

Bloodflow through the heart and great vessels has certain characteristics that can be measured using Doppler ultrasound. For the purpose of understanding flow patterns in the heart it is important to recognise the difference between Laminar (or normal) flow and Turbulent (or disturbed) flow. (fig. 3 : 7).

Laminar flow is flow that occurs along smooth parallel lines in a vessel when all the red cells generally accelerate and decelerate at approximately the same speed. Flow in most of the cardiovascular system is normally laminar. Normal bloodflow through the heart rarely exceeds 1.5 meters per second, whereas in contrast, turbulent flow is said to be present when there is some obstruction that results in a disruption of the normal laminar pattern. This causes the orderly movement of red blood cells to become disorganised and produces various whirls and eddies of differing velocities and directions.

Obstructions to flow usually also results in some increase in velocity, thus turbulent flow is characterised by disordered directions of bloodflow in combination with many different red cell velocities. If the obstruction is significant, some of the red blood cells may move at higher velocities than normal and may reach speeds of 5 - 6 meters per second. Turbulent flow is usually an abnormal finding and is considered indicative of some underlying cardiovascular lesion.

Laminar flow

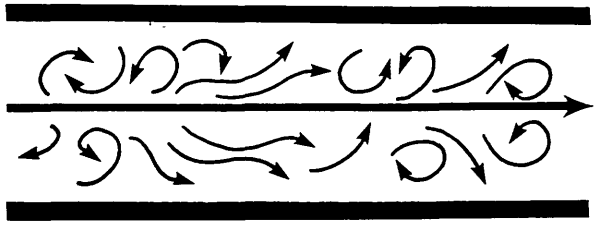

Turbulent flow

fig. 3 : 7. Diagrammatic illustration of Laminar and Turbulent blood flow.

3 : 4. THE DOPPLER SPECTRUM.

The Doppler shift gives information in two formats ; the Audible Signal and the Doppler Spectral Display. This is a graphic analysis of the blood velocity charted against time.The changing velocities (frequencies) detected by the Doppler instrument are converted into audible sounds, and after filtering and processing are emitted from a speaker within the machine. High pitched sounds are obviously the result of large Doppler shifts and indicate the presence of high velocities, whereas low pitched sounds are the result of lesser Doppler shifts. The audio output also allows the operator to easily differentiate laminar from turbulent flow. Laminar flow produces a smooth, pleasant tone because of the narrow, uniform shape of the Doppler Spectrum whereas turbulent flow because of the presence of many different velocities, commonly results in a high - pitched whistling or raspy sound.

Audio output is one of the oldest and simplest forms of Doppler display;never the less it remains a indespensible guide to the machine operator for achieving proper orientation of the ultrasound beam, even when the Doppler is being used in conjunction with an ultrasound image. The audio output from an Doppler machine may superficially resemble the sounds produced by the amplified stethoscope or a phonocardiogram; it is therefore worth emphasising that Doppler is neither of these. The sounds detected with a stethoscope are transmitted vibrations or pressure waves from the heart and great vessels due to the rapid accelerations and decelerations of the blood. The Doppler output in contrast is an audible display of the Doppler Frequency Shift Spectrum produced by the red cells moving in the path of the ultrasound beam. It is a sound produced by the Doppler that does not occur in nature and therefore does not originate from the heart.

The Doppler Spectrum displays the Doppler Shift as either frequency or velocity; therefore blood flowing towards the transducer is displayed above the baseline and blood receding from the transducer is shown below the line. (fig. 3 : 8).

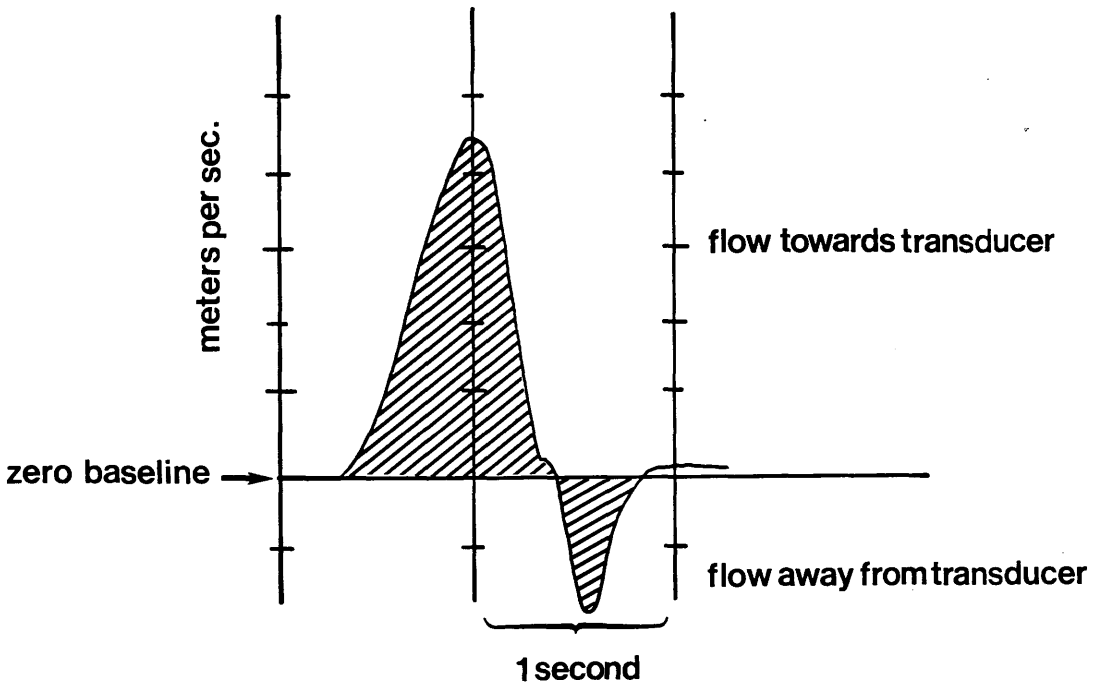

fig. 3 : 8. The Doppler Spectrum.

3 : 5. PULSED AND CONTINUOUS WAVE DOPPLER.

There are two types of Doppler echocardiographic systems in common use today; Continuous Wave (CW) and Pulsed Wave (PW). They differ in transducer design and operation as well as signal processing and in the types of information provided.

Continuous Wave Doppler. (CW)

This is the oldest and electronically most simple of the two forms of Doppler. As the name implies, CW Doppler involves continuous generation of ultrasound waves coupled with continuous generation of ultrasound reception. This dual function is accomplished by a two - crystal transducer, with one crystal dedicated to each function. (fig. 3 : 9). The main advantage of CW Doppler is its ability to measure high blood velocities accurately and record the highest velocities in any valvular or congenital heart disease. The main disadvantage of CW Doppler is its lack of selectivity or depth discrimination. Since CW Doppler is constantly transmitting and receiving from two different crystals, there is no provision for real - time imaging or range gating to allow selective placing of a given Doppler sample volume.

The output from a CW examination contains Doppler Shift data from every red blood cell reflecting ultrasound back to the transducer along the course of the ultrasound beam. However, as is the case with most scientific equipment, the disadvantage of not being able to image a Doppler sample for CW Doppler has been overcome with a new generation of echocardiography systems. (Toshiba SSH - 140A). This equipment is unfortunately very expensive (> £80K) and is therefore outwith the expenditure of most Veterinary Institutions, who must continue with the stand - alone technique.

Pulsed Wave Doppler. (PW).

PW Doppler transducers have 3 - 4 crystal transducers which alternate transmission and reception of ultrasound similar to that of an M - mode

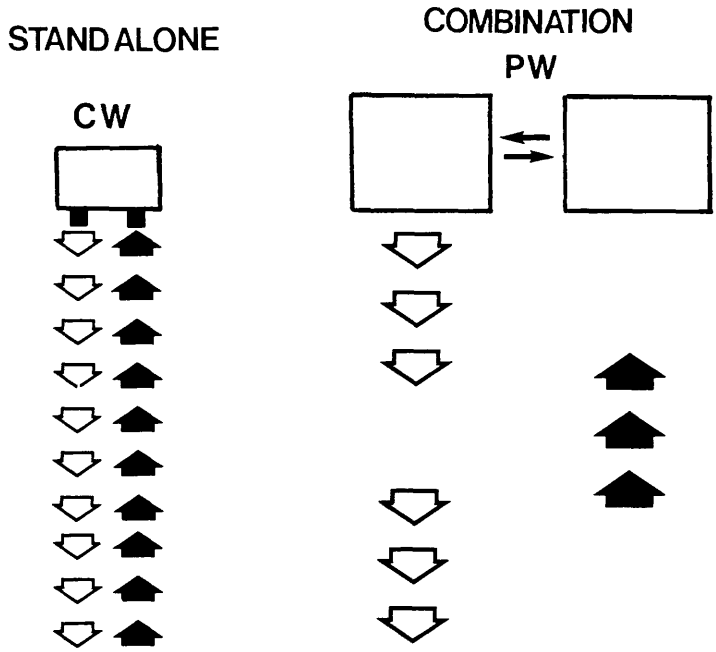

fig. 3 : 9. Comparison of Pulsed Wave and Continuous Wave ultrasound

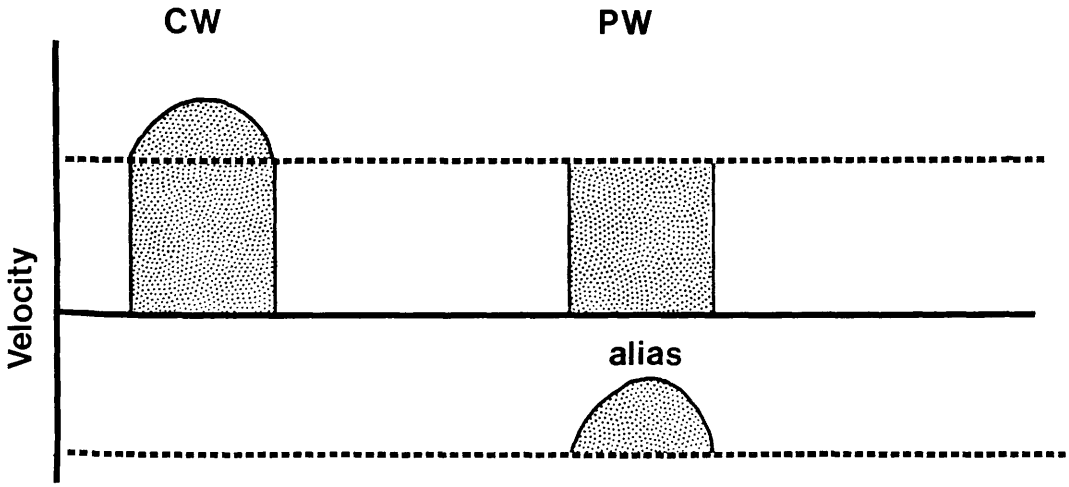

	range sample	maximum velocity limitation
Pulse wave	+	+
Continuous wave	-	

fig. 3 : 10. Comparison of Pulsed Wave and Continuous Wave techniques.

transducer. (fig. 3 : 9). One main advantage of PW Doppler is its ability to provide Doppler Shift data selectively from a small segment along the ultrasound beam, referred to as the Sample Volume. The location of the sample volume is operator controlled. The transducer transmits in short pulses and waits for the reflected signal to return before it sends out another impulse. Another main advantage of pulsed Doppler is the fact that some real - time imaging may be carried on alternatively with the Doppler, and thus the sample volume may be shown on the actual two - dimensional display for guidance.

The main disadvantage of PW Doppler is its inability to accurately measure high blood velocities, such as may be found in certain types of valvular and congenital heart disease. (fig. 3 : 10). The maximum detectable velocity within the sample site is limited because of the pulsed wave's relatively slow sampling rate, also known as the Pulse Repetition Frequency (P.R.F.). This limit is called the "Nyquist Limit " which is equal to half the P.R.F. High sampling values are required to measure high velocities, therefore for the deeper sample volumes, a lower P.R.F. is required to allow the time for a pulse to reach and return from the range gate. The lowering of the P.R.F. or the sampling site lowers the the Nyquist and therefore limits the maximum velocity that can be measured.

Recent technology has extended the range of PW Doppler with the introduction of a High Pulse Repetition Frequency mode (H.P.R.F.) (fig. 3 : 11). High P.R.F. is intermediate between PW and CW modes, and allows the measurement of higher velocities while retaining some information of depth. High P.R.F. mode increases the P.R.F. over pulsed mode which results in the simultaneous placement of multiple range gates in the anatomy. This range gating is basically a timing mechanism that only samples the returning Doppler Shift data from a given region. The range gate is calibrated so that as the operator chooses a particular location for the sample volume, the range gate circuit will only permit Doppler Shift data from inside that area to be displayed as output, all other returning ultrasound information is essentially " ignored ".

Velocities exceeding the Nyquist Limit give a condition known as " Aliasing ".

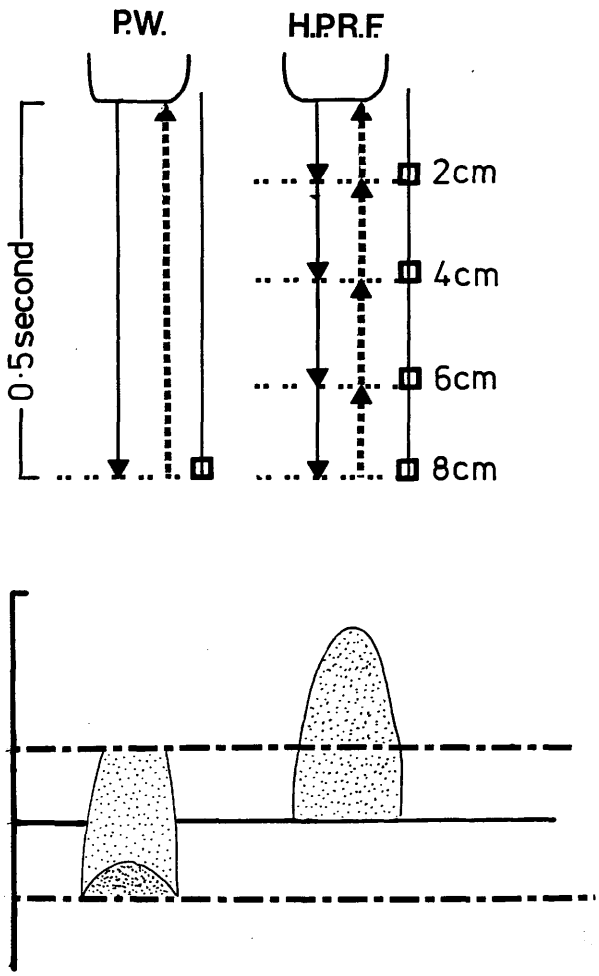

fig. 3 : 11. Comparison of Pulse Wave and High Pulse Repetition Frequency.

3 : 6. ALIASING.

The Aliasing phenomenon occurs when the abnormal velocity being studied exceeds the ability of the pulsed wave system to read it properly. An aliased signal causes the Doppler signal to fold over the spectral display so that the maximum velocity peak above the baseline is cut off and displayed below the baseline (fig. 3 : 12). This is the reason why aeroplane propellers and wagon wheels appear to rotate backwards on a movie film since the film frame rate per second is too slow to accurately keep up with the rapidly moving structures.

As previously described the Nyquist limit defines when aliasing will occur using P.W. Doppler. The Nyquist limit specifies that measurements of frequency shifts are accurate only if the P.R.F. is at least twice the maximum velocity (or Doppler Shift frequency) encountered in the sample volume. It is obviously desirable to use as high a P.R.F. as possible for recording abnormally elevated velocity jets. The problem is that the maximum P.R.F. is limited by the distance that the sample volume is placed into the heart. The closer the sample volume is located to the transducer, the higher the maximum P.R.F. that can be used. Conversely, the farther the sample volume is placed into the heart, the lower becomes the maximum P.R.F. The effect of a reduction in the Nyquist limit is also shown in fig. 3 : 12., where mild aliasing is met when a high velocity jet is in the near field (A). Progressively more severe aliasing with distortion of the full profile occurs if this same jet is encountered at ever increasing distances from the transducer face (B, C, and D). Finally at point D, the aliased profile is so distorted as to be unrecognisable.

It is important to realise that the maximum recordable velocities in any blood flow relate to the frequency of the P.W. transducer being operated. A low - frequency transducer increases the ability of a P.W. system to record high velocities. If an operator encounters aliasing with a 5 MHz transducer at a given depth, use of a 3.5. MHz transducer may allow the recording of the entire profile without distortion. The second and most practical method to overcome aliasing is to either move the zero baseline up or down depending on the direction of flow or to increase the vertical scale.

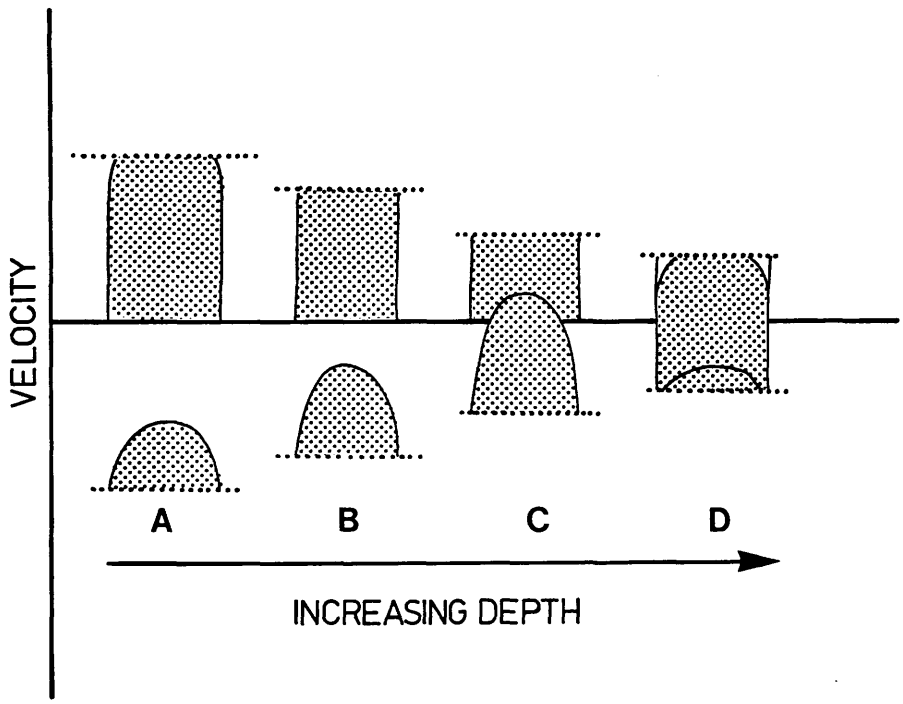

fig. 3 : 12. The effect of reduction in the Nyquist limit.

CHAPTER 4.
MATERIALS AND METHODS.

4 : 1 THE ANIMALS.

The animals used in this study comprised of two breeds of dog ; Greyhounds and Beagles. Twelve Beagles of between the ages of 7 months and 3 years along with three Greyhounds aged between 4, 5 and 7 years respectively were examined.

All the dogs in the study had no previous history of cardiac anomalies and were in good health and condition.

4 : 2. THE SCANNERS.

Three ultrasound systems were used in this study ; the Interspec XL Series 3 Duplex Imaging Scanner, (fig. 4 : 1) the Interspec Apogee Duplex Imaging Scanner, (fig. 4 : 2), (both Interspec, Pennsylvania, U.S.A.) and the Toshiba SSH - 140A Colour Flow Scanner. (fig. 4 : 3), (Toshiba Medical Systems, Crawley, U.K.)

These scanners allow the recording of high resolution, two - dimensional , M - mode and Doppler echocardiography. Being Duplex systems they have the capacity to simultaneously image and display both Pulsed Wave (PW) and Continuous Wave (CW) Doppler signals. The Interspec Apogee is a new generation scanning system replacing the Interspec XL series. It has a high definition screen and combined with Annular array capabilities, allows more greater detailed imaging. The Toshiba scanner has the same facilities as the Apogee but also includes steerable CW and Colour Flow Mapping of blood flow.

The Interspec controls are arranged in functional groups on the front panel around a 7" display screen and on a separate keyboard, whereas all the controls on the Apogee and the Toshiba scanners are contained in their keyboards.

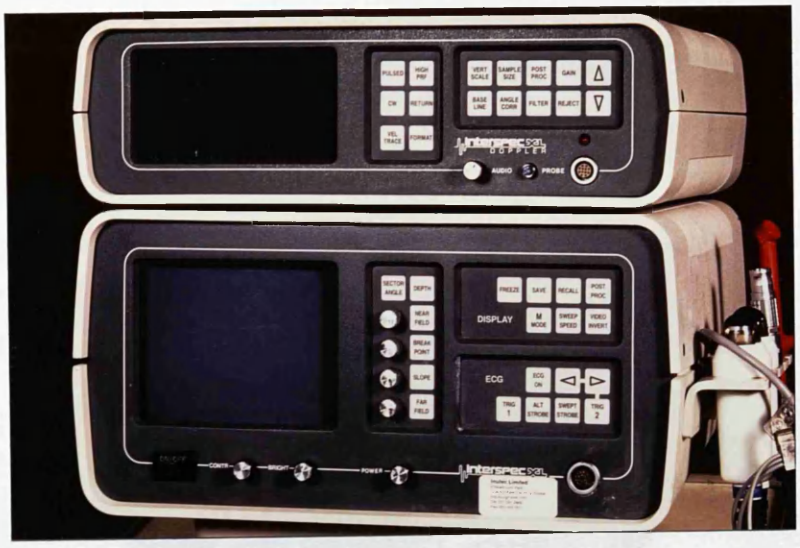

fig. 4 : 1. Interspec scanner.

fig. 4 : 2. Apogee scanner.

fig. 4 : 3. Toshiba colour flow scanner.

IMAGE CONTROLS.

Proper adjustment of the sector angle, depth, gain and power controls is vital in achieving the best possible scan image. The sector angle control allows the choice of a wider or narrower field of view. The depth control as the name implies, enables examination on a shallower or deeper field of view. The gain control adjusts the amplification of the returning signals from specific portions of the image and along with the power control, (which increases or decreases the intensity of the ultrasound energy leaving the transducer) allows the quality of the scanned image to be improved.

In general the power control is set at 100% although it can be set from 10 - 100% in increments of ten. When structures at shallow depths are being viewed and when high TGC settings are being used, the power may be reduced. The Apogee and Toshiba scanners with their annular array transducers and high definition screens can produce images of exceptional quality at only 7% power settings.

Ultrasound signals returning from shallow structures are stronger than the echoes from deeper structures, therefore to allow adjustment of these signals the display image is divided into three areas ; the near field. the slope field and the far field region. (fig. 4: 4) The image in the near and far fields can be amplified independently with the Time Gain Compensation (TGC) controls to display the best possible image. Also the angle of the slope can be adjusted to obtain a rapid or gradual rise in gain throughout the slope region.

The TGC curve is a graphic display of the interaction of all the afore mentioned controls. The three segmented line graphically displays the gain control settings with the top segment representing the near field , the middle segment representing the slope and the bottom segment the far field.

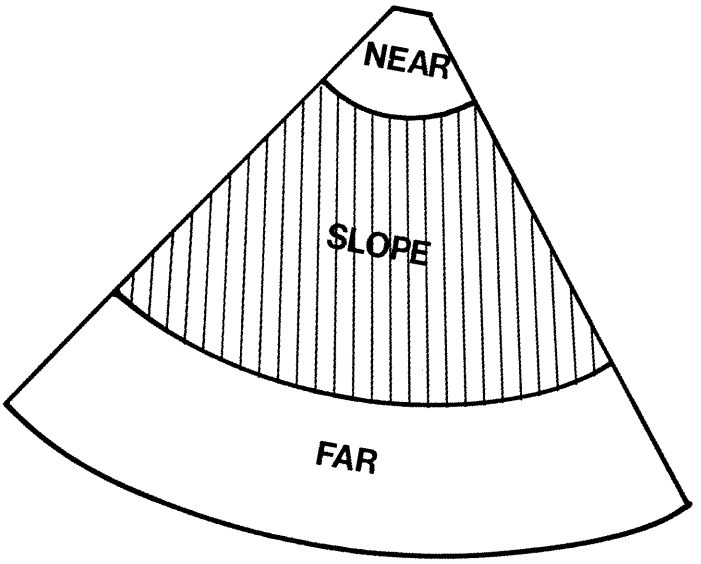

fig. 4 : 4. Image display areas.

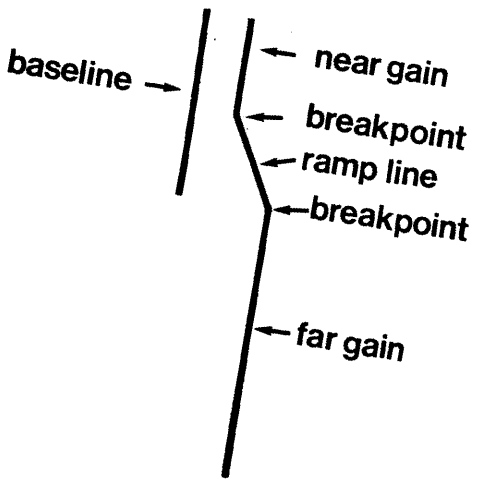

fig. 4 : 5. The T.G.C. curve.

DISPLAY CONTROLS.

The display controls allow the operator to freeze , save and recall images in the scanners memory, select gray - scale settings, enter and exit M - mode, and also choose sweep speeds. In M - mode, the sweep speed control chooses between a two second (50mm/sec.) and a four second (25mm/sec.) display. The time intervals in the M - mode are displayed as vertical columns of dots, the interval between the columns being one second.

In 2 - D mode, the sweep speed is used to choose between a two or four second echocardiograph (ECG) display. Eight 2 - D sector images can be frozen and stored in the scanner's memory, and a ninth frozen. These images can be retrieved from memory with the recall control. M - mode images can be frozen , but cannot be stored in the save memory. The post - processing control is used to select levels of gray - scale assigned to specific returning ultrasound frequencies allowing a difference in the appearance of the monitor display.

KEYBOARD CONTROLS.

The Interspec XL uses a standard typewriter style keyboard that allows annotation of text (plus patient details) on the screen. There is also a marker and calculation function which permits the measurement of distance and area of structures being scanned.

During PW Doppler scanning, the sample volume is positioned by means of a joystick located on the keyboard. The Apogee and the Toshiba operate a similar keyboard except that all their display and image controls are located on the keyboard and not the scanner itself, and the joystick is replaced by a roll - ball for the positioning of the sample volume.

4 : 3 TRANSDUCERS.

Four transducers of varying frequencies were employed for the heart scans in this study, (fig. 4 : 6) they were ;

1) A 2 MHz Continuous Wave (CW) Transducer.

This dedicated Doppler probe performed only CW Doppler images, (via a split wave crystal) and did not have 2D or M - mode capabilities. This probe was used for the measurement of high velocity cardiac flow which could not be measured accurately with PW Doppler (e,g, aortic flow) in both the suprasternal and subcostal imaging planes.

2) A 3.5 MHz Pulsed Wave (PW) Transducer.

This medium focus (13 mm) duplex transducer, allowed both 2D, M - mode and Doppler scanning. The probe was used on the Greyhounds as it gave the greater penetration required for deep chest configuration of this breed. The viewing windows employed with this probe were the right and left parasternal, and the subcostal. In the Beagles however, it was only operated in the suprasternal position as the 5 MHz transducer allowed sufficient detailed penetration for the right and left parasternal views.

3) 5 MHz Pulsed Wave (PW) Transducer.

A short focus (10 mm) duplex probe with the same capabilities as the 3.5 MHz probe was used for the right and left parasternal views in the Beagles. It s use was suitable due to the smaller chest size of this breed.

4) A 3.5 MHz Annular Phased Array Transducer.

This probe employed dynamic beam focusing to obtain the highest resolution possible and was composed of several concentric rings of elements. The Interspec Apogee scanner made it possible to control the transmitted and received signals of the probe to provide focusing in three dimensions. This improved lateral resolution and penetration, allowing greater definition than the non - annular 3.5 MHz transducer.

Steerable CW was also used with the Toshiba scanner with a probe containing two separate transducers. This probe contained a fluid path standoff which contained two separate transducers. A 3.5 MHz crystal was located near the handle of the probe intended for imaging, and a split crystal 5 MHz pulsed, high PRF and Doppler crystal was located near the soft membranous nose. The split crystal Doppler transducer provided all Doppler modes including steerable CW and could be angled by the roller tracking ball on the scanner to achieve the optimum blood velocity signals.

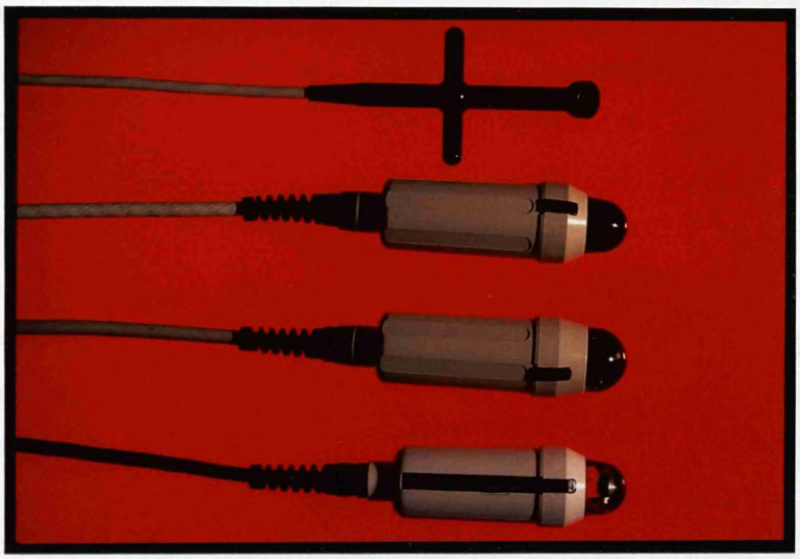

fig. 4 : 6. Range of transducers.

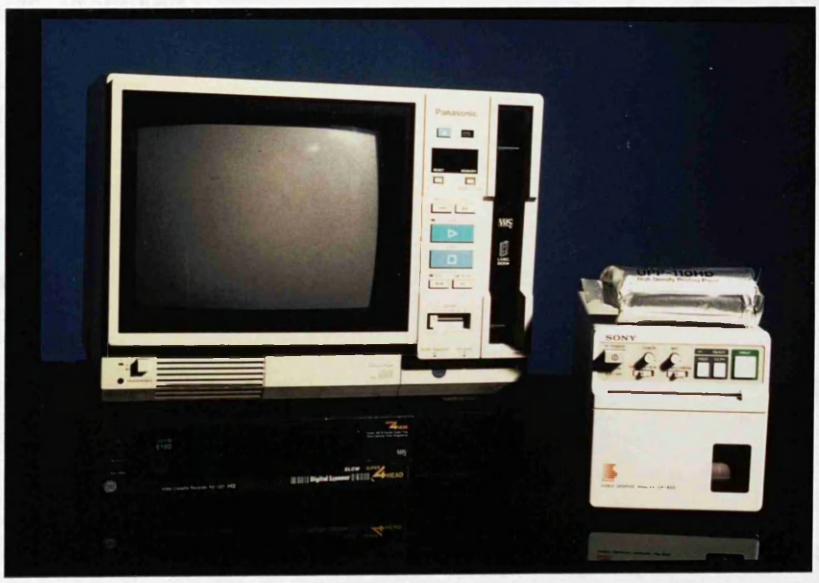

fig. 4 : 7. Video players and printer

4 : 4. RECORDING OF RESULTS.

All the dog echocardiology scans in the study were recorded on VHS video tapes, using a video cassette recorder. (Panasonic NV - G21 HQ) (fig. 4 : 7) Taped ultrasound scans were reviewed later on a video - monitor player which had single frame and freeze frame capabilities for the analysis of sequential heart movements or still pictures. (Panasonic AG - 500)

The selected images from the video tapes were transferred into a video graphic printer by means of a video outlet from the monitor, and printed out on sensitised paper. (Sony UPP - 110 HD)

4 : 5. ANATOMY OF THE HEART

A study of the gross anatomy of the canine heart was carried out before any ultrasound scanning was performed. Initially this was done with the heart viewed in situ in the cadaver. The orientation of the heart in the thoracic cavity was examined in both the left and right lateral recumbency. The heart was then removed and the location and association of the chambers to the great vessels, identified.

To appreciate the anatomy of the heart during an ultrasound scan, the heart was placed in a clear, water - filled plastic bag, and scanned with the transducer applied to the bag's outer surface. This gave both a visual display of the internal anatomy on the display screen and also allowed the observation of the position of the probe in relation to the heart. This proved extremely useful in understanding the internal anatomy of the heart in both short and long axis scans.

The heart was then sectioned with a post - mortem knife through the various imaging planes and the internal structures identified and used as a source of reference for the images recorded on the ultrasound scanner.

4 : 6. PRE - SCANNING PREPARATION.

The dogs were all examined without the administration of an anaesthetic or sedation. The examinations were carried out in a quiet, dimly lit room, as this proved to induce a more relaxed state in the dogs being scanned, and also allowed better interpretation of the ultrasound image on the display screen.

The sites for examination were firstly clipped to remove body hair, and then closely shaved with a razor to allow maximum contact with the transducer. Finally, the skin was smeared with a water soluble medical coupling gel to maximise the contact with the chosen transducer. (Siel Sound Gel, Inutec, Ltd. Edinburgh.)

4 : 7. TRANSDUCER LOCATION SITES.

Four transducer locations were employed in the heart scans of the dogs, they were ;

1) Right Parasternal View. (fig. 4 : 8)

The dog was laid in right lateral recumbency position with the transducer placed between the third, fourth or fifth intercostal space, and approximately five centimetres lateral to the sternal edge.

2) Left Parasternal View.

The dog was laid in left lateral recumbency with the transducer placed between the third to sixth intercostal space and within five centimetres lateral to the sternal edge.

3) Subcostal View. (fig. 4 : 9)

The dog was held in semi - dorsal recumbency (seated) position with the transducer placed on the left mid - line, next to the xiphoid cartilage, and directed cranially.

4) Suprasternal View. (fig. 4 : 10)

The dog was held in a prone sitting position and the transducer placed at the thoracic outlet and directed caudally.

fig. 4 : 8. Right parasternal position.

fig. 4 : 9 Subcostal position.

fig. 4 : 10. Suprasternal position.

Two orthogonal planes were used to examine the heart with 2D echocardiography, (fig. 4 : 11) they were ;

1) The Long Axis Plane.

This plane transected the heart perpendicular to the dorsal and ventral surfaces of the body, and parallel to the long axis of the heart.

2) The Short Axis Plane.

This plane transected the heart perpendicular to the dorsal and ventral surfaces of the body, but perpendicular to the long axis of the heart and was obtained by rotating the probe through 90 from the long axis plane.

4 : 8. ULTRASOUND SCANNING TECHNIQUES.

The dog was firstly examined in the right parasternal position. The transducer was held with the directional marker placed under the thumb. (fig. 4 : 11) This enabled the image being viewed on the monitor to be related to the orientation of the transducer. The heart on being located was viewed in the short axis plane by means of rotating the transducer through 90°so that the ultrasound beam was perpendicular to the long axis of the heart. This was achieved by visualisation of the heart valves at the base of the heart. The orientation was adjusted to obtain circular tomographic images of the left ventricle at various levels , and by tilting the beam gradually from the apex to the base, (ventral to dorsal) a continuous serious of cross - sections was obtained.

M - mode sections were taken in two short axis planes using anatomical structures as landmarks. The first short axis plane was taken in the area between the papillary muscles of the left ventricle, and was used to measure the left ventricular function. (L.V.F.) This was obtained by calculating the shortening fraction (S.F.) using the following equation ;

$$SF = \frac{LVEDD - LVESD}{LVEDD} \times 100$$

where LVEDD is the left ventricular end diastolic diameter, and LVESD the left ventricular end systolic diameter.

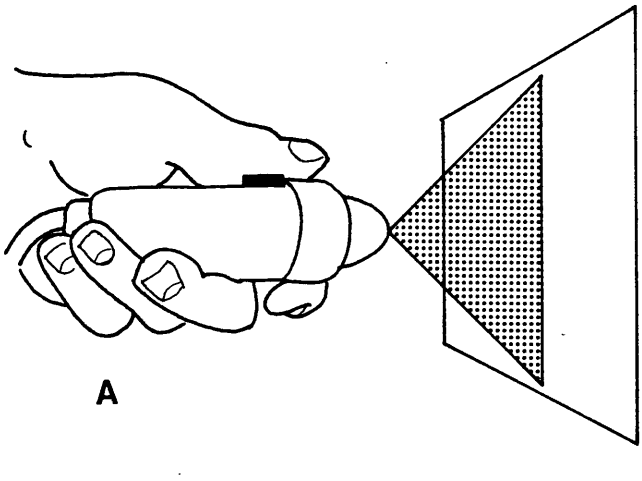

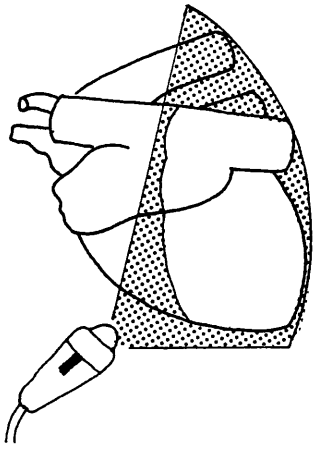

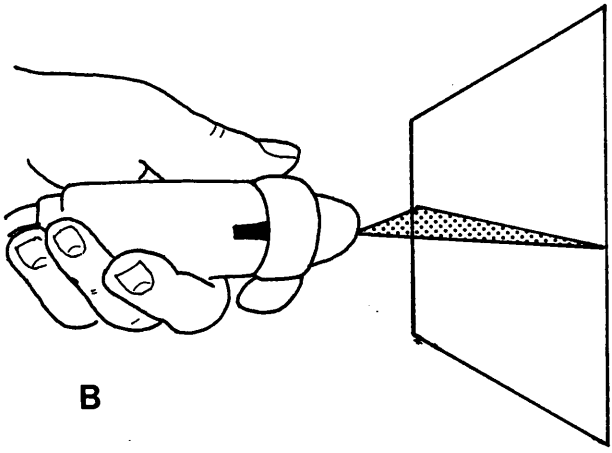

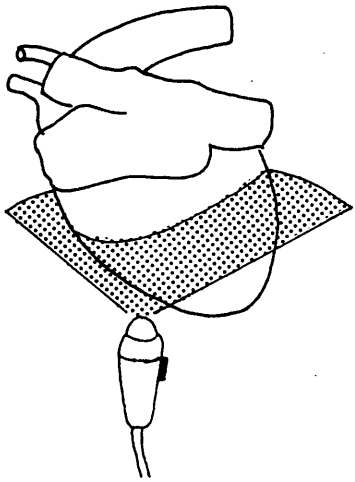

fig. 4 : 11. Transducer orientation ; A. long axis, B. short axis.

The second short axis plane was taken through the mitral valve which was recognised by it's "fish - mouth" like appearance. Both M - mode sections were achieved by placing a line cursor through the required plane and selecting the M - mode control on the scanner. A split - screen image was then obtained of the real - time scan in the top half of the screen and the M - mode trace below. Finite placement of the cursor could be made to achieve the best possible M - mode image. Once this was achieved, a full screen M - mode could be called up and labelled accordingly.

To obtain long axis views of the left heart, the echo beam plane was orientated perpendicular to the dog's long axis and then rotated slightly clockwise to approximately a parallel line drawn between the caudal border of the scapula and xyphoid. The correct position was identified by the clear visualisation of the left ventricle, interventricular septum, papillary muscles, mitral valve and left atrium. From this view both M - mode and Doppler scans were sampled. The M - mode scans were taken in the region between the papillary muscles and the cusps of the mitral valve to allow comparison of the left ventricular function in long axis with that in the short axial plane.

PW Doppler measurements of bloodflow velocity were also recorded in this view. A cursor with a movable sample volume area was placed in the ventricular side of the mitral valve and the peak velocity recorded. The same split screen facility as in the M - mode was used to allow accurate placing of the sample volume, and once this was achieved the full screen image of the Doppler signal was engaged. After this reading was taken, the sample volume was moved to the atrial side of the mitral valve and the valve scanned for mitral regurgitation.

To image the left ventricular out - flow tract, aortic valve and ascending aorta, the beam was rotated clockwise to a slightly more cranially orientation. Likewise as with the mitral valve, bloodflow velocities were also recorded from both sides of the aortic valve by means of PW Doppler. The images were displayed with the apex to the left and the base to the right, as viewed by the operator, following the format recommended for human echocardiography.

Examination of the right heart proved difficult from this view due to the interference from the lungs and only slight glimpses of the tricuspid valve could be made when further dorsal angulation was made. To permit viewing of the right heart the left parasternal position was employed.

The available echo window on the left side varied from the third to seventh intercostal spaces and from one to to five centimetres lateral to the sternum. Two locations between the third and fourth interspaces and fifth to sixth interspaces however gave consistent images in several planes.

As in the right parasternal view, scanning on the left began with a short axis view of the heart between the third and fourth intercostal space. From this view the probe was rotated clockwise through 90°in the transverse plane of the chest and a cross - section of the base of the heart was located. An image of all four chambers was achieved from this plane with the mitral , aortic and tricuspid valves clearly visible. All the intercostal views were displayed with the root of the ascending aorta passing from left to right on the screen, and this resulted in the four chamber view being displayed with the left ventricle to the left and the right ventricle to the right on the monitor.

Doppler examination of the aortic, mitral and tricuspid valves was also carried out in this plane. Imaging of the pulmonary valve was achieved from this plane by rotating the the probe through 90°anti - clockwise until the aortic outflow tract was viewed in the long axis plane. The whole probe was then moved slightly medially and directed approximately 45°ventrally to where imaging of the pulmonary valve and outflow tract was gained and Doppler examination recorded.

True high velocity flow cannot be measured accurately by PW Doppler ultrasound, due to the aliasing of the received signal, therefore continuous wave ultrasound was employed. The main draw back with this form of scanning was that there was no signal converted into a real - time image, and therefore only the image of bloodflow, recorded as a trace of velocity against time was received. To establish in which way the probe should be directed, a pulsed -

wave probe was used, as this gave a real - time view of the heart. The dog was placed in a semi - dorsal position and examined from the subcostal location. The investigating probe was placed on the left of mid - line, next to the xiphoid cartilage, and directed cranially. The mitral and aortic valves were viewed from this plane and recorded with both pulsed - wave and continuous wave Doppler.

The final examination was carried out using the suprasternal imaging plane. The dog was placed in a sitting prone position and 2 MHz CW transducer was placed in the region of the thoracic outlet and directed caudally. Aortic outflow velocities were recorded from this site but pulsed wave imaging could not be achieved due to the narrowness of the thoracic outlet.

CHAPTER 5.

REAL - TIME AND DOPPLER ECHOCARDIOGRAPHY OF THE CANINE HEART.

Right parasternal view.

fig. 5 : 1. Gross anatomical transverse section through dog heart showing right ventricle (RV), interventricular septum (IVS), left ventricle (LV), and papillary muscles.(PM)

fig. 5 : 2. Short axis scan through Greyhound heart illustrating, IVS,LV, PM and left ventricular free wall.(LVFW)

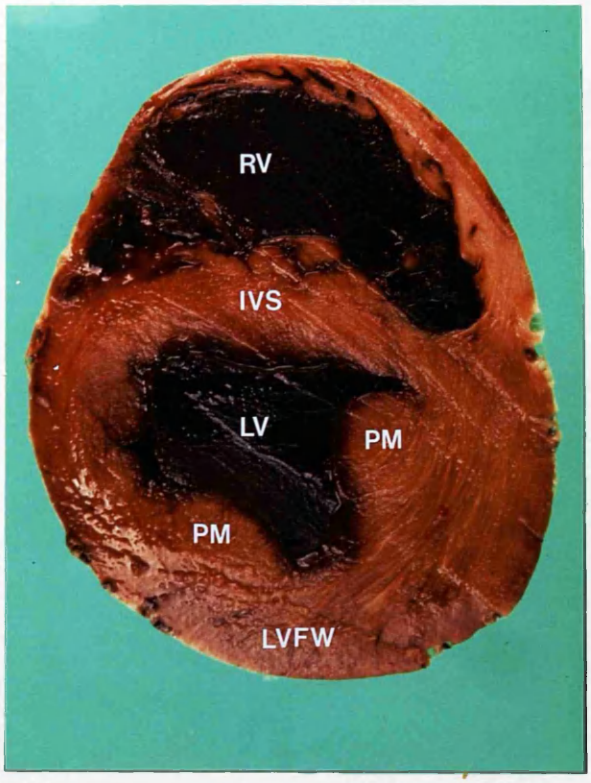
RV
IVS
LV
PM
PM
LVFW

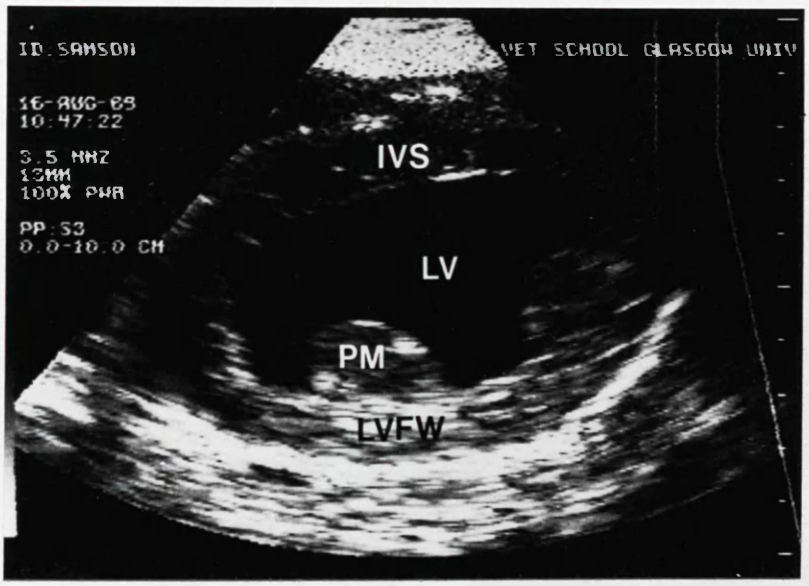
ID SAMSON
VET SCHOOL GLASGOW UNIV
16-AUG-88
10:47:22
3.5 MHZ
12MM
100% PWR
PP:53
0.0-10.0 CM
IVS
LV
PM
LVFW

fig. 5 : 3. Short axis scan through Greyhound heart showing placement of the M - mode cursor.

fig. 5 : 4. Split screen format of both 2D and M- mode imaging, illustrating PM and LV.

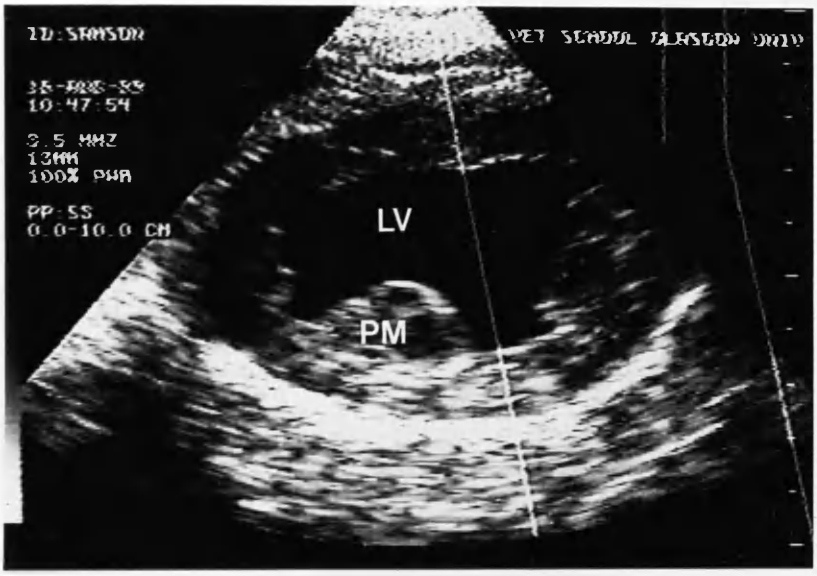
LV
PM

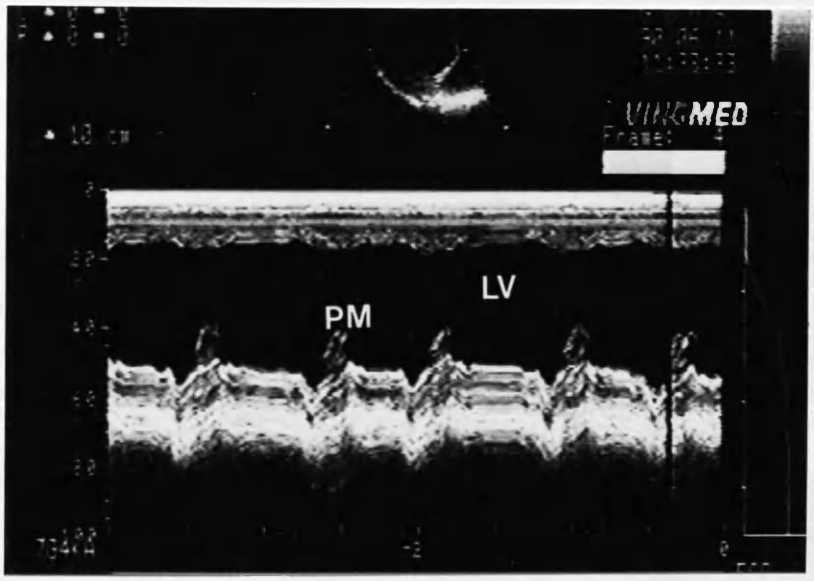
LV
PM

fig. 5 : 5. Short axis scan of Greyhound heart,with the M - mode cursor transecting through the mitral valve.(MV)

fig. 5 : 6. Split screen image showing the MV in 2D and M - mode format.
D = Diastole
E = MV fully opened
A = Atrial systole
C = MV closed


16-AUG-89
10:49:56
3.5 MHZ
13MM
100% PWR
PP:S3
0.0-10.0 CM
MV

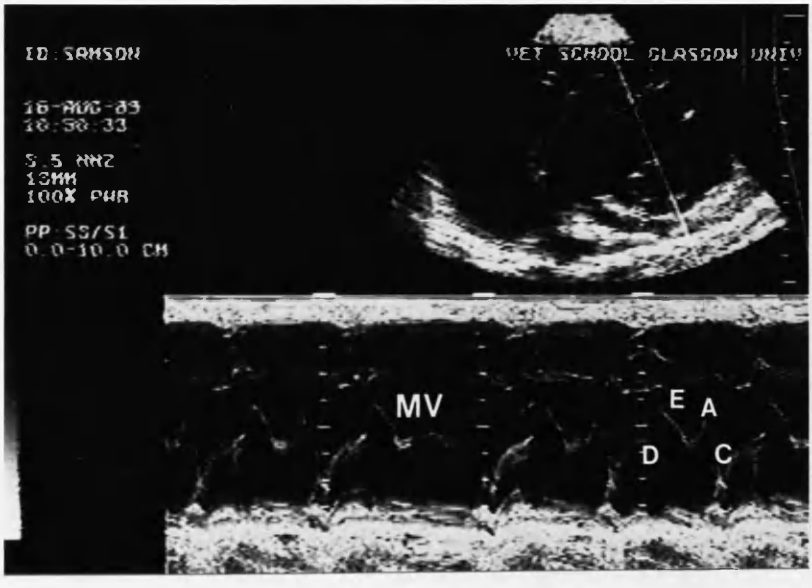
ID:SAMSON
VET SCHOOL GLASGOW UNIV
16-AUG-89
10:50:33
3.5 MHZ
13MM
100% PWR
PP:S3/S1
0.0-10.0 CM
MV
E
A
D
C

fig. 5 : 7. Split screen scan of Beagle heart illustrating the RV, IVS and LV in 2D and M - mode format.

fig. 5 :8. Split screen image illustrating MV in 2D and M - mode format.

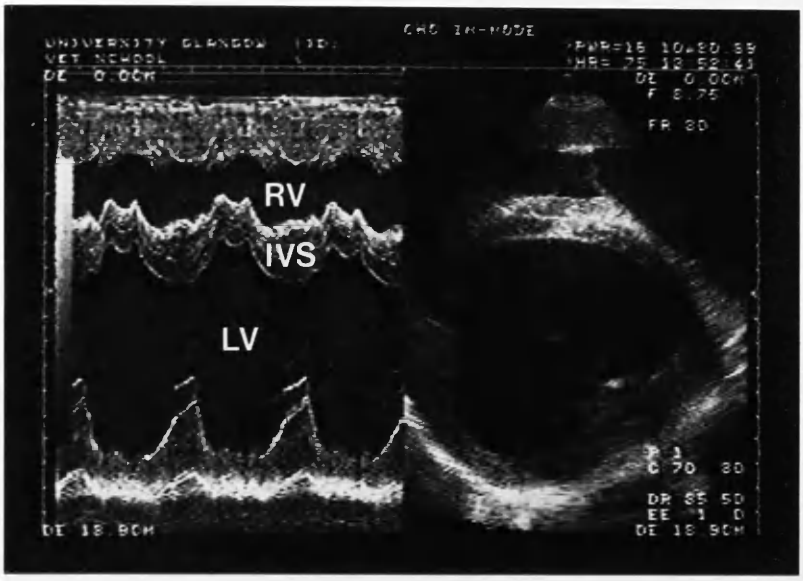
RV
IVS
LV

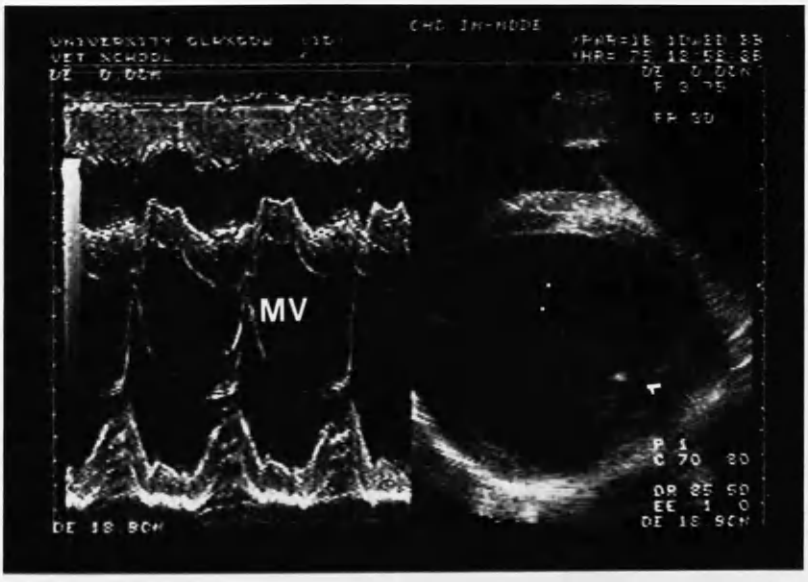
MV

fig. 5 : 9. Short axis scan of Greyhound heart illustrating M - mode cursor placement through AV.
a. = left cusp. b. = septal cusp. c = right cusp.

fig. 5 : 10. Split screen image of Greyhound heart showing AV and AO in both 2D a M - mode format.

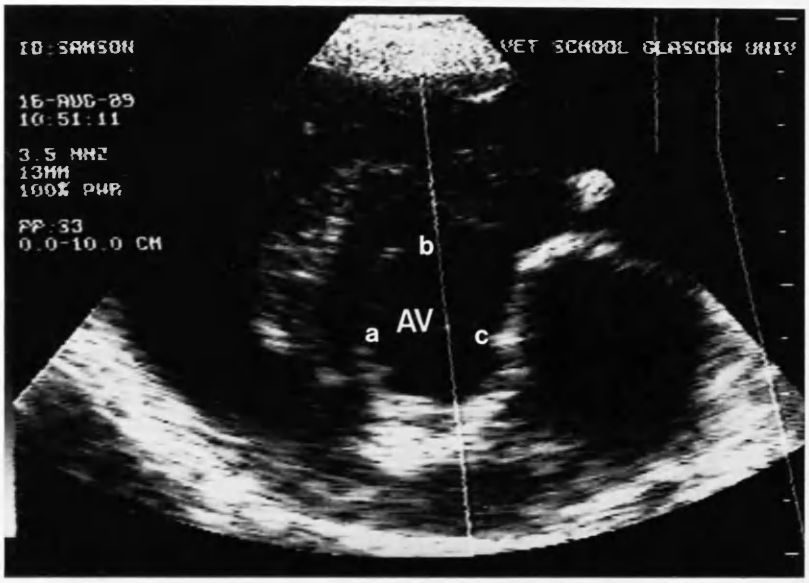
ID:SAMSON
VET SCHOOL GLASGOW UNIV
16-AUG-89
10:51:11
3.5 MHZ
13MM
100% PWR
PP:33
0.0-10.0 CM
b
a
AV
c

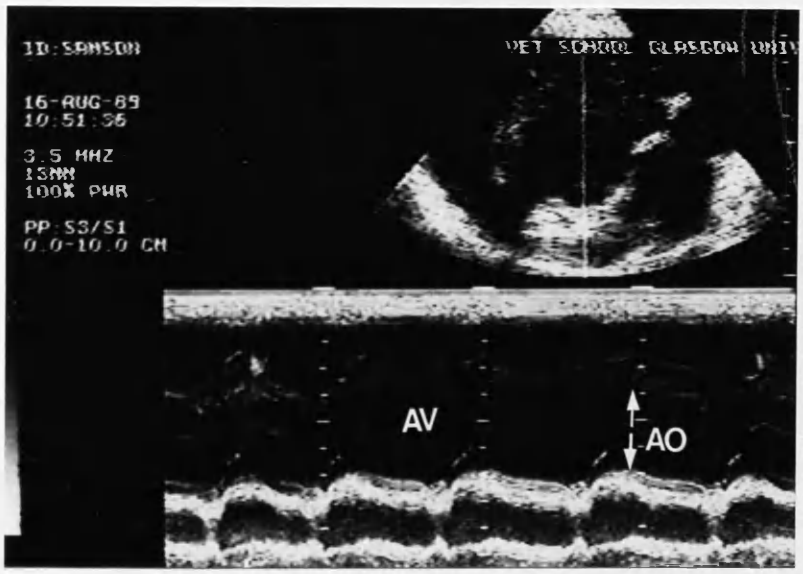
ID:SAMSON
VET SCHOOL GLASGOW UNIV
16-AUG-89
10:51:56
3.5 MHZ
15MM
100% PWR
PP:S3/S1
0.0-10.0 CM
AV
AO

fig. 5 : 11. M - mode scan of Greyhound heart showing IVS, LV and LVFW.

fig. 5 : 12. M - mode of Beagle heart showing diastolic and systolic measurements of LV to establish left ventricular function. (LVF)

fig. 5 : 13. M - mode of Beagle heart showing diastolic and systolic measurements of LV to establish LVF.

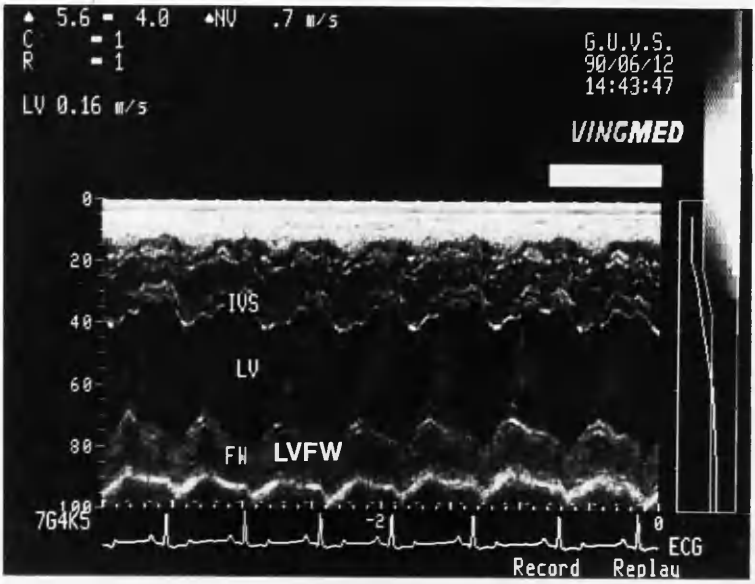
▲ 5.6 ▬ 4.0 ▲NV .7 m/s
C ▬ 1
R ▬ 1
LV 0.16 m/s
G.U.V.S.
90/06/12
14:43:47
VINGMED
0
20
40
60
80
100
IVS
LV
FW
LVFW
7G4K5
-2
0
ECG
Record Replay

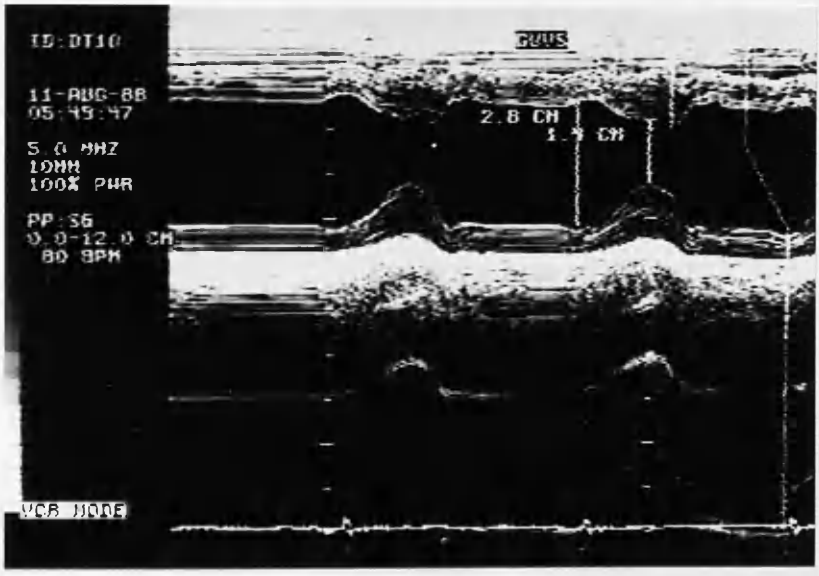
ID:DT10
11-AUG-88
05:45:47
5.0 MHZ
10MM
100% PWR
PP:56
0.0-12.0 CM
80 BPM
GUUS
2.8 CM
1.4 CM
VCR MODE

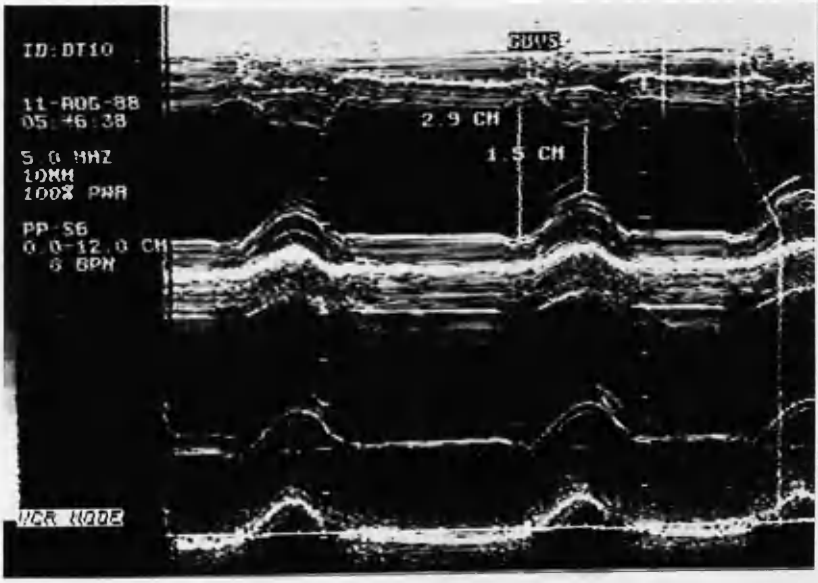
ID:DT10
11-AUG-88
05:46:38
5.0 MHZ
10MM
100% PWR
PP:56
0.0-12.0 CM
6 BPM
GUUS
2.9 CM
1.5 CM
VCR MODE

fig. 5 : 14. Gross, anatomical longitudinal section through dog heart to show RV, LV, AV, PM, LA, MV and IVS.

fig. 5 : 15. Long axis 2D scan of Greyhound heart with measurement of LA in diastole.

fig. 5 : 16. Long axis scan of Greyhound heart with measurement of LA at onset of systole.

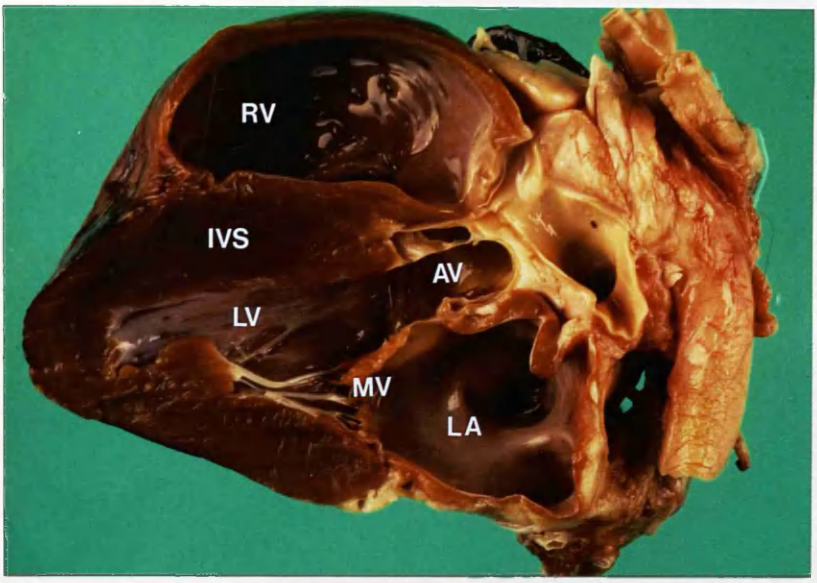
RV
IVS
AV
LV
MV
LA

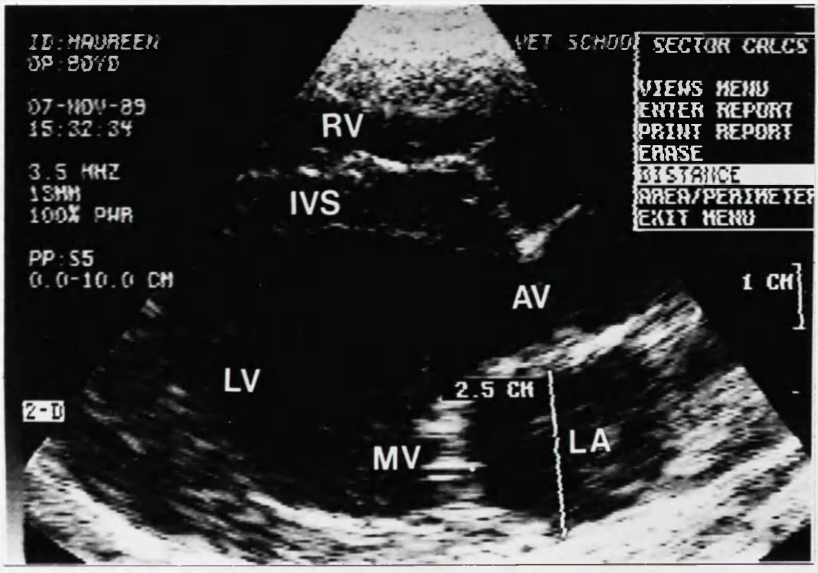
ID:MAUREEN
DR:BOYD
07-NOV-89
15:32:34
3.5 MHZ
13MM
100% PWR
PP:55
0.0-10.0 CM
VET SCHOOL
SECTOR CALCS
VIEWS MENU
ENTER REPORT
PRINT REPORT
ERASE
DISTANCE
AREA/PERIMETER
EXIT MENU
RV
IVS
AV
1 CM
LV
2.5 CM
2-D
MV
LA


ID:MAUREEN
DR:BOYD
07-NOV-89
15:36:39
3.5 MHZ
13MM
100% PWR
PP:55
0.0-10.0 CM
VET SCHOOL
SECTOR CALCS
VIEWS MENU
ENTER REPORT
PRINT REPORT
ERASE
DISTANCE
AREA/PERIMETER
EXIT MENU
1 CM
4.4 CM
2-D
VCR MODE

fig. 5 : 17. Schematic diagram illustrating the cardiac cycle.

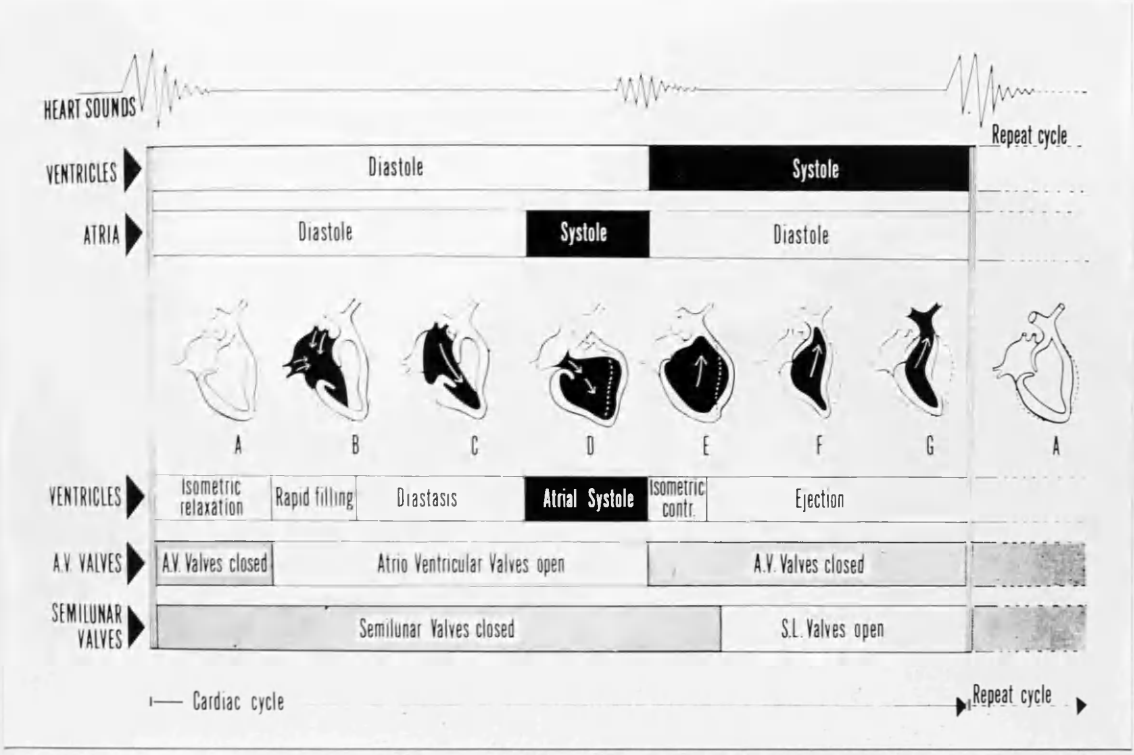
HEART SOUNDS
Repeat cycle
VENTRICLES
Diastole
Systole
ATRIA
Diastole
Systole
Diastole
A
B
C
D
E
F
G
A
VENTRICLES
Isometric relaxation
Rapid filling
Diastasis
Atrial Systole
Isometric contr.
Ejection
A.V. VALVES
A.V. Valves closed
Atrio Ventricular Valves open
A.V. Valves closed
SEMILUNAR VALVES
Semilunar Valves closed
S.L. Valves open
Cardiac cycle
Repeat cycle

fig. 5 : 18. Gross, anatomical, longitudinal section of dog heart showing RV, RA, IVS, AV, AO, LV, MV and left ventricular outflow tract. (LVOT)

fig. 5 : 19. Long axis scan of Greyhound heart, showing pulsed wave Doppler (PW) sample site in LA.

fig.5 : 20. Split screen format showing both 2D and PW images of bloodflow velocity through the MV from the LA site.

E = E peak

A = A peak

* = Valve " click "

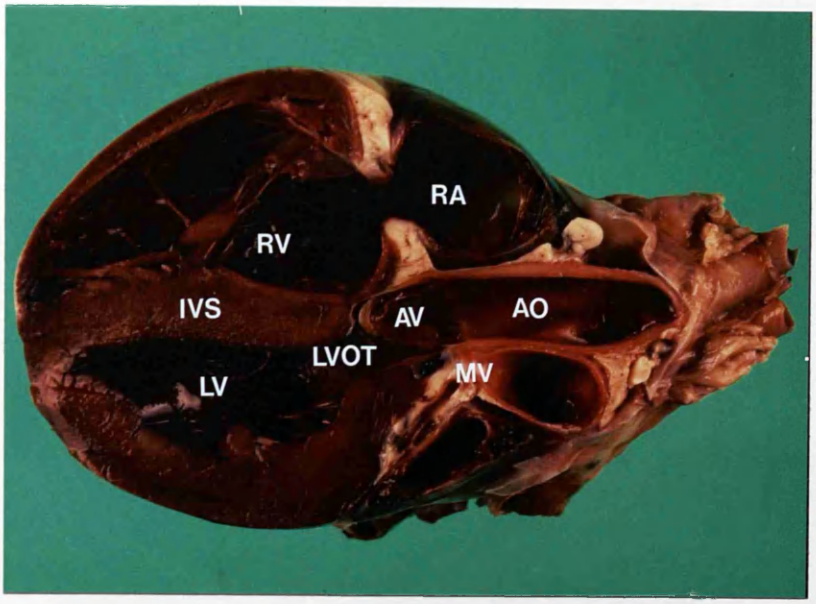
RA
RV
IVS
AV
AO
LVOT
MV
LV

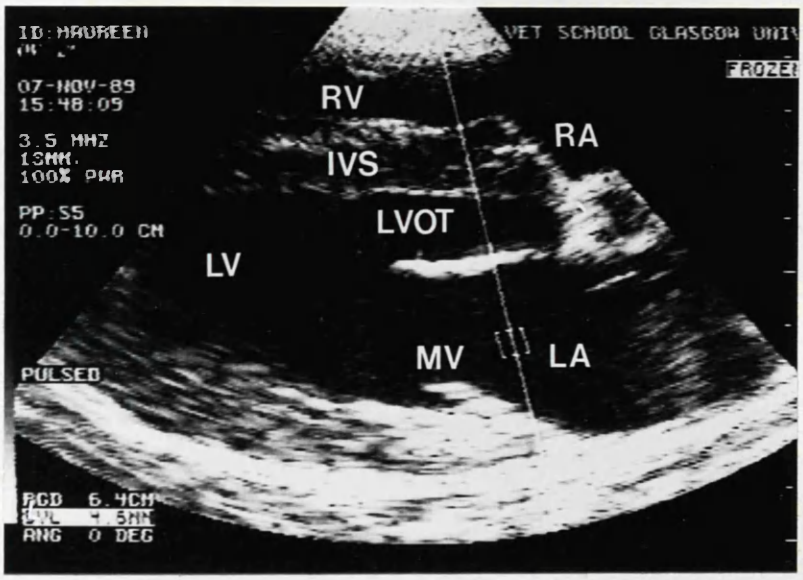
ID:MAUREEN
07-NOV-89
15:48:09
3.5 MHZ
19MM
100% PWR
PP:55
0.0-10.0 CM
VET SCHOOL GLASGOW UNIV
FROZEN
RV
RA
IVS
LVOT
LV
MV
LA
PULSED
RGD 6.4CM
SVL 4.8MM
ANG 0 DEG

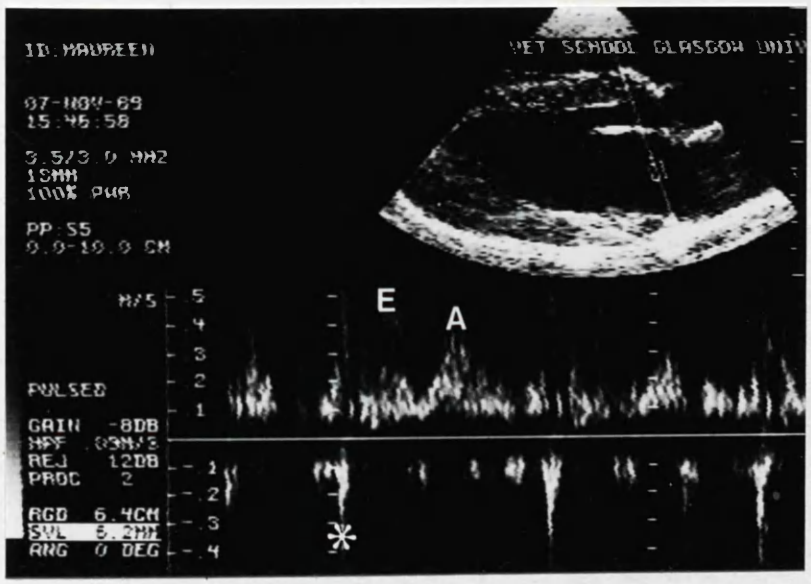
ID:MAUREEN
07-NOV-89
15:46:58
3.5/3.0 MHZ
19MM
100% PWR
PP:55
0.0-10.0 CM
VET SCHOOL GLASGOW UNIV
M/S
5
4
3
2
1
E
A
PULSED
GAIN -8DB
MPF 03M/S
REJ 12DB
PROC 2
RGD 6.4CM
SVL 8.2MM
ANG 0 DEG
1
2
3
4

fig. 5 : 21. Long axis scan of Greyhound heart with PW sample site in the LV side of MV during diastole.

fig.5 : 22. Long axis scan of Greyhound heart with the PW sample site in the LV side of the MV during the onset of systole.

fig. 5 : 23. Split screen format showing bloodflow velocity through the MV from the LV sample site.


ID:MAUREEN
VET SCHOOL GLASGOW UNI
FROZE
07-NOV-89
15:25:10
3.5 MHZ
13MM
100% PWR
PP:55
0.0-10.0 CM
LV
MV
PULSED
RGD 6.4CM
SVL 6.2MM
ANG 0 DEG


ID:MAUREEN
VET SCHOOL GLASGOW UNIV
07-NOV-89
15:34:47
3.5 MHZ
13MM
100% PWR
PP:55
0.0-10.0 CM
MV
LV
PULSED
RGD 6.3CM
SVL 6.2MM
ANG 0 DEG

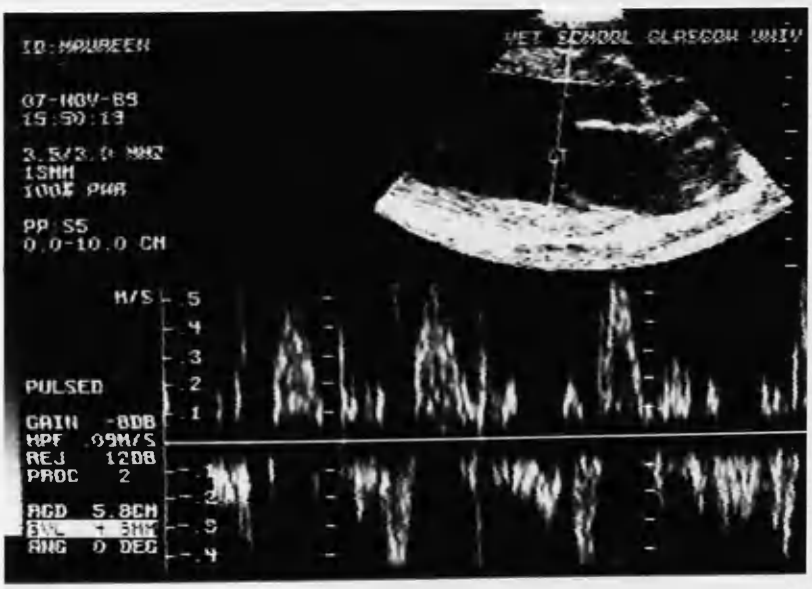
ID:MAUREEN
VET SCHOOL GLASGOW UNIV
07-NOV-89
15:50:19
3.5/3.0 MHZ
13MM
100% PWR
PP:55
0.0-10.0 CM
M/S
5
4
3
2
1
PULSED
GAIN -8DB
WPF .09M/S
REJ 12DB
PROC 2
RGD 5.8CM
SVL 6.3MM
ANG 0 DEG

fig. 5 : 24. Long axis view of AV in Greyhound heart showing LVOT, RV, AO and positioning of PW sample site.

fig. 5 : 25 Split screen scan of both 2D and M - mode format illustrating aortic bloodflow velocity from the LV sampling site.

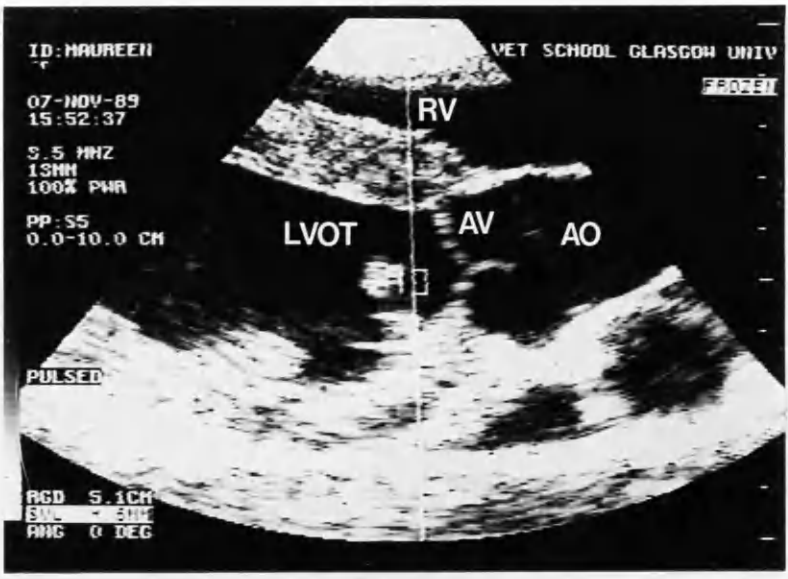
ID:MAUREEN
VET SCHOOL GLASGOW UNIV
FROZEN
07-NOV-89
15:52:37
5.5 MHZ
13MM
100% PWR
PP:55
0.0-10.0 CM
RV
LVOT
AV
AO
PULSED
RGD 5.1CM
SVL 6.8MM
ANG 0 DEG


ID:SAMSON
VET SCHOOL GLASGOW UNIV
16-AUG-89
11:09:04
3.5/3.0 MHZ
13MM
100% PWR
PP:53
0.0-10.0 CM
M/S
.5
PULSED
GAIN 0DB
HPF .16M/S
PROC 1
-.5
-1
RGD 5.2CM
SVL 6.2MM
ANG 0 DEG

fig. 5 : 26. AV valve with the PW sample volume in the Aortic root.

fig. 5 : 27. Split screen format of bloodflow velocity through the AV from the Aortic root sampling site.


ID:MAUREEN
OP:BOYD
07-NOV-89
15:53:49
3.5 MHZ
1SMH
100% PWR
PP:55
0.0-10.0 CM
VET SCHOOL GLASGOW UNIV
LVOT
AV
AO
PULSED
RGD 5.1CM
ANG 0 DEG

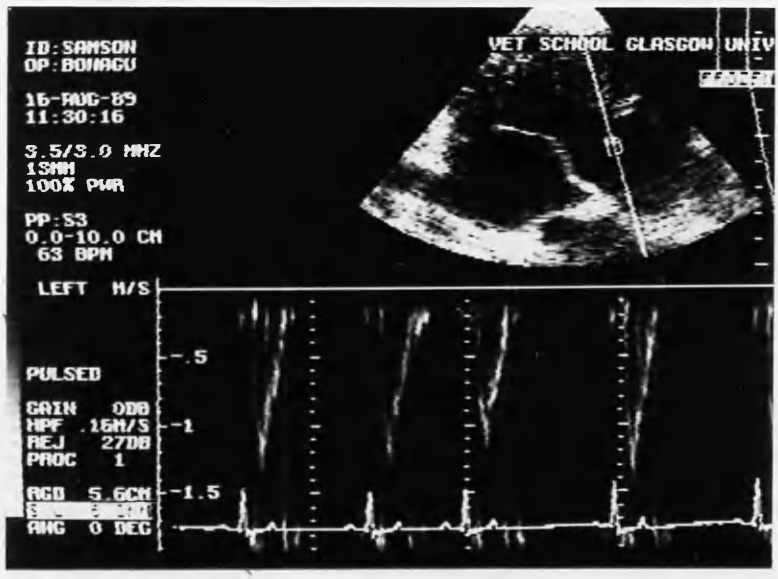
ID:SAMSON
OP:BONAGU
16-AUG-89
11:30:16
3.5/3.0 MHZ
1SMH
100% PWR
PP:53
0.0-10.0 CM
63 BPM
VET SCHOOL GLASGOW UNIV
LEFT M/S
-.5
-1
-1.5
PULSED
GAIN 0DB
HPF .16M/S
REJ 27DB
PROC 1
RGD 5.6CM
ANG 0 DEG

fig. 5 : 28. Gross anatomical longitudinal section of dog heart showing ; tricuspid valve (TV), LV, AV, RA and IVS.

fig. 5 : 29. Long axis view of Greyhound heart showing position of PW sample site in RA.

fig. 5 : 30. Split screen format of 2D and PW mode in Beagle heart.showing bloodflow velocity through the TV.

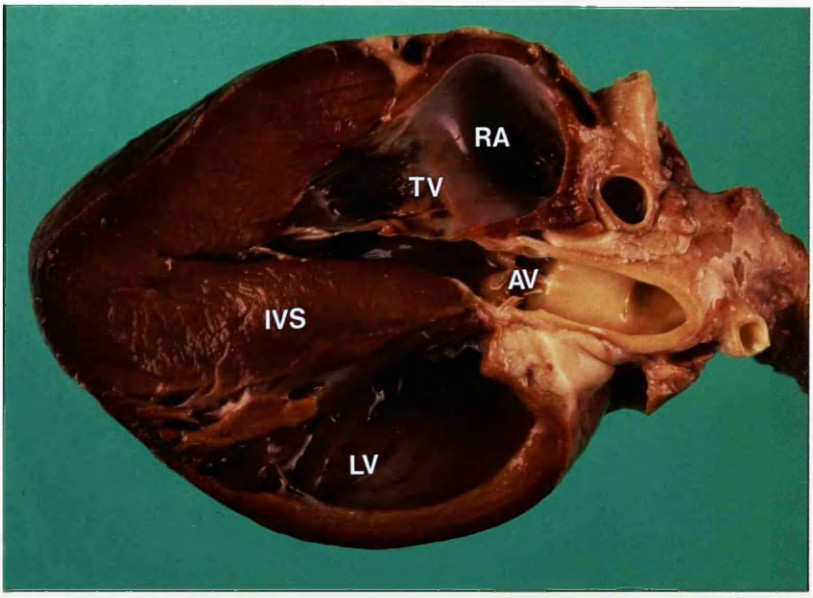
RA
TV
AV
IVS
LV

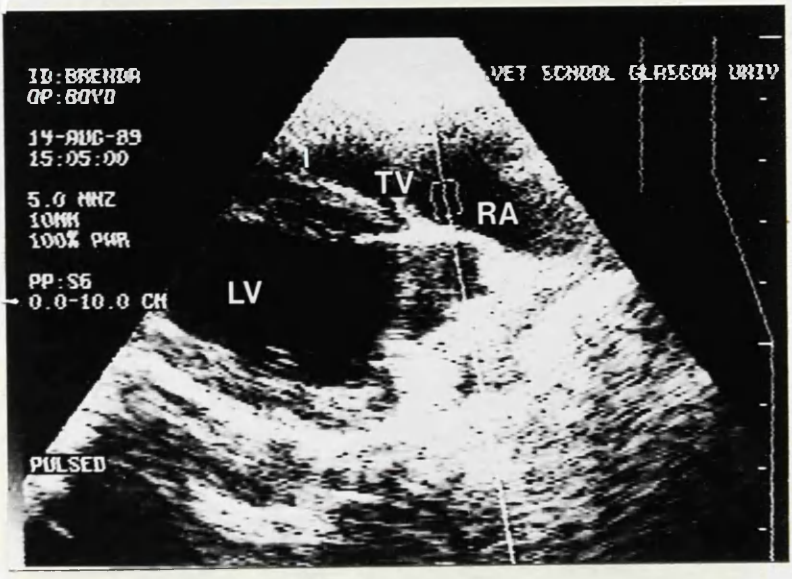
ID:BRENDA
OP:BOYD
14-AUG-89
15:05:00
5.0 MHZ
10MM
100% PWR
PP:S6
0.0-10.0 CM
VET SCHOOL GLASGOW UNIV
TV
RA
LV
PULSED

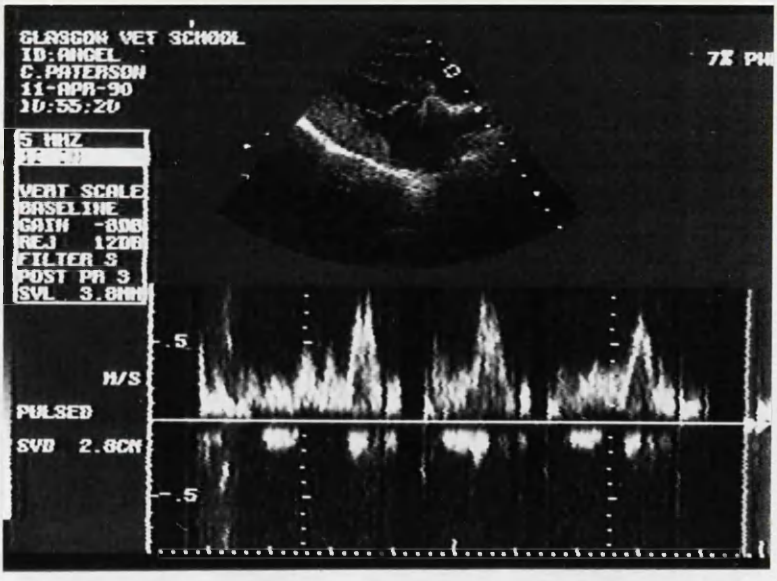
GLASGOW VET SCHOOL
ID:ANGEL
C.PATERSON
11-APR-90
10:55:20
5 MHZ
VERT SCALE
BASELINE
GAIN -8DB
REJ 12DB
FILTER 3
POST PR 3
SVL 3.8MM
.5
M/S
PULSED
SVD 2.8CM
-.5

fig. 5 : 31. Gross, anatomical, longitudinal section of dog heart to show LA, LV, LVOT,IVS,RV,AO,MV, PM and chordae tendineae. (CT)

fig. 5 : 32. Long axis scan of Greyhound heart showing LV, AO,LVOT AV, RV and LA

fig. 5 : 33. Long axis scan of Greyhound heart showing Doppler Colour Flow Mapping.through the MV and AV.

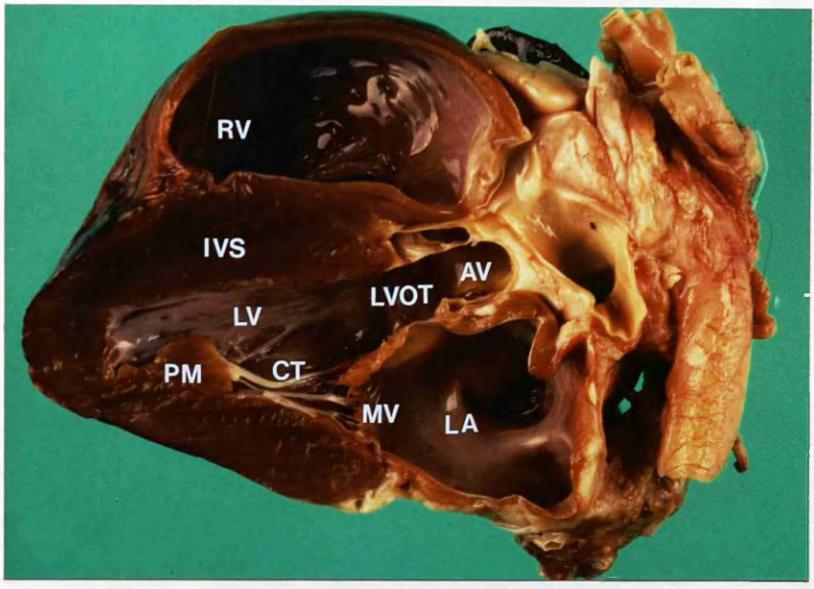
RV
IVS
AV
LVOT
LV
PM
CT
MV
LA

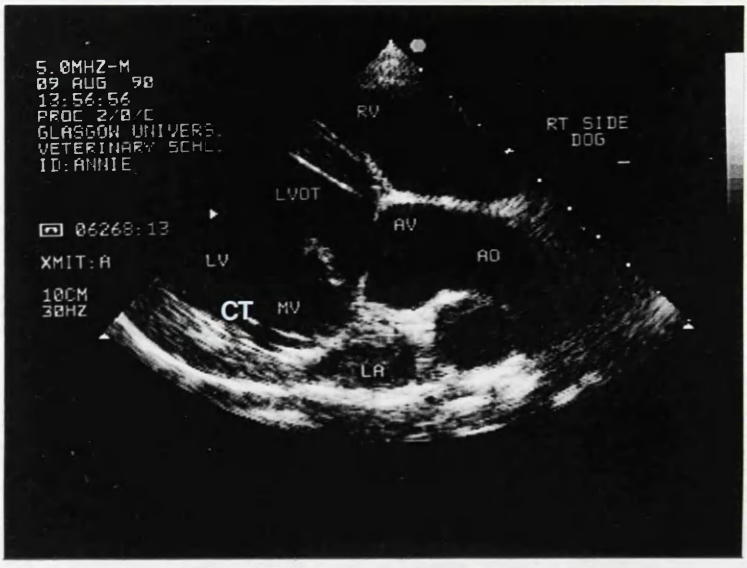
5.0MHZ-M
09 AUG 90
13:56:56
PROC 2/0/C
GLASGOW UNIVERS.
VETERINARY SCHL.
ID:ANNIE
06268:13
XMIT:A
10CM
30HZ
RV
RT SIDE
DOG
LVOT
AV
LV
AO
CT
MV
LA

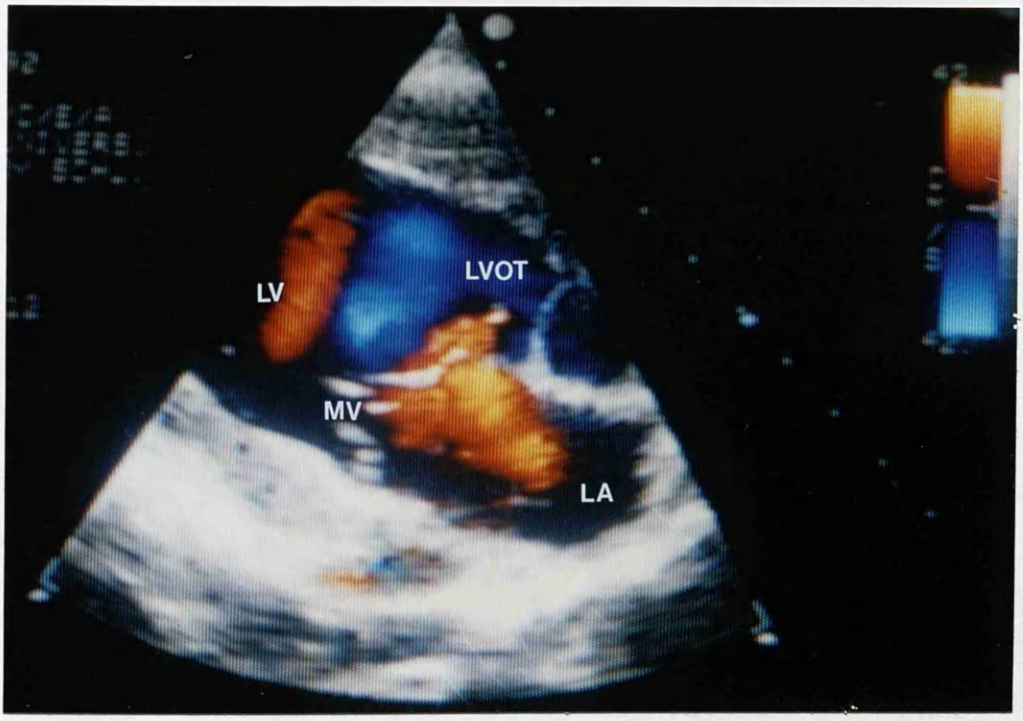
LV
LVOT
MV
LA

fig. 5 : 34a. Black and white print of colour low mapping during long axis scan of Beagle heart showing MV during systole.

fig. 5 : 34b. Long axis scan of Beagle heart showing bloodflow velocity through MV during systole by means of colour flow mapping as described in previous figure,

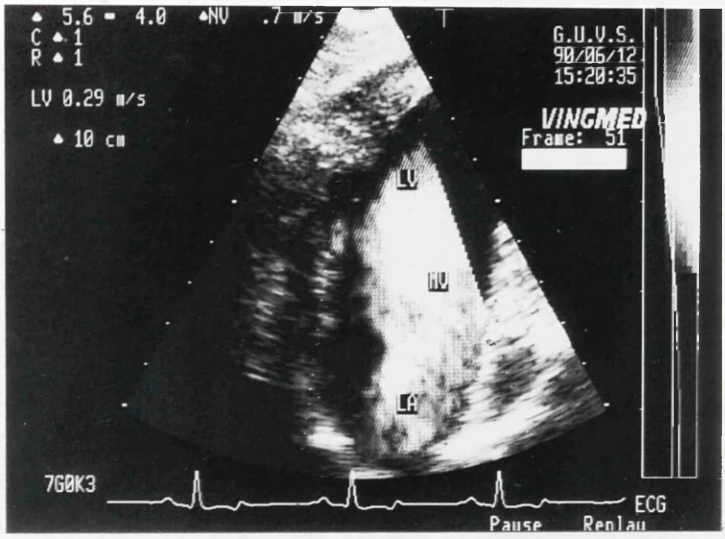
5.6 = 4.0 NV .7 m/s
C 1
R 1
LV 0.29 m/s
10 cm
G.U.V.S.
90/06/12
15:20:35
VINGMED
Frame: 51
LV
MV
LA
7G0K3
ECG
Pause
Replay

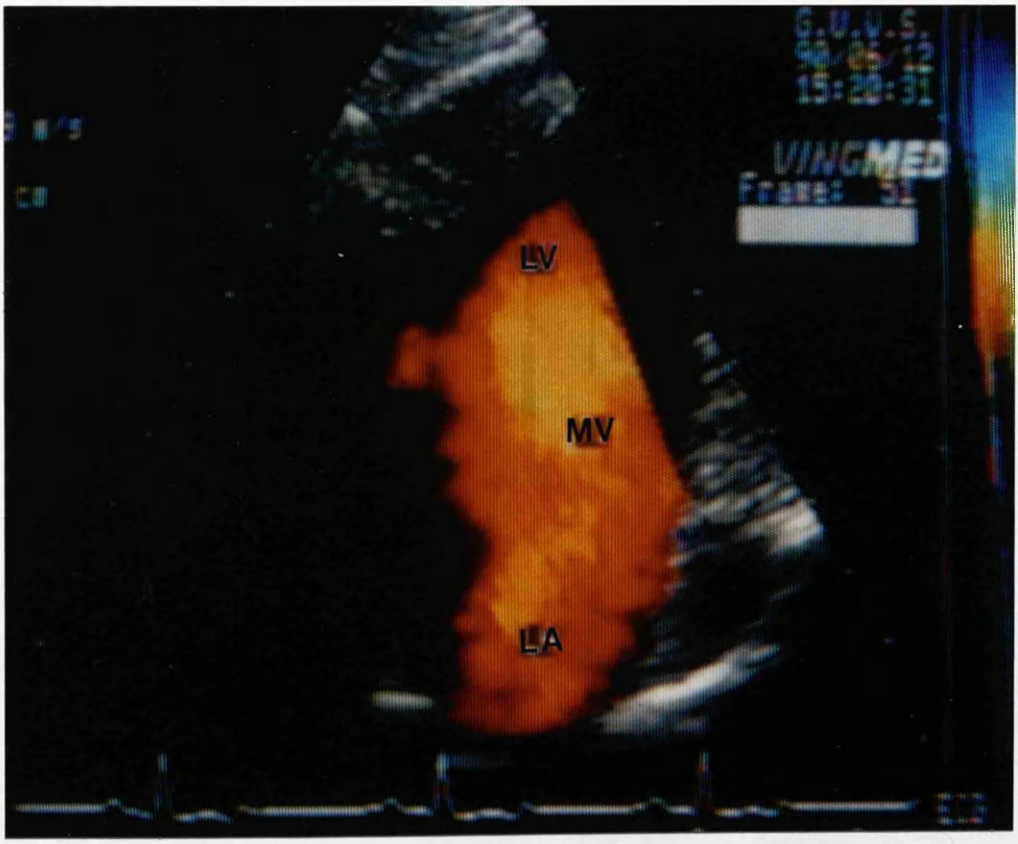
VINGMED
LV
MV
LA

fig. 5 : 35a. Long axis scan of Beagle heart illustrating the MV, LV and LA.

fig. 5 : 35b. Long axis view of Beagle heart showing bloodflow velocity through the MV by means of Colour flow mapping.

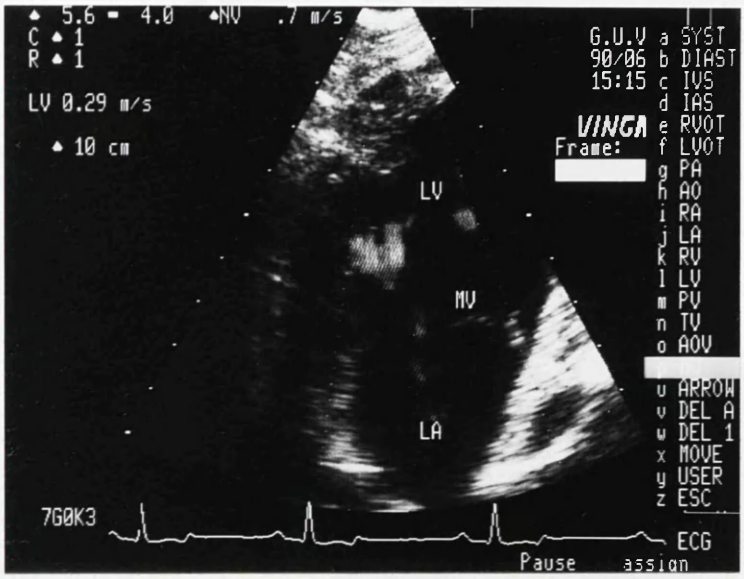
5.6 = 4.0 NV .7 m/s
C 1
R 1
LV 0.29 m/s
10 cm
G.U.V
90/06
15:15
VINGM
Frame:
a SYST
b DIAST
c IVS
d IAS
e RVOT
f LVOT
g PA
h AO
i RA
j LA
k RV
l LV
m PV
n TV
o AOV
u ARROW
v DEL A
w DEL 1
x MOVE
y USER
z ESC
LV
MV
LA
7G0K3
ECG
Pause
assign

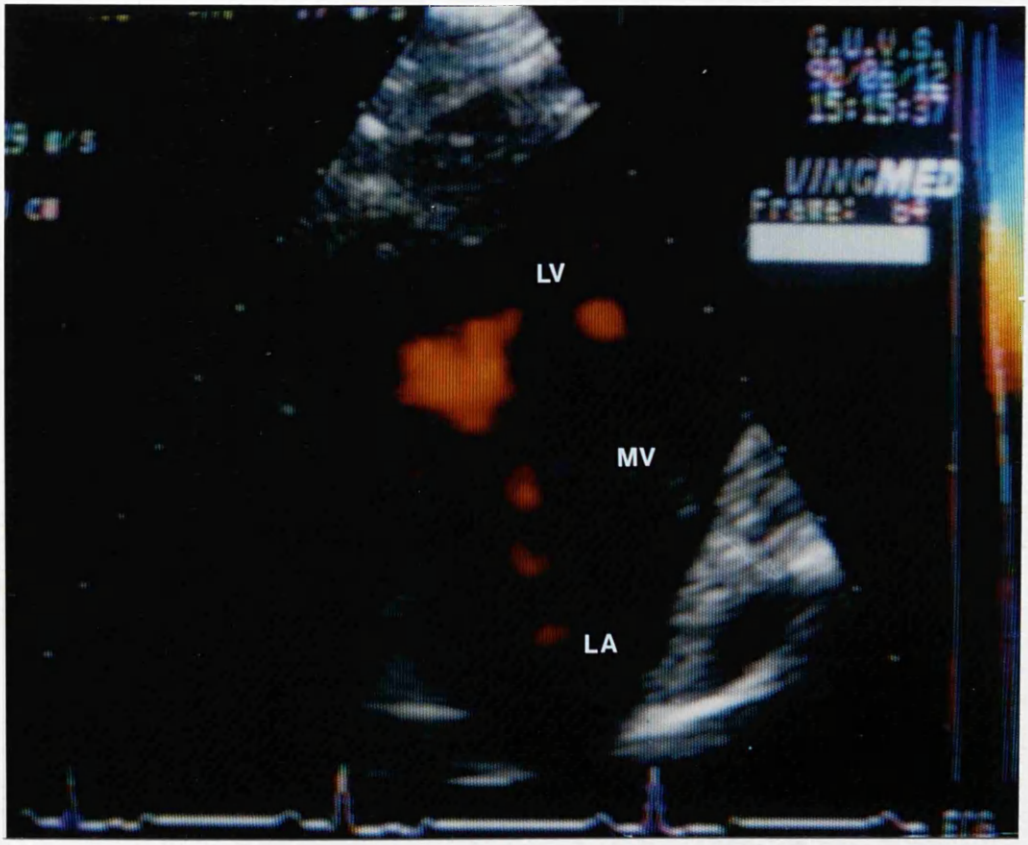
VINGMED
Frame:
LV
MV
LA

fig. 5 : 36. Long axis scan through Beagle heart illustrating RV, LVOT, LV, AO,AV and LA.

fig.5 : 37. Bloodflow velocity through MV illustrated by means of colour flow mapping

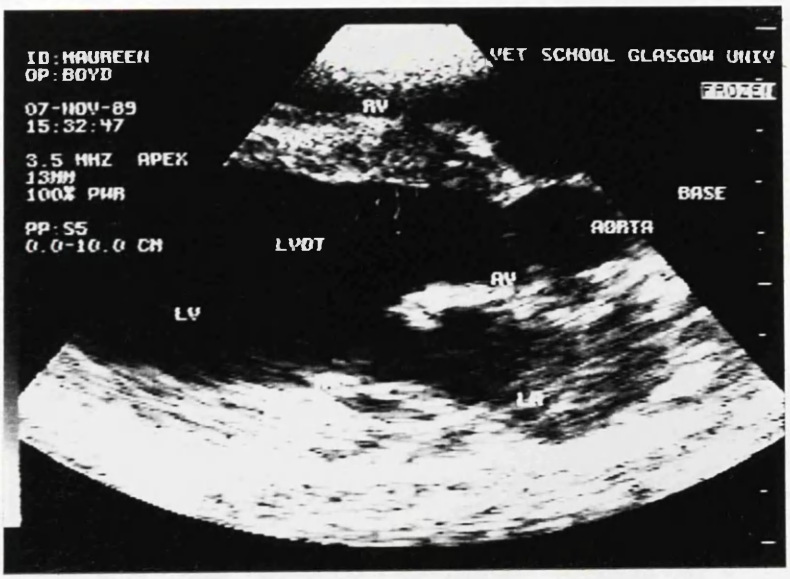
ID:MAUREEN
OP:BOYD
07-NOV-89
15:32:47
3.5 MHZ APEX
13MM
100% PWR
PP:55
0.0-10.0 CM
VET SCHOOL GLASGOW UNIV
FROZEN
RV
BASE
AORTA
LVOT
AV
LV
LA

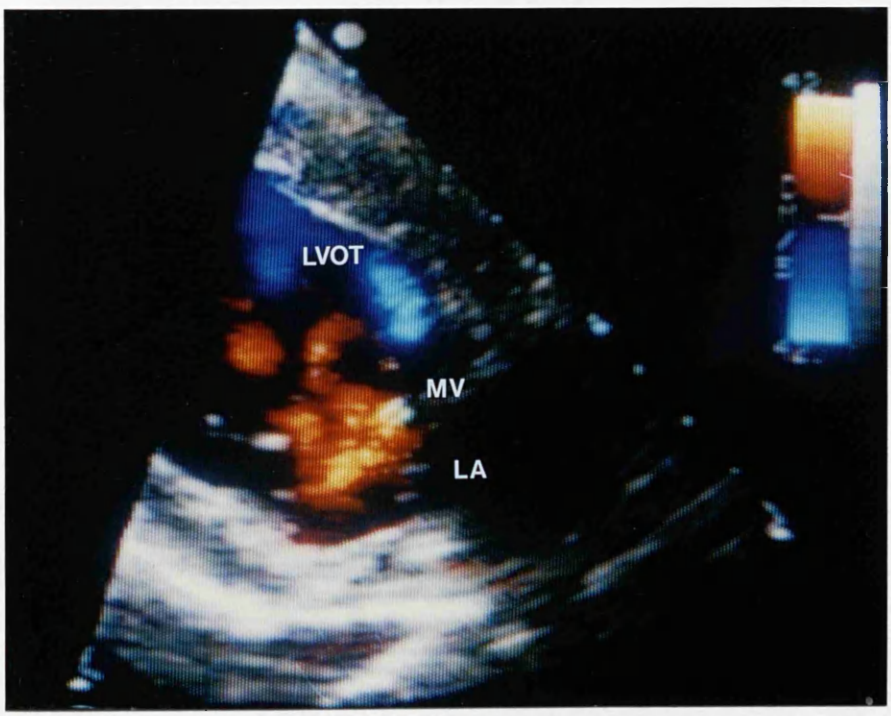
LVOT
MV
LA

Left parasternal view.

fig. 5 : 38. Gross anatomical longitudinal section through dog heart depicting the left parasternal view.

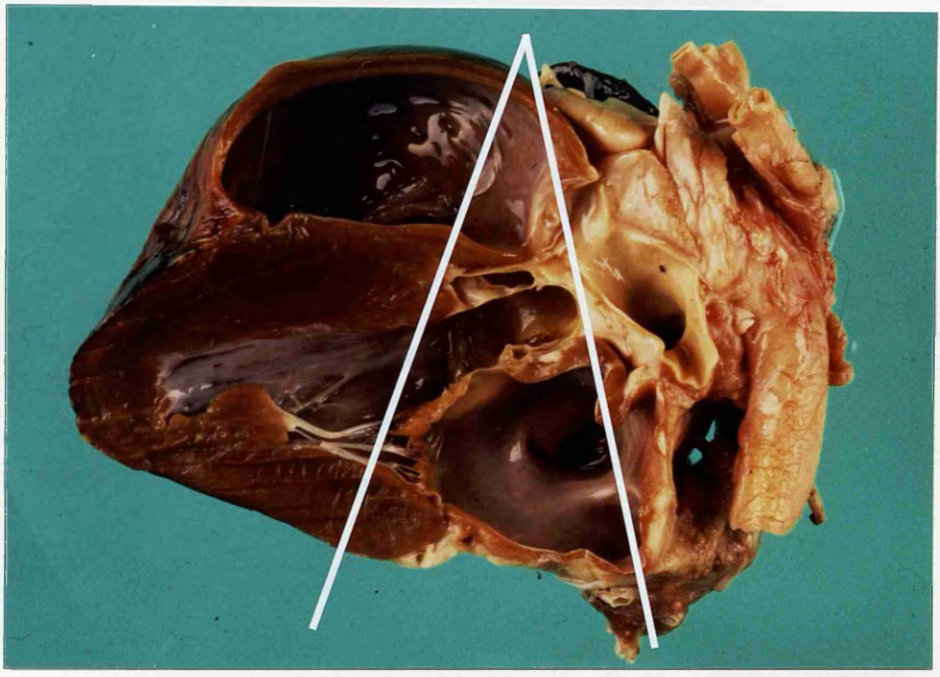

fig. 5 : 39. Long axis view of Greyhound heart showing MV, AV, LV,LA, AO and PM, with the PW sample volume positioned in the LV during diastole.

fig. 5 : 40. Split screen format of 2D and PW showing bloodflow velocity through the MV when sampled from the LV.

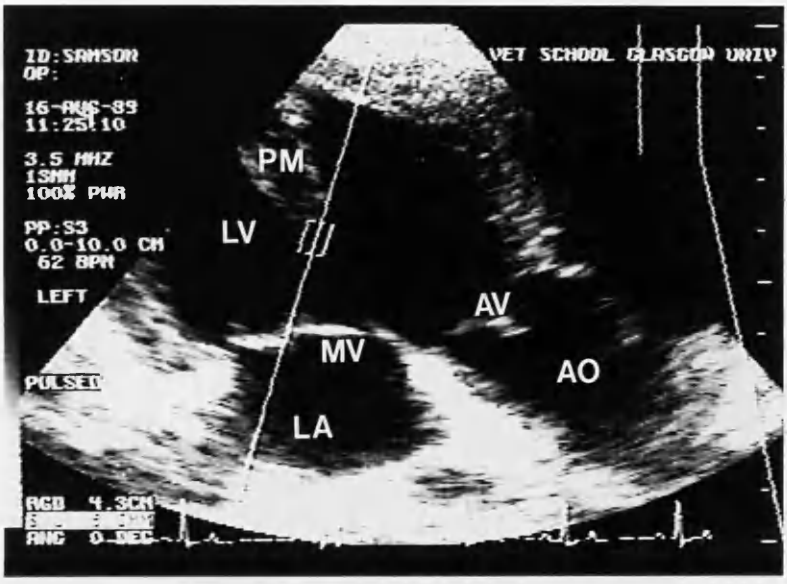
ID:SAMSON
OP:
16-AUG-89
11:25:10
3.5 MHZ
1SNH
100% PWR
PP:S3
0.0-10.0 CM
62 BPM
LEFT
PULSED
RGD 4.3CM
ANG 0 DEG
VET SCHOOL GLASGOW UNIV
PM
LV
AV
MV
AO
LA

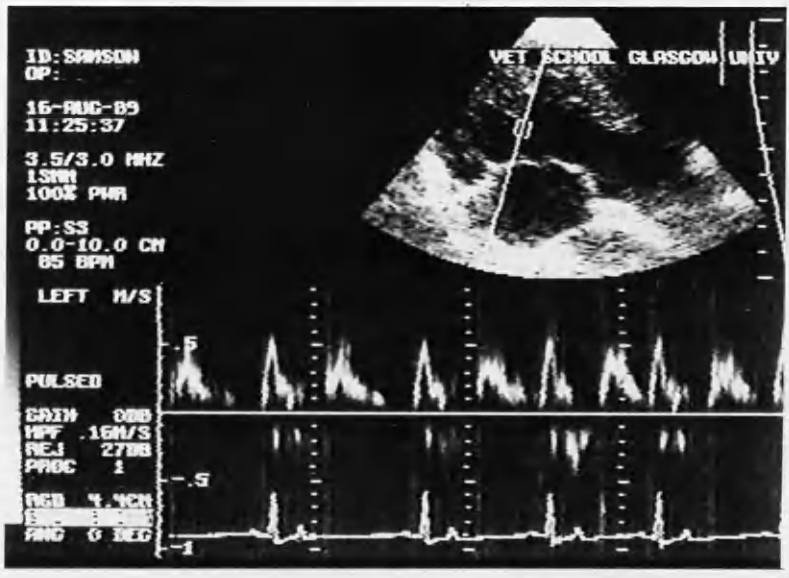
ID:SAMSON
OP:
16-AUG-89
11:25:37
3.5/3.0 MHZ
1SNH
100% PWR
PP:S3
0.0-10.0 CM
85 BPM
LEFT M/S
PULSED
GAIN 0DB
HPF .16M/S
REJ 27DB
PROC 1
RGD 4.4CM
ANG 0 DEG
VET SCHOOL GLASGOW UNIV
.5
-.5
-1

fig. 5 : 41. Long axis view of Greyhound heart with PW sample site in the LV location during systole.

fig. 5 : 42. Split screen format of bloodflow velocity through the MV when sampled in the LV location during systole.

fig. 5 : 43. Split screen format of bloodflow velocity through MV when PW sample volume is located in the LA location during systole

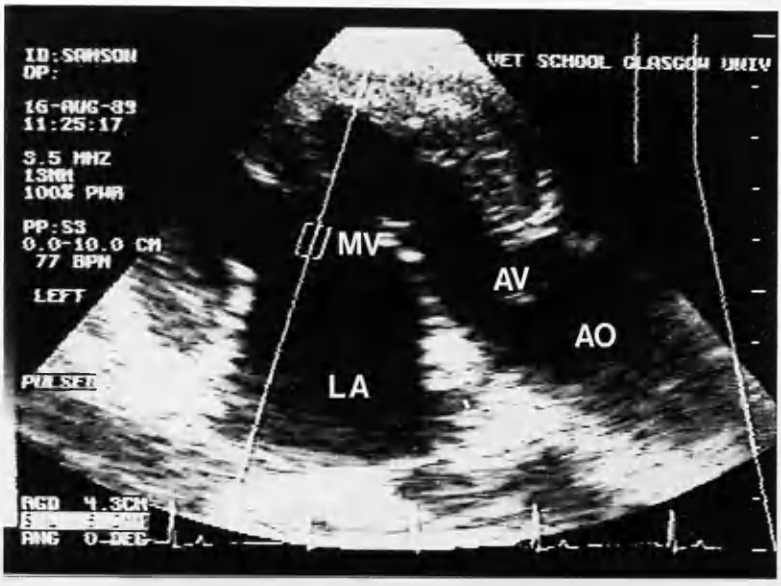
ID:SAMSON
OP:
16-AUG-89
11:25:17
3.5 MHZ
13MM
100% PWR
PP:S3
0.0-10.0 CM
77 BPM
LEFT
PULSED
RGD 4.3CM
ANG 0 DEG
VET SCHOOL GLASGOW UNIV
MV
AV
AO
LA

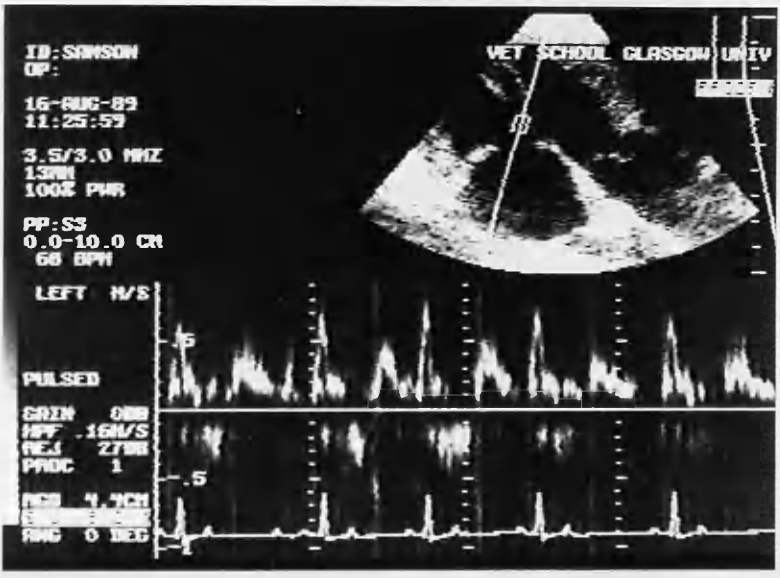
ID:SAMSON
OP:
16-AUG-89
11:25:59
3.5/3.0 MHZ
13MM
100% PWR
PP:S3
0.0-10.0 CM
68 BPM
LEFT M/S
PULSED
GAIN 0DB
HPF .16M/S
REJ 27DB
PROC 1
RGD 4.4CM
ANG 0 DEG
VET SCHOOL GLASGOW UNIV
.5
-.5
-1

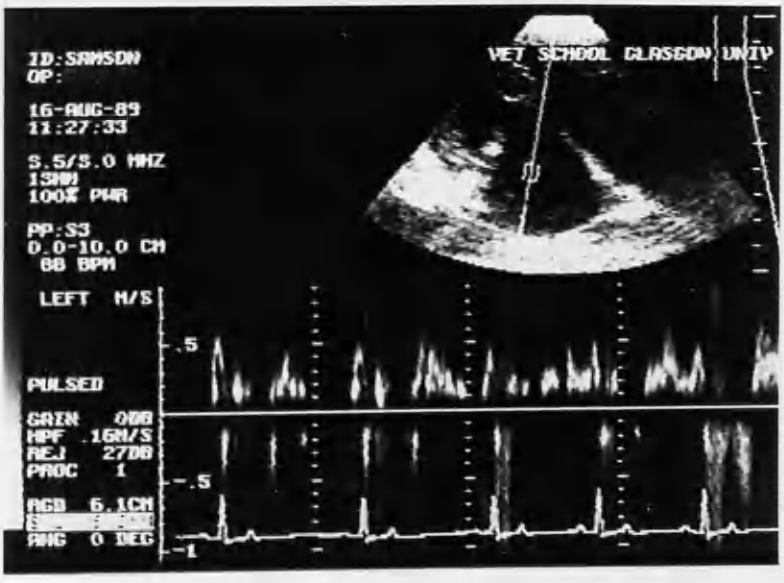
ID:SAMSON
OP:
16-AUG-89
11:27:33
3.5/3.0 MHZ
13MM
100% PWR
PP:S3
0.0-10.0 CM
68 BPM
LEFT M/S
PULSED
GAIN 0DB
HPF .16M/S
REJ 27DB
PROC 1
RGD 6.1CM
ANG 0 DEG
VET SCHOOL GLASGOW UNIV
.5
-.5
-1

fig. 5 : 44a. Split screen format of PW bloodflow velocity through MV.

fig. 5 : 44b. PW trace of bloodflow velocity through MV showing measurement of Pressure half - time and also the E peak (initial filling phase corresponding to the initial opening of the MV) and A peak. (period of flow ending with LA contraction)

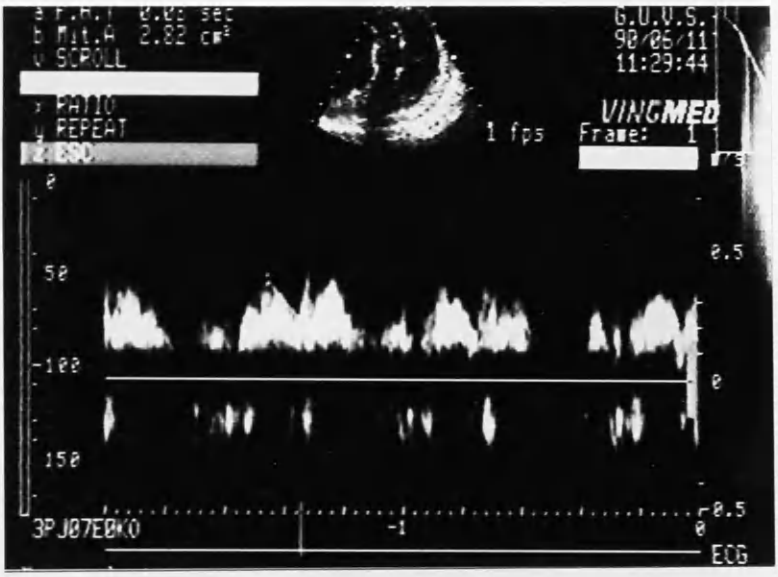
b Mit.A 2.82 cm²
v SCROLL
x RATIO
y REPEAT
G.U.V.S.
90/05/11
11:29:44
VINGMED
1 fps
Frame: 1
0
50
100
150
0.5
0
-0.5
-1
ECG

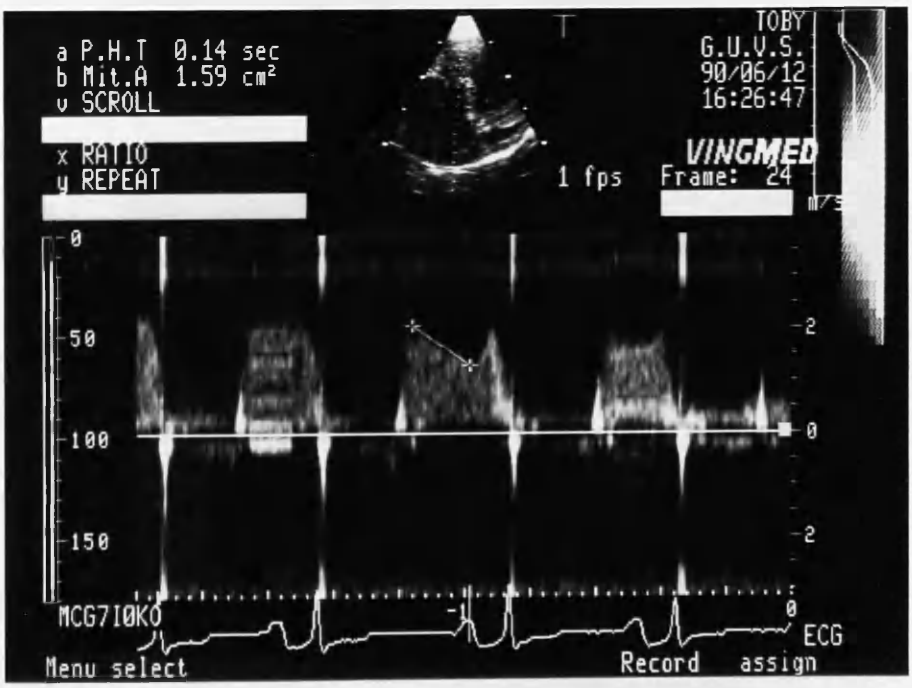
a P.H.T 0.14 sec
b Mit.A 1.59 cm²
v SCROLL
x RATIO
y REPEAT
TOBY
G.U.V.S.
90/06/12
16:26:47
VINGMED
1 fps
Frame: 24
0
50
100
150
2
0
-2
-1
ECG
Menu select
Record assign

fig. 5 : 45. Long axis view of Greyhound heart showing LVOT, AV and AO.

fig. 5 : 46. Long axis view showing PW sample volume in the LV location.

fig. 5 : 47. Split screen format showing PW bloodflow velocity through AV.

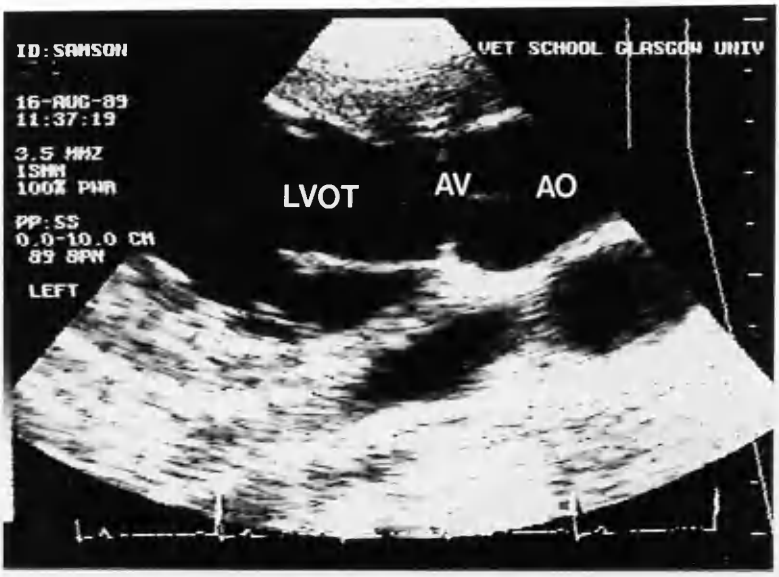
ID:SAMSON
VET SCHOOL GLASGOW UNIV
16-AUG-89
11:37:19
3.5 MHZ
15MM
100% PWR
PP:55
0.0-10.0 CM
89 BPM
LEFT
LVOT
AV
AO

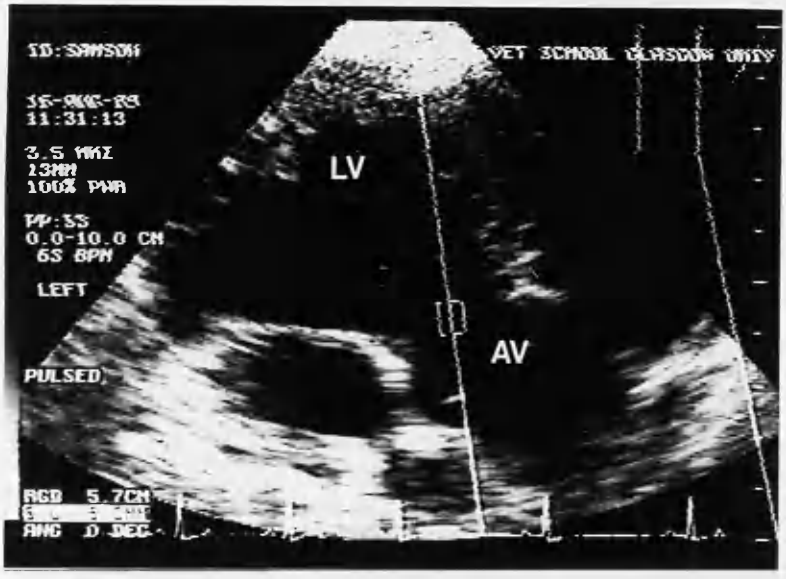
ID:SAMSON
VET SCHOOL GLASGOW UNIV
3.5 MHZ
13MM
100% PWR
PP:55
0.0-10.0 CM
65 BPM
LEFT
PULSED
LV
AV
RGD 5.7CM
ANG 0 DEG

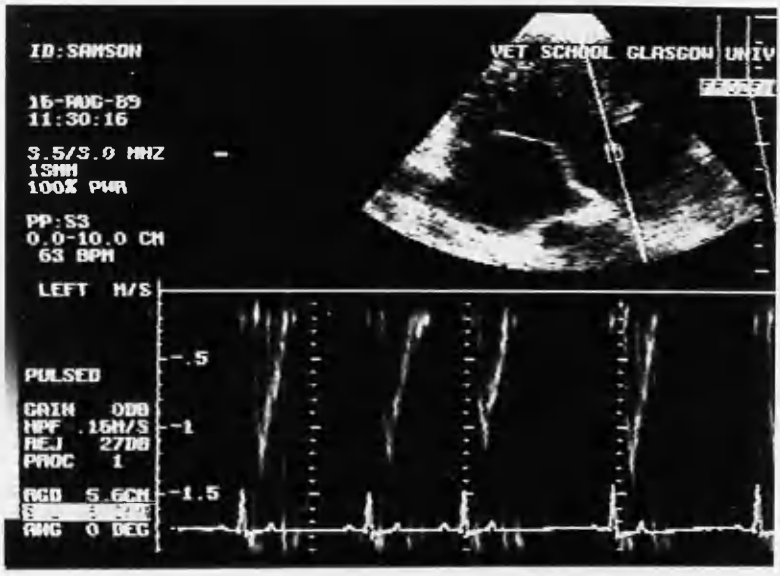
ID:SAMSON
VET SCHOOL GLASGOW UNIV
16-AUG-89
11:30:16
3.5/3.0 MHZ
13MM
100% PWR
PP:53
0.0-10.0 CM
63 BPM
LEFT M/S
PULSED
GAIN 0DB
HPF .15M/S
REJ 27DB
PROC 1
RGD 5.6CM
ANG 0 DEG
-.5
-1
-1.5

fig. 5 : 48. Sequential long axis scans through Greyhound heart illustrating the movement of the MV and AV during diastole and systole.

a) Diastole; both MV and AV closed.

b, c,d.) MV allows blood to pass from LA into LV.

e) Systole; MV closed, LV contracts and pushes blood through the now open AV.

a

b

c

d

e

fig. 5 : 49. Long axis scan of Greyhound heart showing MV, LV, AV and LA.

fig. 5 : 50. Long axis scan through MV illustrating bloodflow velocity with colour flow mapping

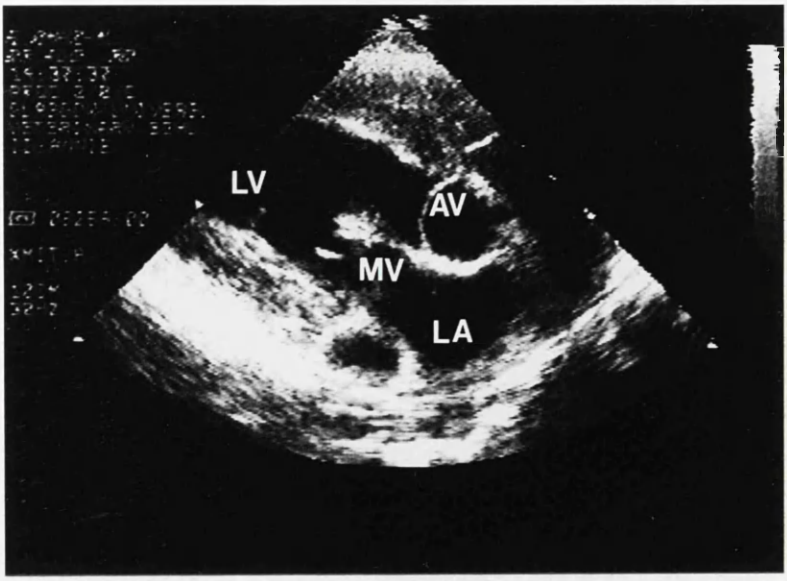
LV
AV
MV
LA

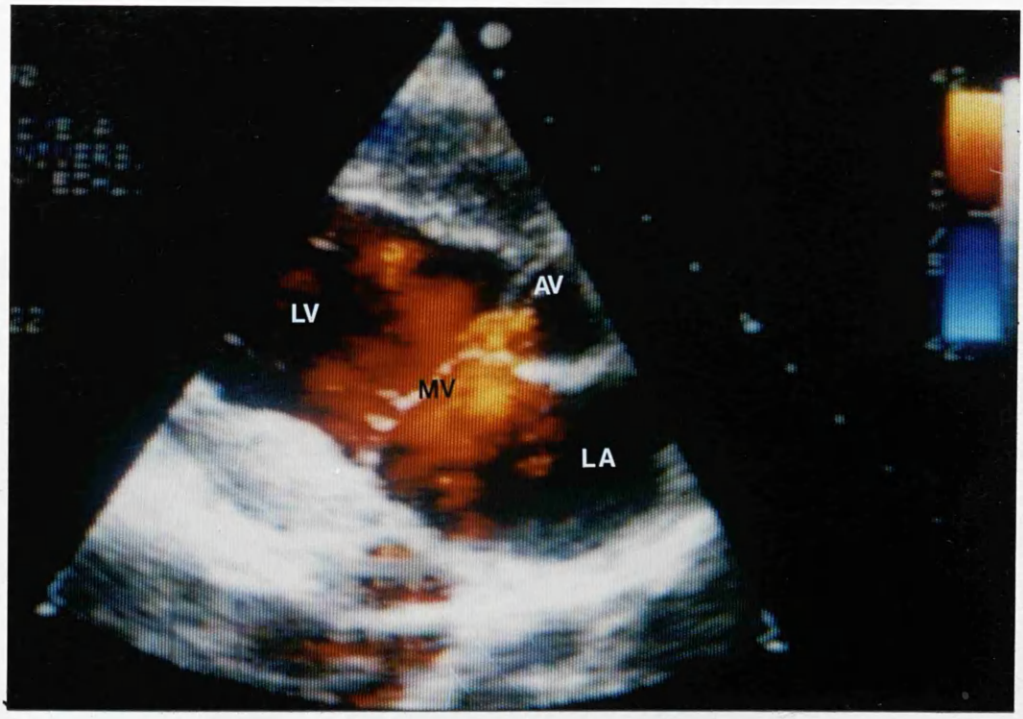
AV
LV
MV
LA

fig.5 : 51. Long axis scan of Greyhound heart showing MV, AV LV.and LA.

fig. 5 : 52. Long axis scan showing bloodflow velocity through the MV with Colour flow mapping. The red spectrum indicates bloodflow towards the transducer, whereas the blue spectrum indicates bloodflow away from the transducer.

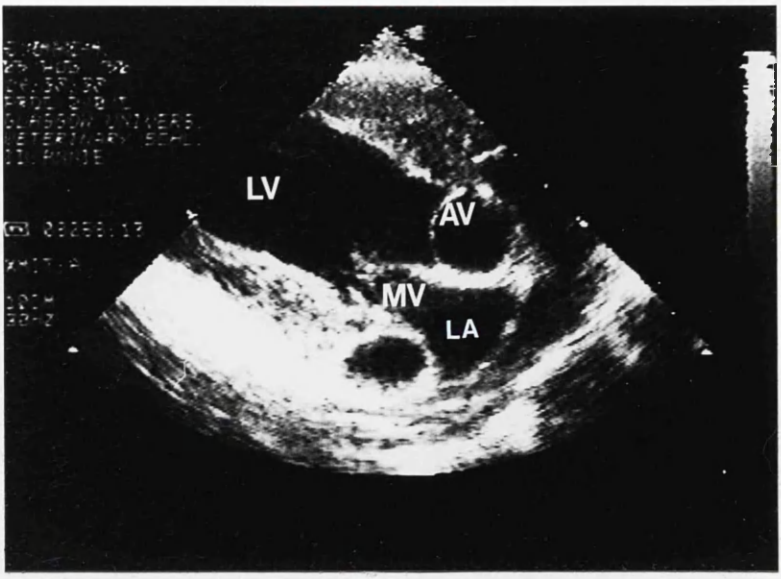
LV
AV
MV
LA

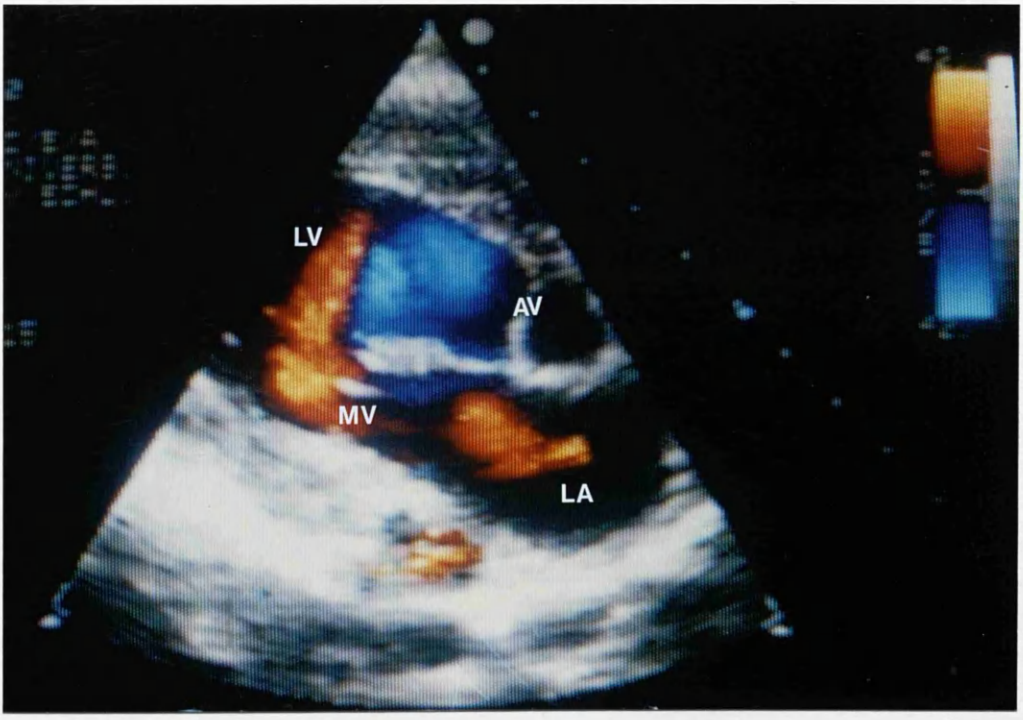
LV
AV
MV
LA

fig. 5 : 53. Long axis scan through Greyhound heart showing MV and AV.

fig. 5 : 54. Long axis scan showing bloodflow velocity through the MV with Colour flow mapping.

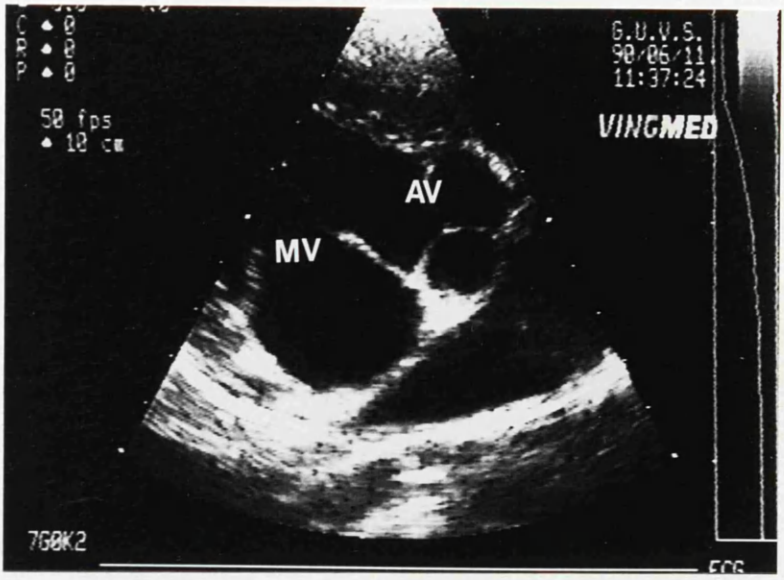
G.U.V.S.
90/06/11
11:37:24
VINGMED
50 fps
10 cm
AV
MV
7G0K2

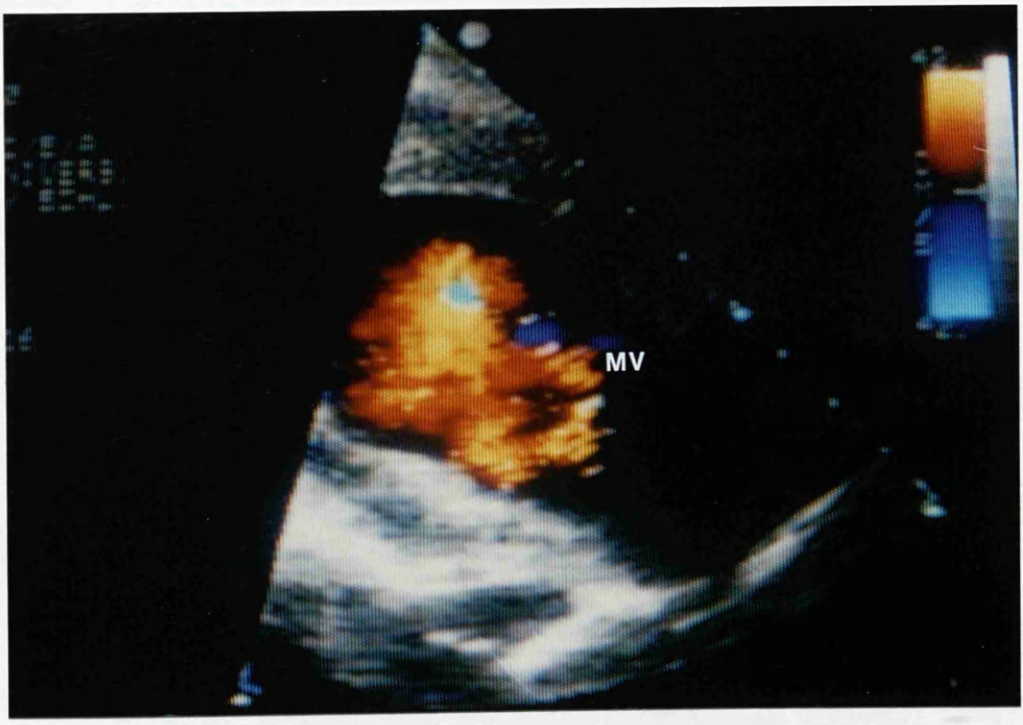
MV

fig. 5 : 55. Long axis scan of Greyhound heart in diastole, showing MV, AV, LA LV and chordea tendineae (CT).

fig. 5 : 56. Long axis scan of bloodflow velocity in LV with colour flow mapping.

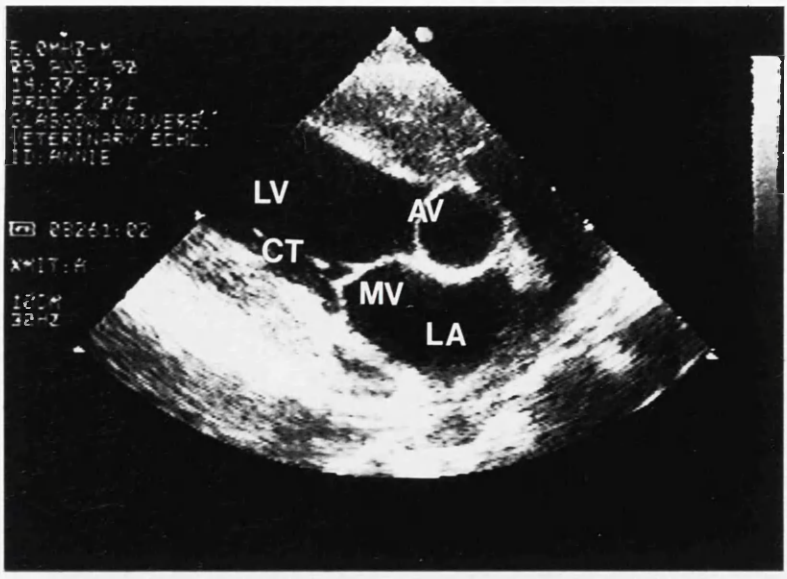
LV
AV
CT
MV
LA

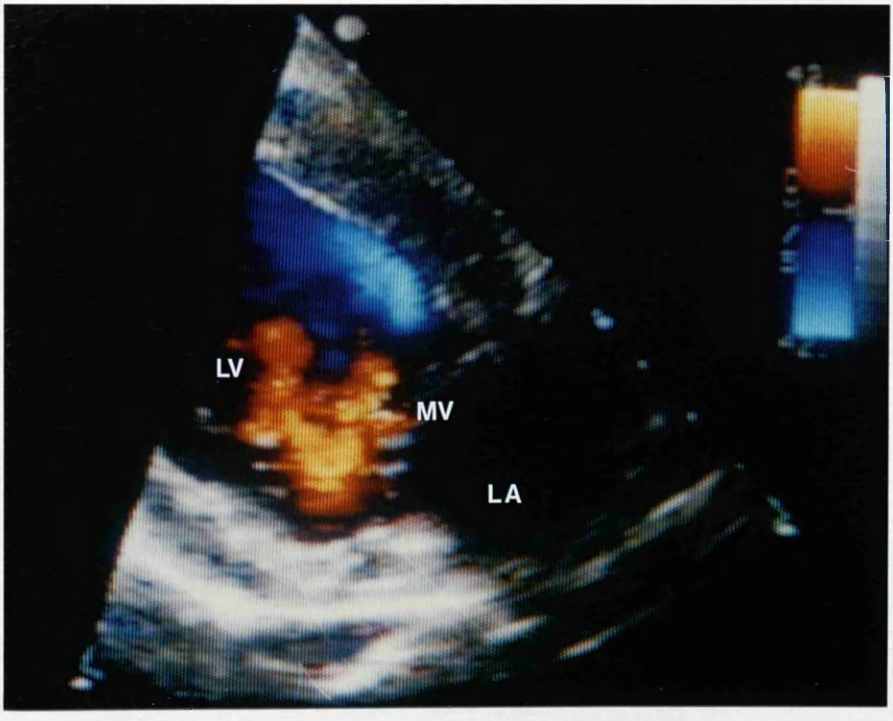
LV
MV
LA

fig. 5 : 57a. Long axis scan of Greyhound heart showing RV, LV, LVOT, AV, MV and LA.

fig. 5 : 57b. Bloodflow velocity through the MV illustrated with colour flow mapping.

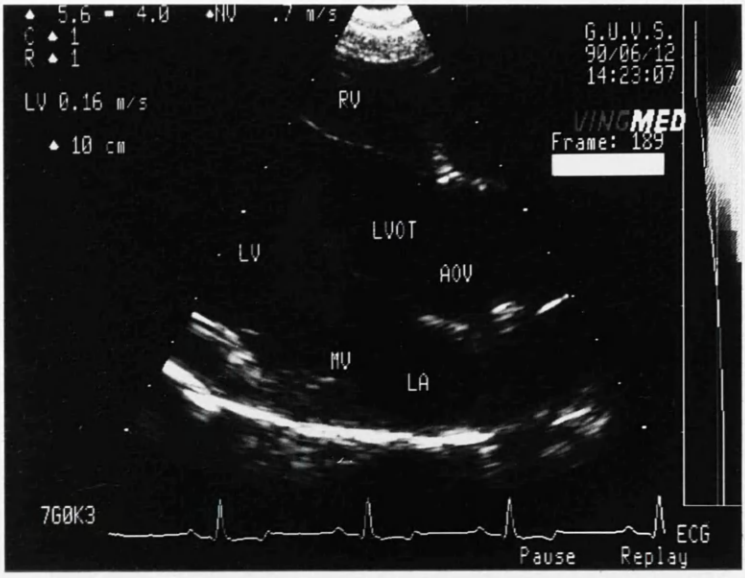
5.6 4.0 NV .7 m/s
G 1
R 1
LV 0.16 m/s
10 cm
RV
LVOT
LV
AOV
MV
LA
G.U.V.S.
90/06/12
14:23:07
VINGMED
Frame: 189
7G0K3
ECG
Pause
Replay

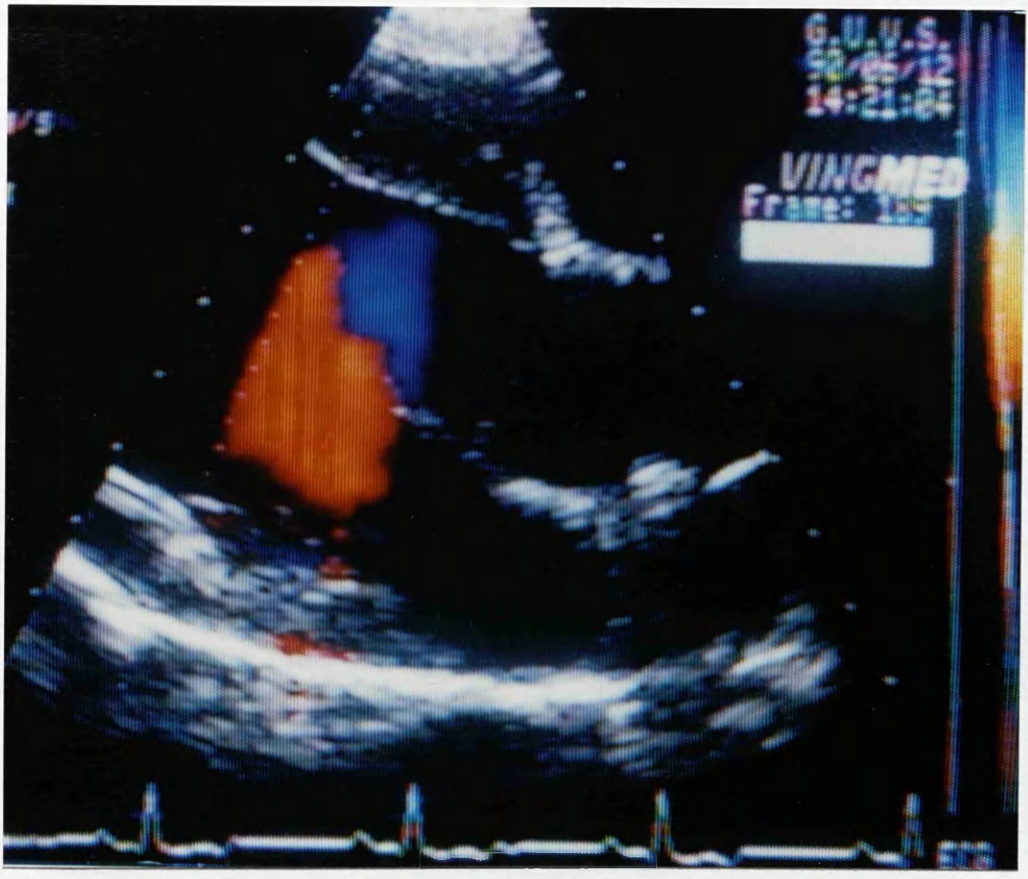
G.U.V.S.
VINGMED

fig. 5 : 58a. Long axis scan of Greyhound heart showing LVOT, AV, AO, MV and LA.

fig. 5 : 58b. Bloodflow velocity through MV turning into LVOT illustrated with colour flow mapping.

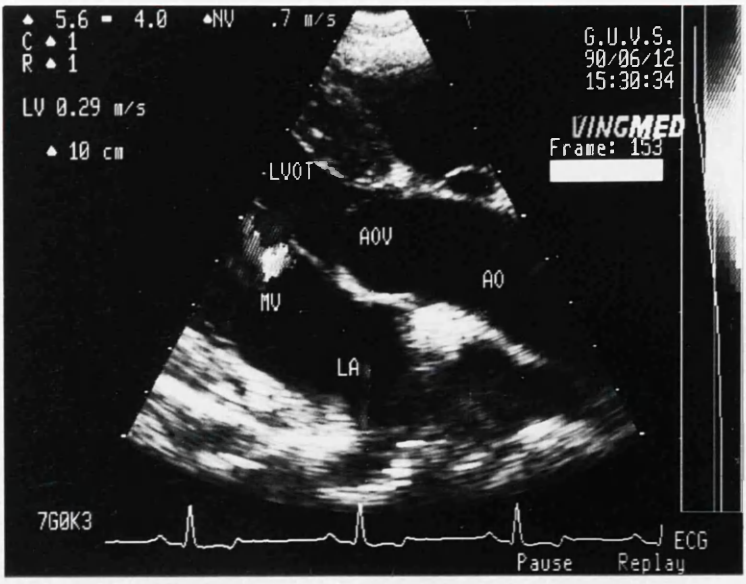
▲ 5.6 ▬ 4.0 ▲NV .7 m/s
C ▲ 1
R ▲ 1
LV 0.29 m/s
▲ 10 cm
G.U.V.S.
90/06/12
15:30:34
VINGMED
Frame: 153
LVOT
AOV
AO
MV
LA
7G0K3
ECG
Pause
Replay

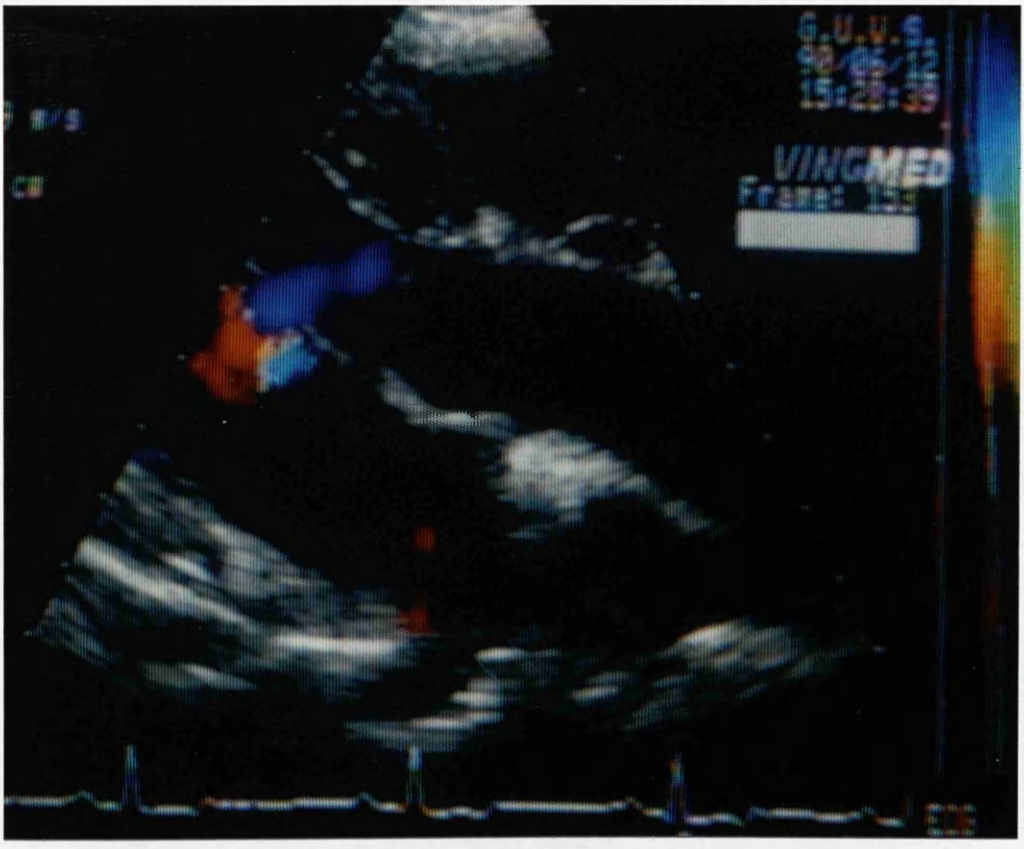
VINGMED

fig. 5 : 59a. Long axis scan of Greyhound showing RV, LVOT, AV and AO.

fig. 5 : 59b. Bloodflow velocity through AV illustrated with colour flow mapping. The blue spectrum indicating all sampled flow moving away from the transducer.

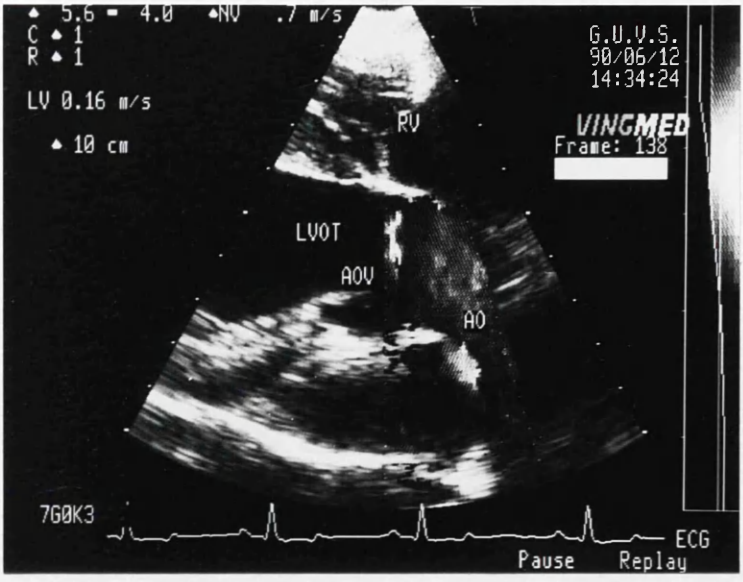
▲ 5.6 ▬ 4.0 ▲NV .7 m/s
C ▲ 1
R ▲ 1
LV 0.16 m/s
▲ 10 cm
G.U.V.S.
90/06/12
14:34:24
VINGMED
Frame: 138
RV
LVOT
AOV
AO
7G0K3
ECG
Pause
Replay

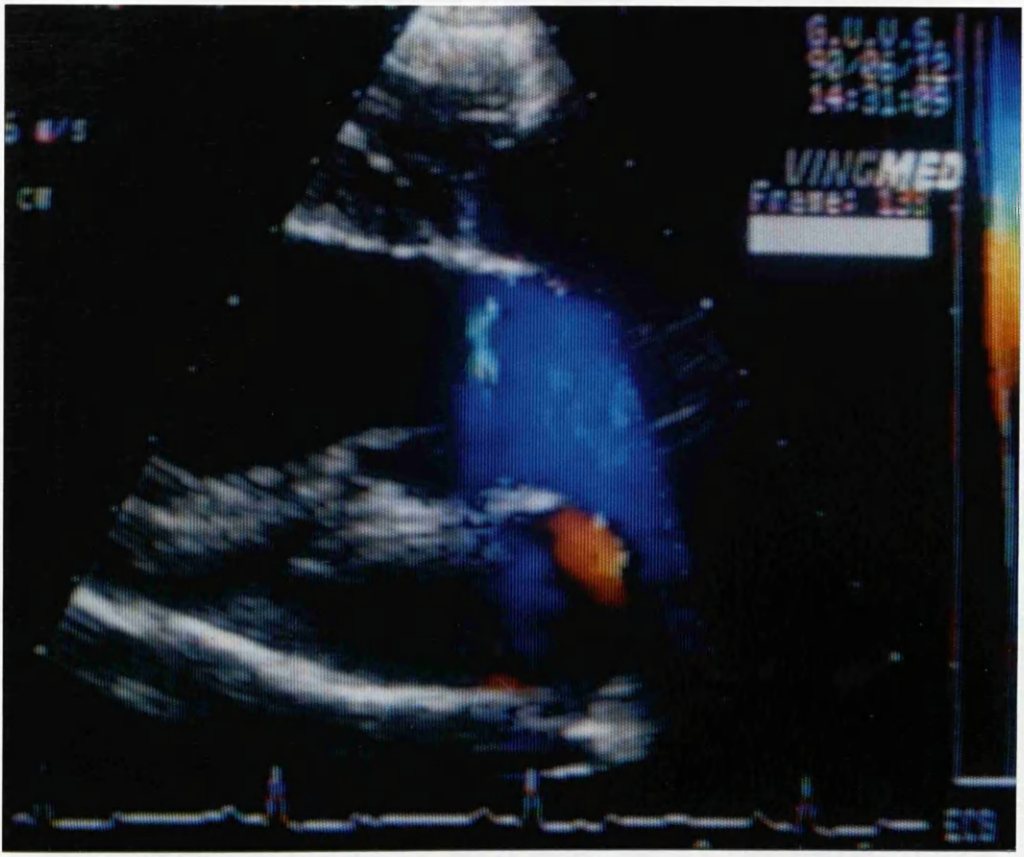
VINGMED

fig. 5 : 60. Gross anatomical transverse section through dog heart showing AO, TV, RA, and RV.

fig. 5 : 61. Short axis scan of Greyhound heart showing AO, RA, TV and RV with PW sample volume in the RV.

fig. 5 : 62. Split screen format showing bloodflow velocity through the TV.

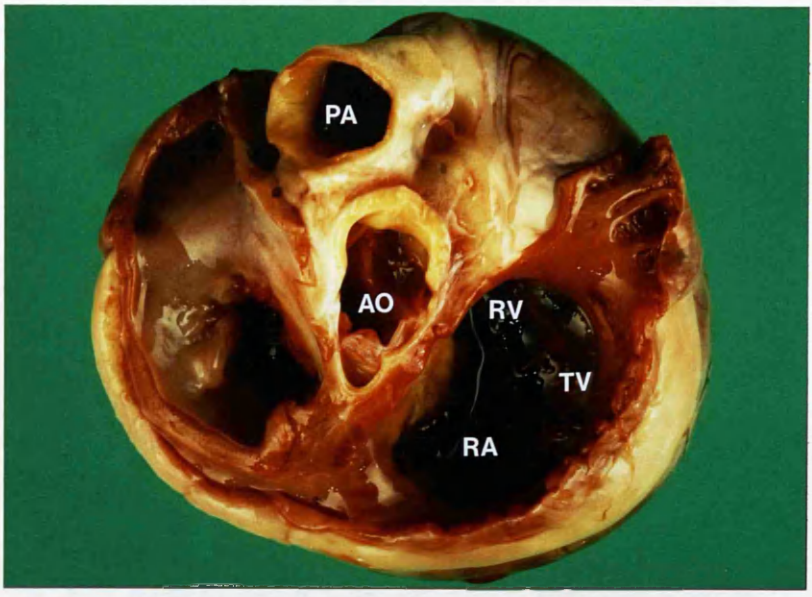
PA
AO
RV
TV
RA

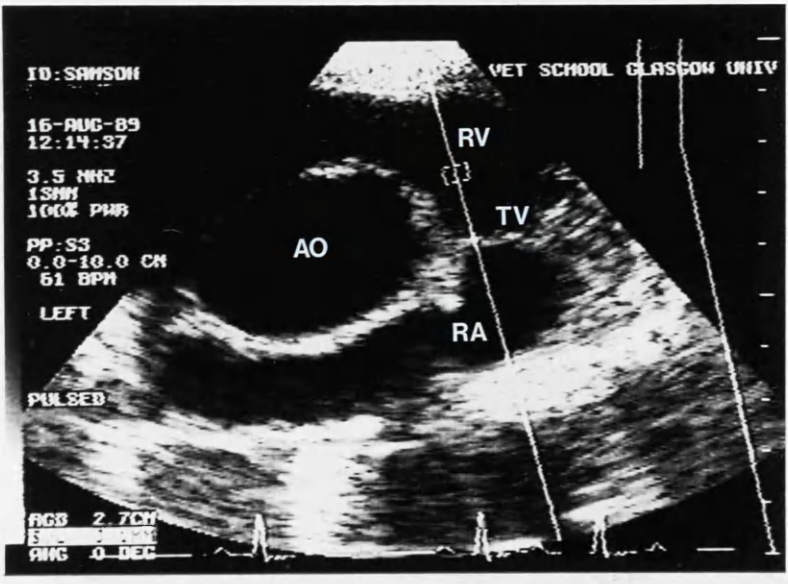
ID:SAMSON
VET SCHOOL GLASGOW UNIV
16-AUG-89
12:14:37
3.5 MHZ
13MM
100% PWR
PP:S3
0.0-10.0 CM
61 BPM
LEFT
PULSED
AGB 2.7CM
ANG 0 DEG
RV
TV
AO
RA

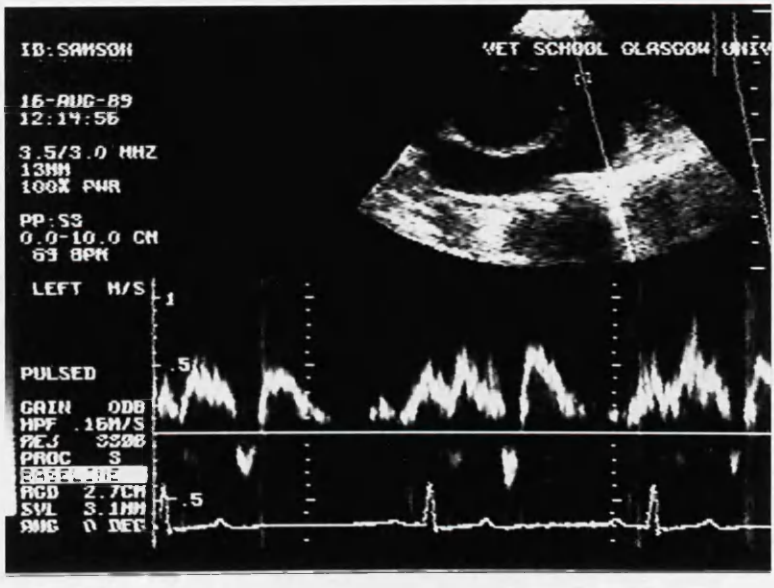
ID:SAMSON
VET SCHOOL GLASGOW UNIV
16-AUG-89
12:19:56
3.5/3.0 MHZ
13MM
100% PWR
PP:S3
0.0-10.0 CM
69 BPM
LEFT M/S
PULSED
GAIN 0DB
HPF .16M/S
REJ 33DB
PROC S
SCREEN 0%
AGD 2.7CM
SVL 3.1MM
ANG 0 DEG
1
.5
.5

fig. 5 : 63. Short axis scan of of Greyhound heart showing PW sample volume in the RA.

fig. 5 : 64. Split screen format showing bloodflow velocity through the TV.

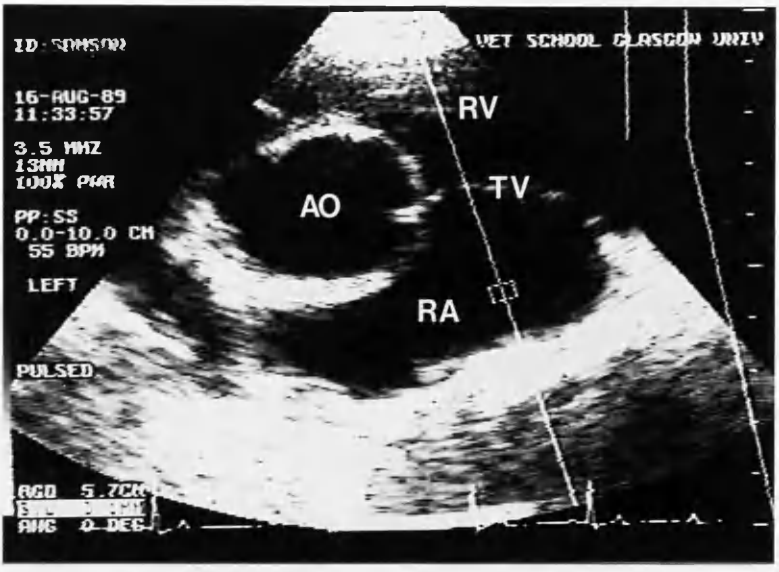
ID:SAMSON
VET SCHOOL GLASGOW UNIV
16-AUG-89
11:33:57
3.5 MHZ
13MM
100% PWR
PP:SS
0.0-10.0 CM
55 BPM
LEFT
PULSED
RGD 5.7CM
ANG 0 DEG
RV
TV
AO
RA

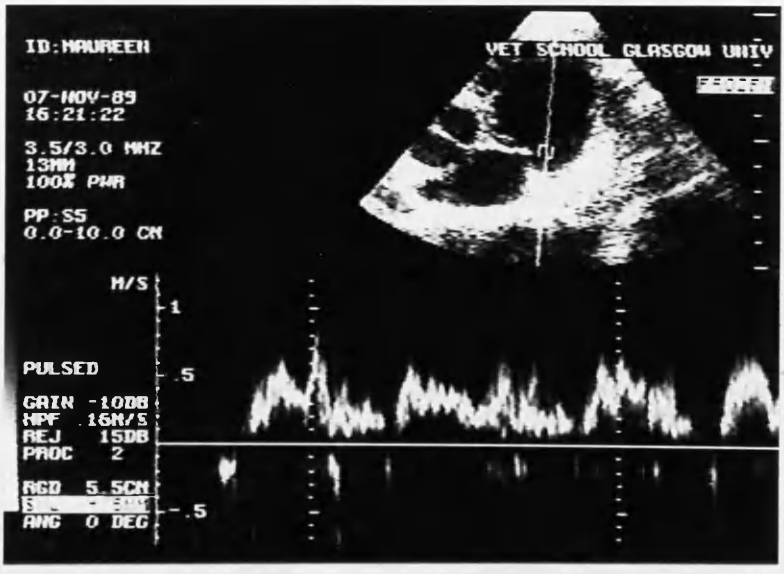
ID:MAUREEN
VET SCHOOL GLASGOW UNIV
07-NOV-89
16:21:22
3.5/3.0 MHZ
13MM
100% PWR
PP:SS
0.0-10.0 CM
M/S
1
.5
PULSED
GAIN -10DB
HPF .16M/S
REJ 15DB
PROC 2
RGD 5.5CM
ANG 0 DEG
.5

fig. 5 : 65a. Short axis scan of Greyhound heart showing RV, TV, RA, LV and IVS.

fig. 5 : 65b. Short axis scan showing bloodflow velocity through the TV and MV with colour flow mapping.

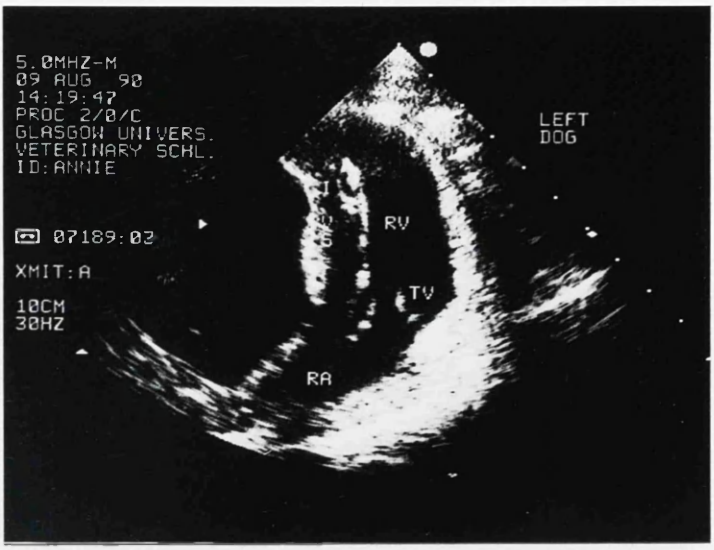
5.0MHZ-M
09 AUG 98
14:19:47
PROC 2/0/C
GLASGOW UNIVERS.
VETERINARY SCHL.
ID:ANNIE
07189:02
XMIT:A
10CM
30HZ
LEFT
DOG
RV
TV
RA

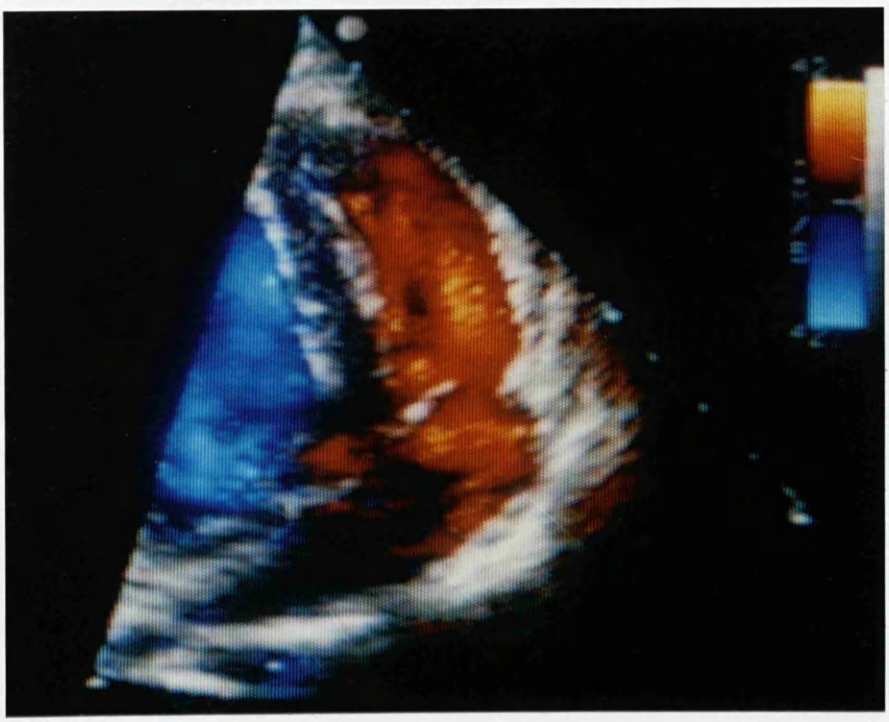

fig. 5 : 66. Short axis scan of Greyhound heart showing bloodflow velocity through the TV with colour flow mapping.

fig. 5 : 67. Short axis scan of Greyhound heart showing TV closed with bloodflow velocity in the RV and bloodflow reflux in the RA (*) illustrated with colour flow mapping.

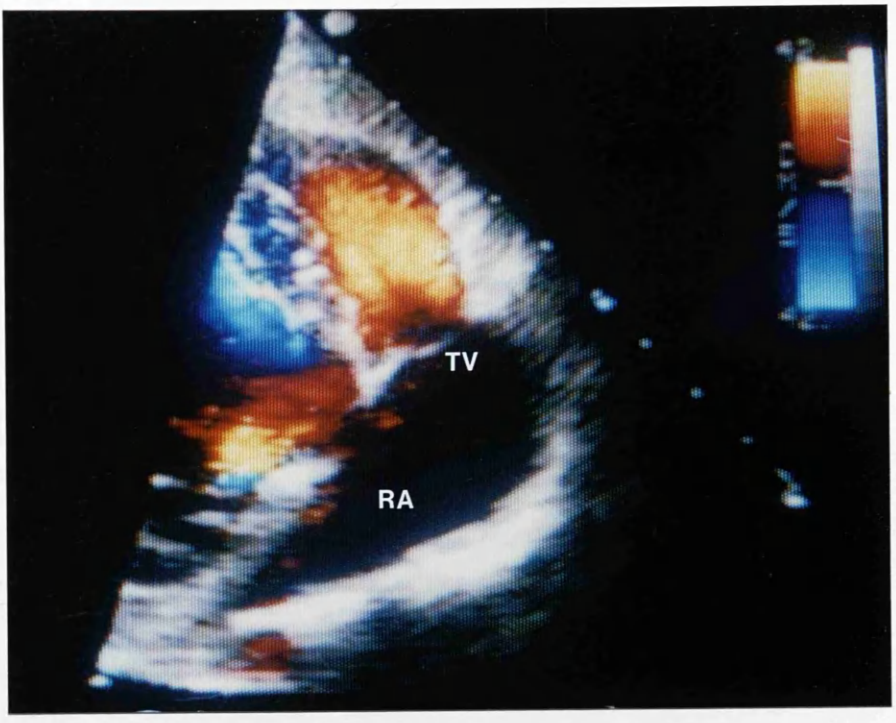
TV
RA

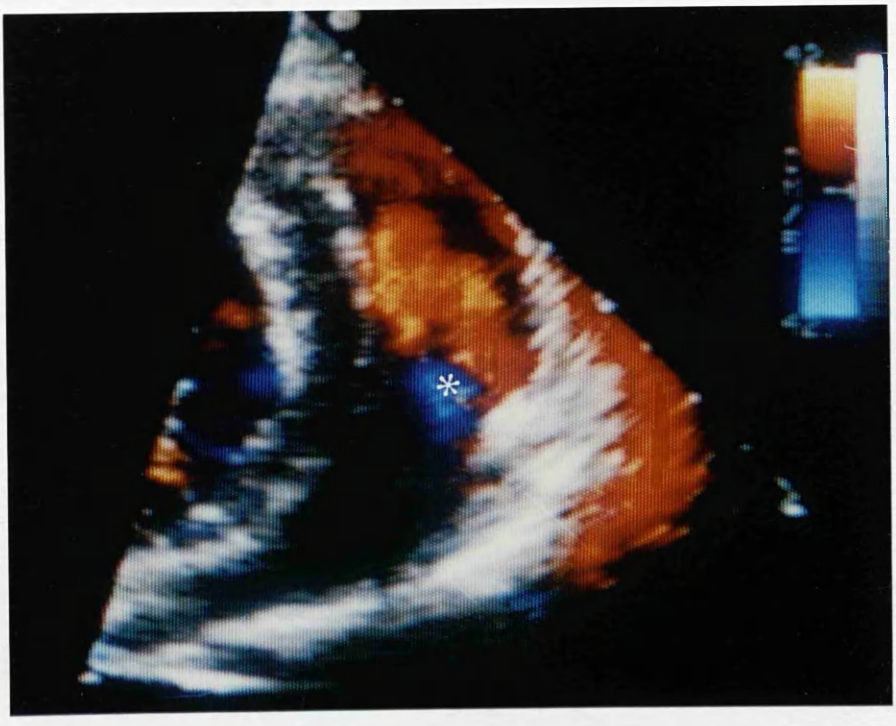
*

fig. 5 : 68a. Short axis scan of Greyhound heart showing RV, TV, LVOT, LV and IVS.

fig. 5 : 68b. Short axis scan showing bloodflow velocity through the TV with colour flow mapping.

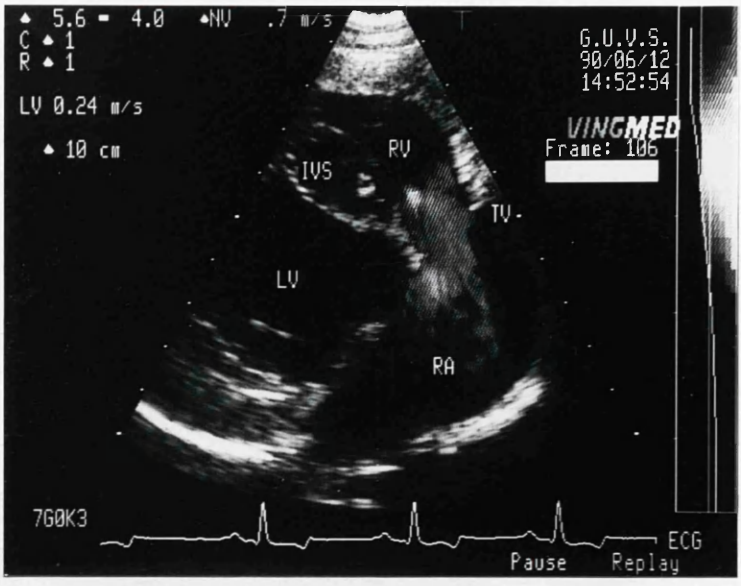
▲ 5.6 ▬ 4.0 ▲NV .7 m/s
C ▲ 1
R ▲ 1
LV 0.24 m/s
▲ 10 cm
G.U.V.S.
90/06/12
14:52:54
VINGMED
Frame: 106
IVS
RV
TV
LV
RA
7G0K3
ECG
Pause
Replay


G.U.V.S.
VINGMED

fig. 5 : 69. Gross anatomical transverse section through the base of dog heart showing pulmonary valve (PV), pulmonary artery (PA) and AO.

fig. 5 : 70. Short axis scan of Greyhound heart showing PV, PA, LA, MV with the PW sample volume in the PA.

fig. 5 : 71. Split screen format showing bloodflow velocity through the PV with colour flow mapping.

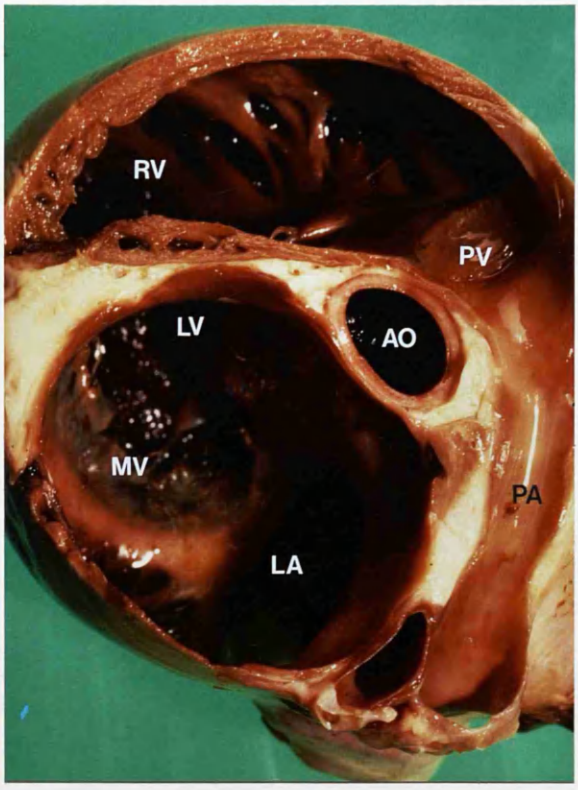
RV
PV
LV
AO
MV
PA
LA

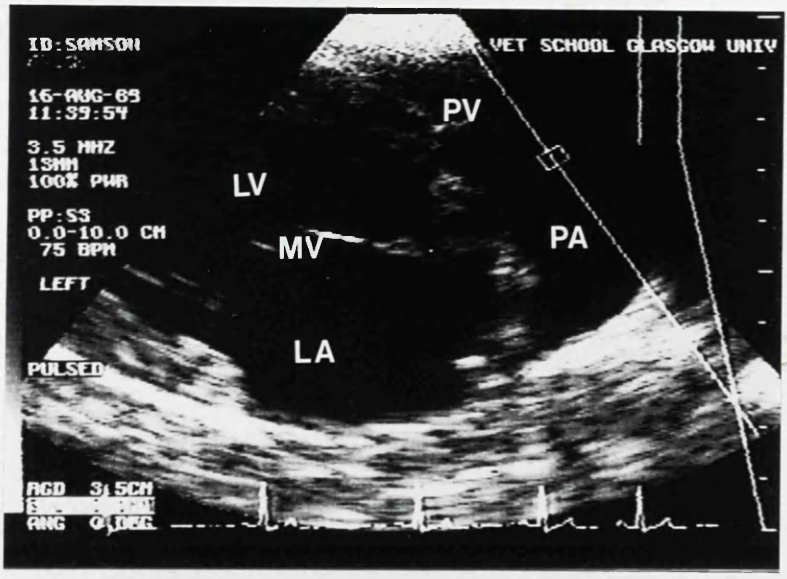
ID:SAMSON
VET SCHOOL GLASGOW UNIV
16-AUG-89
11:39:54
3.5 MHZ
13MM
100% PWR
PP:53
0.0-10.0 CM
75 BPM
LEFT
PULSED
PV
LV
MV
PA
LA
AGD 3.5CM
ANG 0 DEG

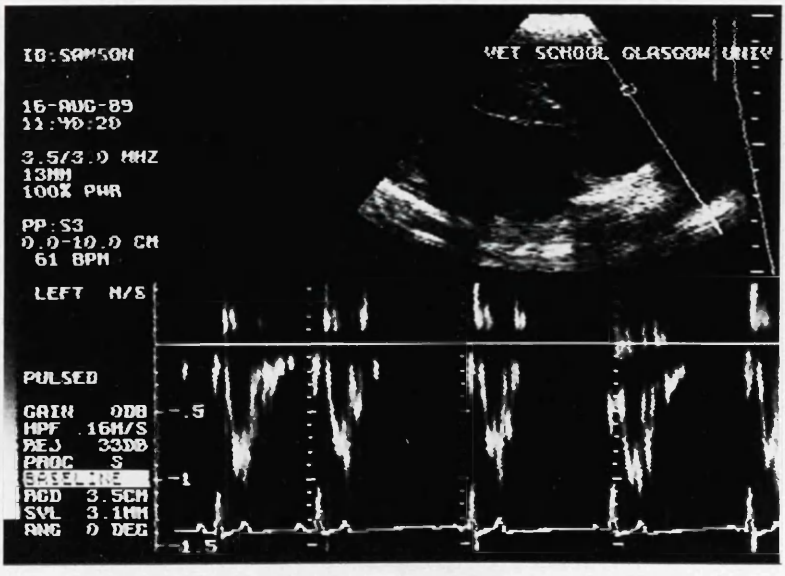
ID:SAMSON
VET SCHOOL GLASGOW UNIV
16-AUG-89
11:40:20
3.5/3.0 MHZ
13MM
100% PWR
PP:53
0.0-10.0 CM
61 BPM
LEFT M/S
PULSED
GAIN 0DB
HPF 16M/S
REJ 33DB
PROC S
BASELINE
AGD 3.5CM
SVL 3.1MM
ANG 0 DEG
-.5
-1
-1.5

fig. 5 : 72. Split screen format showing bloodflow velocity through the PV of a Greyhound by means of PW.

fig. 5 : 73. Split screen format of bloodflow velocity through the PV of a Greyhound by means of steerable continuous wave Doppler.

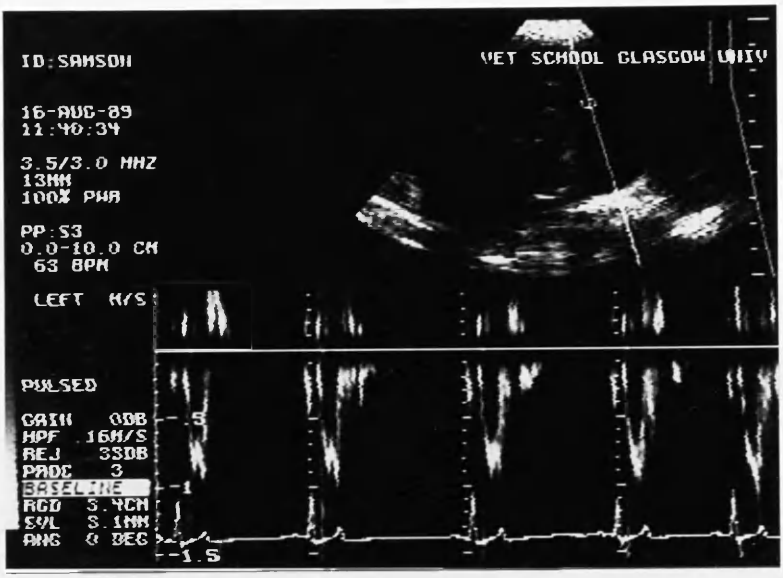
ID:SAMSON
VET SCHOOL GLASGOW UNIV
16-AUG-89
11:40:34
3.5/3.0 MHZ
13MM
100% PWR
PP:S3
0.0-10.0 CM
63 BPM
LEFT M/S
PULSED
GAIN 0DB
HPF 16M/S
REJ 3SDB
PROC 3
BASELINE
RGD 5.4CM
SVL 5.1MM
ANG @ DEG
5
1
-1.5

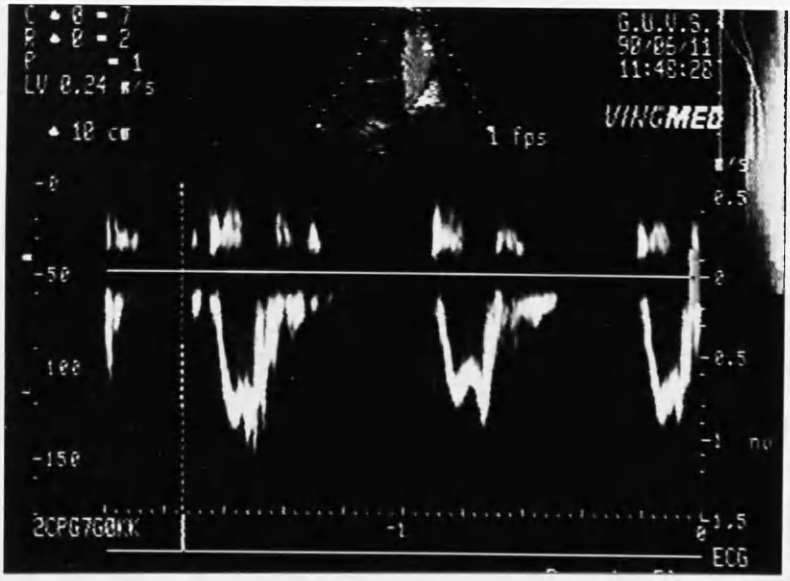
G.U.V.S.
90/05/11
11:48:28
VINGMED
LV 0.24 M/s
10 cm
1 fps
0
-50
100
-150
0.5
-0.5
-1
m/s
2CPG760MK
ECG

fig. 5 : 74a. Short axis view of Greyhound heart showing right ventricular outflow tract (RVOT), PV and PA.

fig. 5 : 74b. Bloodflow velocity through the PV illustrated with colour flow mapping indicating bloodflow away from the transducer. The AO to the left is used as a landmark when locating the PV.

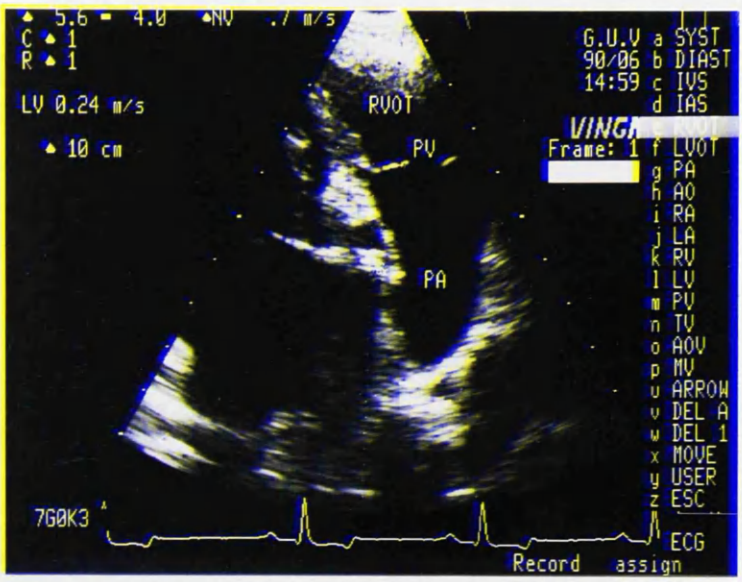
5.6 - 4.0
NV .7 m/s
C 1
R 1
LV 0.24 m/s
10 cm
RVOT
PV
PA
G.U.V
90/06
14:59
Frame: 1
a SYST
b DIAST
c IVS
d IAS
f LVOT
g PA
h AO
i RA
j LA
k RV
l LV
m PV
n TV
o AOV
p MV
u ARROW
v DEL A
w DEL 1
x MOVE
y USER
z ESC
7G0K3
ECG
Record assign

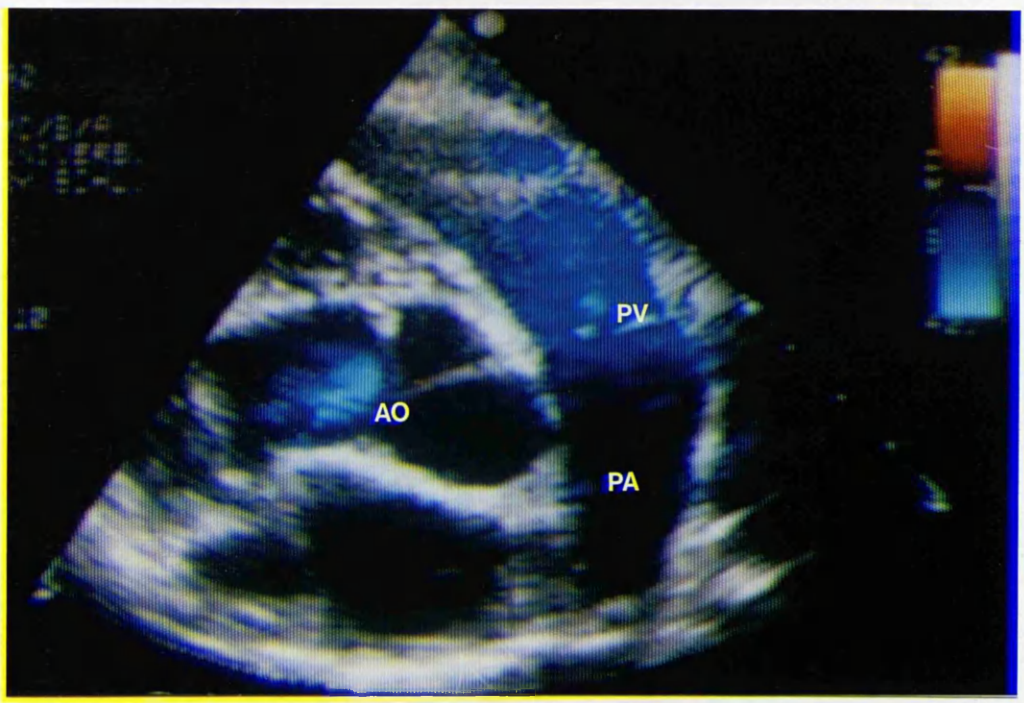
PV
AO
PA

Subcostal view.

fig. 5 : 75. Gross anatomical longitudinal section through the dog thorax showing position of scanning planes in relation to the orientation of the heart in a) subcostal and
b) suprasternal scans.

fig. 5 : 76. Split screen format scanned from the subcostal view showing bloodflow velocity through the MV of a Beagle with the PW sample volume in the LA

fig. 5 : 77. Split screen format of bloodflow velocity through the MV of a Beagle with the PW sample volume in the LV

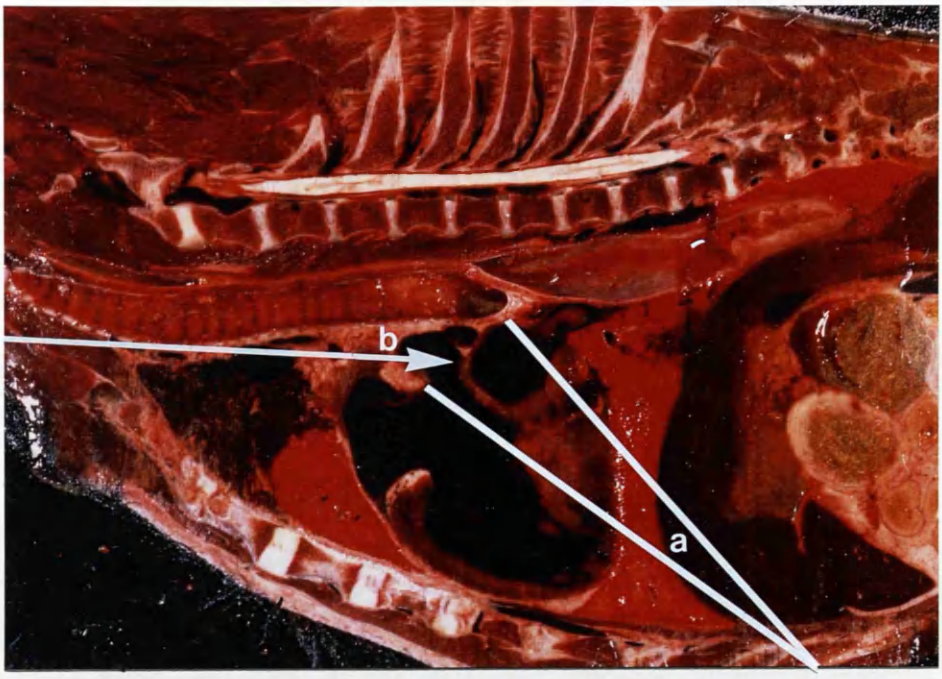
b
a

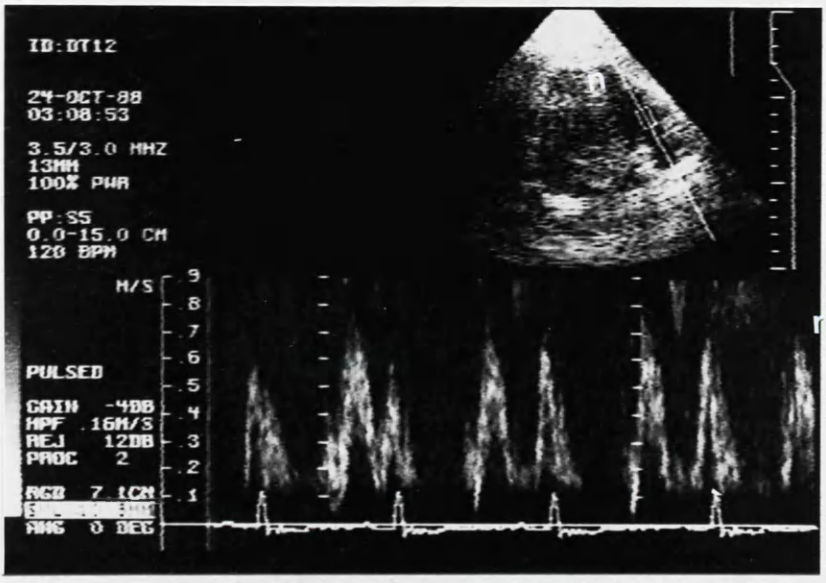
ID:DT12
24-OCT-88
03:08:53
3.5/3.0 MHZ
13MM
100% PWR
PP:SS
0.0-15.0 CM
120 BPM
M/S
9
8
7
6
5
4
3
2
1
PULSED
GAIN -4DB
HPF .16M/S
REJ 12DB
PROC 2
RGD 7.1CM
ANG 0 DEG

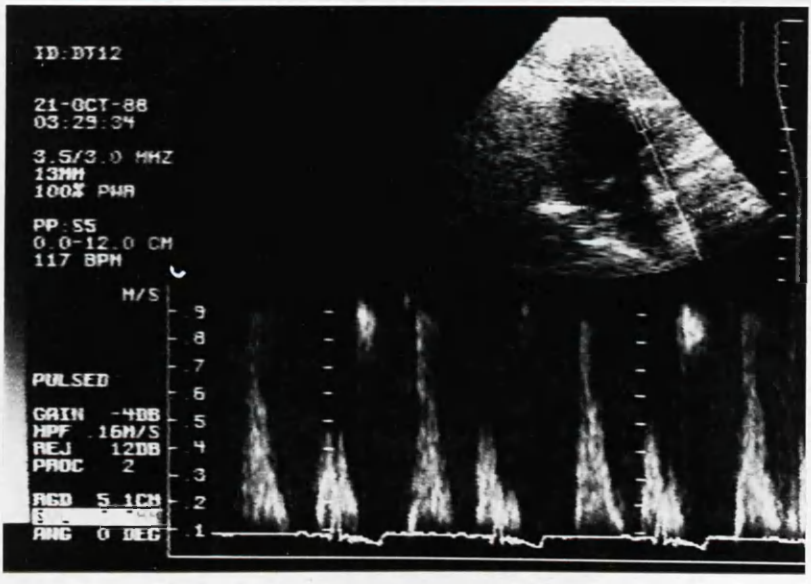
ID:DT12
21-OCT-88
03:29:34
3.5/3.0 MHZ
13MM
100% PWR
PP:SS
0.0-12.0 CM
117 BPM
M/S
9
8
7
6
5
4
3
2
1
PULSED
GAIN -4DB
HPF .16M/S
REJ 12DB
PROC 2
RGD 5.1CM
ANG 0 DEG

fig.5 : 78. Continuous wave (CW) velocity trace of MV from subcostal view in a Beagle.

fig. 5 : 79. CW bloodflow velocity trace of MV from the subcostal view in a Beagle with the vertical scale increased.

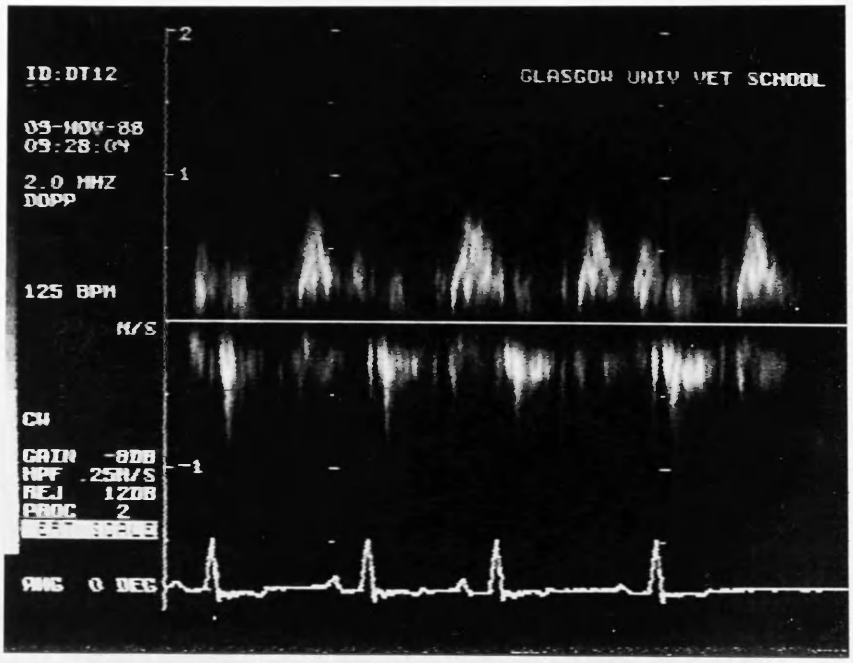
ID:DT12
GLASGOW UNIV VET SCHOOL
09-NOV-88
09:28:04
2.0 MHZ
DOPP
125 BPM
M/S
CW
GAIN -8DB
HPF .25M/S
REJ 12DB
PROC 2
ANG 0 DEG
2
1
-1

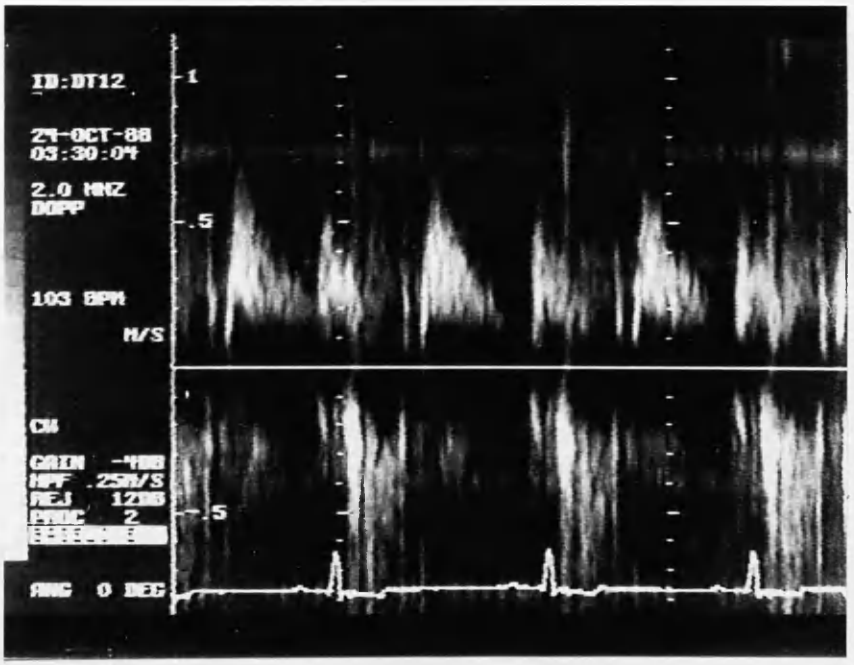
ID:DT12
24-OCT-88
03:30:04
2.0 MHZ
DOPP
103 BPM
M/S
CW
HPF .25M/S
REJ 12DB
PROC 2
ANG 0 DEG
1
.5
.5

fig. 5 : 80. Short axis scan of Beagle heart with PW sample volume in the LV in front of AV.

fig. 5 : 81. Split screen format of bloodflow through AV by means of PW.

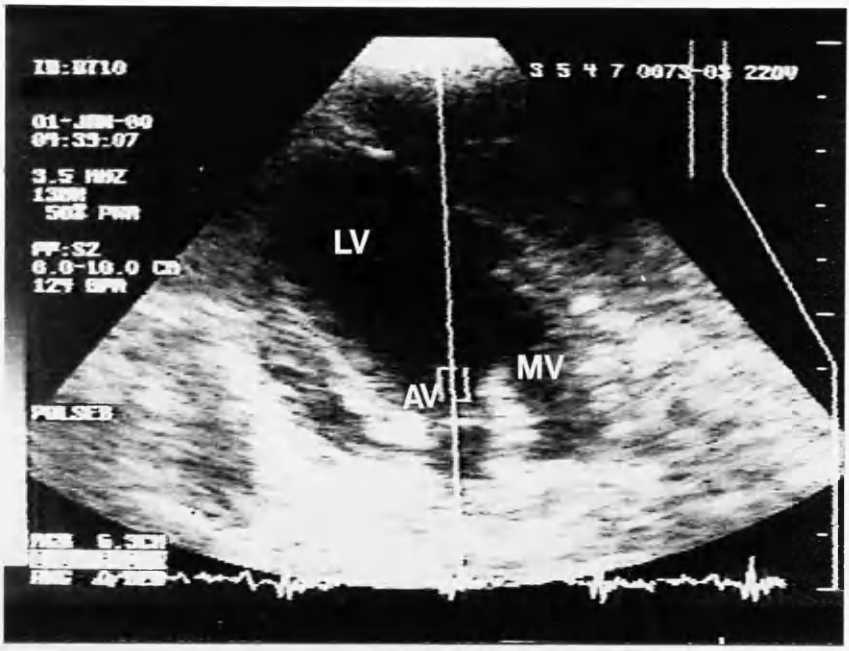
ID:BT10
01-JAN-80
09:33:07
3.5 MHZ
13MM
PWR
PP:SZ
6.0-18.0 CM
129 BPM
PULSED
LV
MV
AV

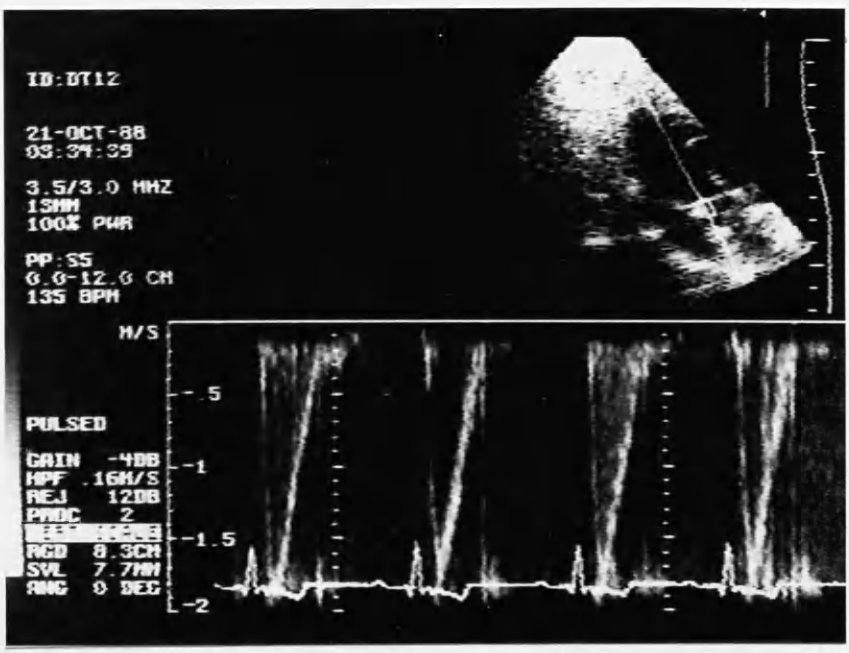
ID:BT12
21-OCT-88
03:34:39
3.5/3.0 MHZ
13MM
100% PWR
PP:55
6.0-12.0 CM
135 BPM
M/S
.5
1
1.5
2
PULSED
GAIN -4DB
HPF .16M/S
REJ 12DB
PWDC 2
RCD 8.3CM
SVL 7.7MM
ANG 0 DEG

fig. 5 : 82. CW trace of bloodflow velocity through the AV in a Beagle from the subcostal location. The trace is in the lower channel as bloodflow is moving away from the transducer.

Suprasternal view.

fig. 5 : 83. CW trace of bloodflow velocity through AV in a Beagle from the suprasternal view. The trace is in the upper channel as bloodflow is moving towards the transducer.


ID:DT12
21-OCT-88
03:52:01
2.0 MHZ
DOPP
126 BPM
M/S
CW
REJ 120B
PROC 2
ANG 0 DEG
-1
-2
-3
-4


ID:DT12
24-OCT-88
03:40:17
2.0 MHZ
DOPP
115 BPM
M/S
CW
REJ 120B
PROC 2
ANG 0 DEG
2
1
-1

CHAPTER 6.
RESULTS.

6 : 1. Right parasternal location.

Images of the heart in this location were obtained in both breeds of dog by the placement of a 5 MHz PW transducer between the third to fifth intercostal space, and one to seven centimetres lateral to the sternum. The heart was first scanned in the short axial plane (fig. 5 : 1, 5 : 2) and from this approach consistent images of the LV, IVS, LVFW and PM's were obtained in all the dogs examined. A continuous series of sections in short axis was achieved by tilting and directing the transducer gradually from the ventral (apex) to the dorsal (base) aspect of the heart. The LV was readily identifiable by its anechoic (black) fluid filled interior and echogenic (grey - shaded) thick muscular walls.

The examination of the LV was carried out during the periods of both diastole and systole. The optimum site for examination of LVF, as described in human echocardiography, was obtained by the location of the two PMs on either side of the ventricle. (fig. 5 : 3) A split screen format of the LV was achieved by the placement of a cursor (controlled by a rollerball on the scanner keyboard) through the bifurcation of the PMs. A 2D image of the heart was displayed on the top of the screen, with the LV in an M - mode format at the bottom. (fig. 5 : 4)

The continual imaging of the heart in 2D, made for accurate placement of the cursor between the PMs, thus allowing an optimum M - mode image of the LV. The LV was recognised in M - mode, as a horizontal anechoic area running from left to right of the M - mode trace. The cursor when moved slightly to the left or the right of the bifurcation in this format, outlined one of the PM's as an echogenic mass on the image. (fig. 5 : 4) LVF was obtained from this location (fig. 5 : 12, 5 : 13) by the calculation of the shortening fraction, (SF) using the formula described in chapter 4. The average SF in the normal heart recorded was 35. 5%. In a heart with mitral or aortic valve incompetence, this value would be greater, due to the extra work rate required to passage blood out of the LV. Further dorsal angulation of the transducer past the PMs, resulted in the imaging of the MV cusps. (fig. 5 : 5) The CT were also identified as strands of bright echogenic echoes stretching from the PM to the MV. (fig. 5 : 31)

The MV was identified by the " fish mouth " appearance of its valvular cusps. As with the LV, an M - mode study of the MV was carried out using the same technique as described previously. The MV was viewed in the split screen, M - mode format which outlined the valve movements during systole and diastole. (fig. 5 : 6) The MV was recognised as an undulating echogenic line running through the centre of the trace and the movement of the valve was examined during a cardiac cycle. Atrial systole occurred at peak A on the cranial MV with the valve completely closed at point C. Diastole corresponded to point D on the trace, and the valve was seen to be fully opened at point D. The RV was also identified at this level as a anechoic area to the top of the M - mode trace along with the IVS which appeared as an echogenic mass between the LV and the RV. (fig. 5 : 7, 5 : 8, 5 : 11)

The IVS was found to be a useful landmark in the M - mode format, in that it gave verification that the transducer was scanning at the proper angle. If a sharp image of the IVS was not evident, optimum LV dimensions could not be recorded.

The AV was next to be scanned in the same short axial plane. Viewing was achieved by tilting the transducer slightly more dorsal, then caudal,until the valve came into view. The AV was readily recognised by its inverted " Y " shaped valve cusps in the centre of the image. (fig. 5 : 9) The septal cusp was located in the upper left region of the AV with the right cusp in the upper right and the left cusp at the bottom of the AO image. The AV like the MV was examined using the split - screen, M - mode format to show its movement in diastole and systole. (fig. 5 : 10) The valve was seen as a echo dense structure in the anechoic aortic root. The AV was identified in the mid position of the aortic root during diastole, and seen to move towards the AO wall before eventually closing at the end of systole.

The heart was now viewed in the longitudinal axial plane, (fig. 5 :14) by rotating the transducer through a plane of 90 from the short axis position. The image was so orientated that the apex of the heart appeared on the left of the scanner screen, and the base to the right. (fig. 5 : 15) The RV positioned at the top of

the screen was divided from the LV at the bottom of the picture by the distinctive echogenic IVS. Further dorsal tilting of the transducer revealed the MV cusps in the lower left portion of the image. During diastole these cusps appeared as dense, thin semicircular lines projecting into the LV. (fig. 5 : 15) whereas in systole, the closed MV appeared as an irregular band separating the LA from the LV. (fig. 5 : 16) The LVOT was visible in the centre of the image as an anechoic area between the septal cusp of the MV and the IVS. (fig. 5 : 16) At this level the RV and RA were also partially imaged cranial to the LV as anechoic areas. Further tilting and slight clockwise rotation revealed the AV and AO root directly in the centre of the screen. (fig. 5 : 23)

The rhythmical movements of the MV were observed between the junction of the LA and LV, along with that of the AV between the LV and the ascending AO. In the long axial view, only two septal cusps of the AV were imaged. This differed from the short axial view, where the three septal cusps were identified. Measurement of the LA dimensions were carried out during diastole and at the onset of systole by means of a cursor placed in a cranial - caudal position that approximately bisected the LA. (fig. 5 : 15, 5 : 16) The average figures recorded in systole were 1.94cms and 4.65cms during diastole. These results concurred with the findings in previous studies. (O'Grady and others 1986)

The anatomy of the left heart having been identified, the bloodflow velocities through the AV and MV were next to be examined. This was carried out by the use of firstly, PW Doppler ultrasound and secondly a combination of CW and steerable CW Doppler ultrasound. The MV was imaged first and located in the long axis plane with the PW Doppler sample volume placed in the LA examination site just cranial to the valve. (fig. 5 :18) The split screen format was again employed, but this time instead of the M - mode trace illustrated below the 2D image, a PW Doppler trace of bloodflow velocity measured in distance (m / sec.) against time (sec.) was displayed. (fig. 5 : 19)

The bloodflow velocity trace appeared as a Doppler spectrum above the baseline, indicating that the direction of flow was positive and towards the transducer. A distinctive twin peak Doppler signature of the MV was clearly

illustrated where the first peak (E) represented the initial filling phase of the LA corresponding to the initial opening of the MV during early diastole. The second peak (A) indicated the period of flow ending with LA contraction in late diastole. This biphasic flow signal was composed of a relatively narrow - ranged frequency spectrum as was shown by the narrow grey scale band on the Doppler display, suggesting that the flow was laminar. No significant Doppler signal was recorded in the MV during systole.

At certain times during the Doppler scans,a bright resonant trace was identified between the end of the A peak and the beginning of the E peak below the baseline. At first this was thought to be bloodflow away from the transducer but was later properly identified as "valve clicks" caused by the MV leaflets as they closed at the onset of ventricular systole. The Doppler examination was repeated with the sample volume located in the LV side of the MV, (fig. 5 : 20, 5 : 21) and bloodflow velocity was again recorded using the split screen format. (fig. 5 : 22) The bloodflow velocity recorded in the dog for the MV with PW Doppler was 0.697 ± 0.076 m/s for the E peak, and 0.468 ± 0.069 m/s for the A peak. There was no significant difference in the readings between the breeds examined in either location.

A similar set of procedures was conducted with the AV, again using PW Doppler. The sample volume was located firstly in the LV, and secondly, in the ascending AO sampling sites and the bloodflow velocities recorded. (fig. 5 : 23, 5 : 24) A single peaked flow with a narrow - ranged frequency spectrum was recorded below the baseline in systole, indicating negative flow away from the transducer. (fig. 5 : 25, 5 : 26) The bloodflow velocity recorded through the AV was 1.584 ± 0.016 m/s. When the sample volume was moved to the ascending AO dorsal to the AV, a similar systolic flow was observed. (fig. 5 : 25. 5 : 26)

With the transducer in the same location, variable portions of the TV and RA were imaged above the IVS, and allowed the examination of velocity flow through the TV with PW Doppler. The Doppler sample volume was placed in the RA side of the TV and blood velocities recorded. (fig. 5 : 28, 5 : 29) The

flow patterns observed at the level of the TV orifice resembled those of MV flow in the left heart. However, some differences in flow pattern through the two atrioventricular valves were noted. TV inflow was found to have a lower peak flow velocity than that of the MV inflow. (0.546 ± 0.043 m/s)

Although PW Doppler proved to be a useful tool in recording bloodflow velocities, it had the limitation that at any point in time,it could only detect Doppler frequency shifts along the one - dimensional path of the ultrasound beam. This was further limited to the one isolated focusing area defined by the sample volume. To overcome these problems a Doppler colour flow scanner was employed. The colour flow scanner operated in the same way as a normal 2D scanner except that it contained a colour converter which presented bloodflow velocity signals from the scanner converter as assigned colours based on the direction and variance of the detected frequency shifts. Bloodflow towards the transducer was coded red, whereas flow away from the transducer was designated blue.

The heart was scanned as before with PW, in the long axis plane, and the MV located in 2D. Colour flow mapping was then introduced and the bloodflow velocity was illustrated as a colour spectrum. (fig. 5 : 33, 5 : 34b) Bloodflow towards the transducer during the onset of systole was seen moving through the MV from the LA into the LV as a red flame like spectrum indicating that the direction of flow was towards the transducer. The flow was also seen to turn away from the transducer and move into the LVOT and was displayed as a blue spectrum. The use of colour flow mapping allowed for clearer visualisation of the direction of bloodflow through the left heart.

6 : 2. Left parasternal location.

The available echo window on the left side of the dog, varied from the third to the seventh intercostal space, and from one to five centimetres lateral to the sternum. In most examinations, the best images were obtained from the third to the sixth intercostal space within four centimetres of the sternal edge. The heart was scanned in the long axial plane and the internal anatomy examined. The transducer was directed dorsally toward the base of the heart and from this plane the MV was clearly identifiable in the centre of the screen with the AV lying directly medial. The LA was located cranially to the MV with the ascending AO imaged running obliquely to the right of the AV. (fig. 5 : 38) In all the studies from the left parasternal location, the LV could only be imaged obliquely and therefore a true LV apex was not achievable.

The anatomy of the left heart having been recognised from this view, the bloodflow velocities through the MV and AV were again recorded by PW Doppler using the same techniques as employed for the right parasternal view. The Doppler sample volume was placed firstly in the LV location in front of the MV and the split screen format was again employed. The familiar twin peak signatures of the MV were identified, and similar velocities to that obtained from the right parastenal location were recorded. (fig. 5 : 39)

On occasion during the examination of a dog in this location, a velocity trace was observed below the baseline indicating velocity flow away from the transducer. (fig. 5 : 41) This signal appeared different from the bright resonating valve "clicks" described previously, as it had a wider wave spectrum. Care had therefore to be taken that the sample volume was placed in the direct line of flow through the MV. The signal was identified as AV flow being picked up by the Doppler sample volume as it strayed into the LVOT due to the movement of the heart within the thoracic cavity. The sample volume was next placed in the LA location and the flow velocity through the valve recorded. The velocity results found at this site were comparable to those recorded from the MV in right parasternal view, (fig. 5 : 42)

The pressure half - time gradient of the MV was also recorded by freezing the PW Doppler trace, and measuring the slope between the E peak and the A peak by means of a cursor. (fig. 5 : 44b) This indicated the time taken between the period of the initial filling of the LA and the opening of the MV, and that of LA contraction in late diastole.

The ultrasound beam was now angled dorsally and somewhat caudally to allow the imaging of the AV in long axis. The LVOT was imaged to the left of the screen, and the ascending AO to the right of the AV. (fig. 5 : 45) The movement of the AV cusps were clearly visible, and once more Doppler studies were carried out in both the LV and the AO sample locations. (fig. 5 : 46) As with the MV readings, similar trace recordings were obtained from the AV when compared to the findings recorded in the right parasternal view.

The movements of the left heart during diastole and systole were recorded by directing the ultrasound beam slightly caudally, and rotating the transducer anti - clockwise until the aortic root was seen in full longitudinal section. The AV was seen in the centre of the image with the MV below. The LV lay obliquely to the MV and AV, with the LA located in the bottom portion of the screen. (fig. 5 : 47) The MV and AV were recorded through a full cardiac cycle, and the VHS tape replayed frame by frame on the video editor. The result was a sequential series of images illustrating the position and movement of the MV and AV at the different stages of bloodflow through the left heart.

As in the right parasternal view, Doppler colour flow mapping was employed to examine the bloodflow velocities through the MV and AV with the transducer in a cranial angulation. Diastolic inflow through the MV was identified as a diffuse red colour throughout the left ventricular inflow tract. (fig. 5 : 50) Systolic outflow was visualised as a blue colour primarily along the IVS,(fig. 5 : 51 - fig. 5 : 56b) and again indicated bloodflow velocity was away from the transducer.

Aliasing, which limited conventional PW Doppler studies of high velocity flow, also occurred in colour flow mapping for the same inherent reasons. Whenever the detected frequency shifts exceeded the Nyquist limit for a given

pulse repetition frequency, aliasing developed and gave a false impression of reversal flow. This resulted in a colour reversal, where red flow areas had a central blue zone (fig. 5 : 54) and blue areas had a central red zone. (fig. 5 : 59b) Frequently areas of significant turbulence were recorded in areas of high bloodflow velocity which caused the flow to appear as a mosaic of colours in the centre of the spectrum. (Fig. 5 : 57b) The movement of the heart muscle chambers could be also picked up by the colour flow mapping, and care had to be taken during the examination that this was not confused with the bloodflow velocities through the cardiac valves.

The transducer was now rotated back to the short axial plane and directed slightly caudally to achieve a short axis view of the AO. The AO was located to the left of the screen along with an oblique view of the RA, TV and RV to the right. PW Doppler examination was carried out in the split- screen PW format to show bloodflow velocities through the TV with the sample volume located firstly in the in the RV position and secondly in the RA. (fig. 5 : 63) The flow patterns recorded at this level of the tricuspid orifice, resembled those found in transmitral flow, however some differences in flow velocity were noted. Tricuspid inflow was found to have a lower velocity than mitral flow during diastole (0.586 ± 0.072 m/s) and occasionally had a slow velocity flow toward the RV in systole.

The transducer was next moved slightly ventrally until the AO disappeared, and with the probe still in the short axis position, the RV, TV, IVS and LV were identified. (fig, 5 : 64a) Doppler colour flow was introduced to study the bloodflow velocities through the TV and the results recorded. Bloodflow during the onset of diastole was illustrated as red, an indication of flow towards the transducer from the RA to the RV, while in the left heart at the same time the bloodflow velocity in the LVOT was transcribed as blue in dictating flow away from the transducer from the LV to the AO. (fig. 5. : 64b) When the TV was fully closed, bloodflow velocity could still be seen as a red spectrum in the RV but the reflux bloodflow in the RA appeared as a blue due to the velocity now flowing away from the transducer. (fig. 5 : 66)

2D examination of the PV was the most difficult of the cardiac valves to achieve. As described in materials and methods, the AO was viewed in long axis and the transducer moved slightly medially and directed ventrally to where the PV was identified (fig. 5 : 73b) The PV and PA were located on the right side of the screen with the AO to the left. During the course of the scan, when the transducer was moved slightly ventrally, the LA, MV and LV replaced the AO on the left side of the screen. (fig. 5 : 69) PW Doppler of the bloodflow velocities through the PV were carried out with the sample volume placed in the RV and PA examination sites.

The bloodflow patterns recorded in the areas just below and above the PV were essentially the same as those found in the corresponding areas of the AV. The difference in wave form between the PA and AO flow was that the velocity drive in the AO had a more rapid increase with a peak velocity which was earlier in systole than that in the PA. (fig. 5 :70) Steerable CW Doppler was also carried out on the PV and compared to PW Doppler. (fig. 5 : 71, 5 : 72) The main advantage of steerable CW as described previously, was that the split crystal within the 5 MHz transducer allowed both a split screen format of both 2 D and a CW Doppler trace. Precise positioning of the sample volume was permitted, but unlike PW Doppler, high bloodflow velocity traces could be recorded due to the continual update of the Doppler signal.. There was a distinct difference in the quality of trace between the two Doppler modes, in that a greater grey - scale spectrum and optimum velocity recording was achieved with the steerable CW, indicating that laminar flow was present.

The Doppler colour flow mapping was again used to study the flow velocity spectrum through the PV. As the bloodflow velocity was flowing from the RV into the PA, in the direction away from the transducer, the flow velocity was illustrated as a blue spectrum. (fig. 5 : 73b)

6 : 3. Subcostal location.

To achieve the optimum bloodflow velocities using PW Doppler in the left heart, the dog was held in a semi - dorsal recumbency position and a 3.5 MHz PW transducer placed on the left mid - line, next to the xiphoid cartilage and directed cranially. This transducer was employed to allow the increased penetration required to examine the heart from this position,due to the dog chest configuration. The degree of penetration however resulted in a loss of image quality due to the distance the soundwaves had to travel.

The rotation of the heart was now displayed with the apex to the top of the screen and the base at the bottom. This positioning allowed for the placement of the Doppler sample volume to be as parallel as possible to the direction of bloodflow through the MV and AV, thus recording the optimum velocities. The sample volume was firstly placed in the LA location behind the MV and using PW Doppler in the split screen format, the familiar twin peak signature of the mitral flow was identified above the baseline indicating flow towards the transducer. (fig. 5 : 75) The sample volume was then moved into the LV location and the procedure repeated. Similar findings were recorded from this location as were found in the LA. In order to achieve the maximum velocities through the MV, a CW Doppler format was employed using a 2 MHz CW transducer. The probe was placed in the same position as the 3.5 MHz PW transducer but had the disadvantage in that the heart could not be visualised. The transducer was manipulated until the MV trace was located. (fig. 5 : 77, 5 : 78) The blood velocity measured through the MV by the CW format was recorded (0.712 ± 0.015 m/s) and was shown to be marginally greater than achieved with the PW.

The AV was located and examined with the 3.5MHz PW in the split - screen format and the Doppler spectrum of normal AO flow recorded. The sample volume was again translocated and placed in the ascending AO and the flow velocity measured. The velocity traces recorded between the two sites proved similar (1.672 ± 0.028 m/s) and appeared as a laminar flow spike below the baseline indicating that bloodflow was away from the transducer. As with the

MV, the AV was examined with a 2 MHz CW transducer. The bloodflow velocity appeared as negative values below the baseline, (fig. 5 : 81) with a slightly greater maximum velocity trace than that recorded with PW. (1.715 ± 0.018 m/s)

6 : 4. Suprasternal location.

The dog was examined from this view in a prone sitting position. The narrowness of the thoracic outlet prohibited the use of a 2D PW Doppler transducer due to the breadth of the sector beam. The 2 MHz CW transducer was therefore employed at the thoracic outlet and directed caudally. Manipulation of the probe was carried out until the spiked trace of flow velocity through the AV was recognised. Unlike the flow from the subcostal location, the trace had a positive value and appeared above the baseline indicating flow towards the transducer. (fig. 5 : 82) The measured flow velocity was found to be similar to that recorded in the AV from the subcostal position.

CHAPTER 7.
DISCUSSION AND CONCLUSIONS.

The current study was planned and carried out to evaluate the use of 2 - D and Doppler ultrasound in both cardiac anatomy and the dynamics of bloodflow in the dog.

Ultrasonography, as described in Chapter 1, is a relatively new imaging modality with many applications, particularly for cardiac and abdominal soft tissue structural evaluation. Despite extensive and detailed descriptions of the 2 - D echocardiography technique as well as experimental and clinical diagnostic applications in humans, its value in the field of Veterinary Medicine is still yet to be fully realised. Investigators and clinicians using the techniques in animals must understand its advantages and limitations along with the anatomical and physiological characteristics of the species being studied.

The detailed descriptions of 2 - D echocardiography technique and cardiac anatomy imaged from several locations in the human, provided an important starting point for undertaking an echocardiographic study of the dog. The differences however in thoracic configuration and cardiac orientation in the dog, prevented direct application of human 2 - D scanning techniques and terminology. In particular, the dog heart was found to be comparatively mobile within a laterally compressed thorax, with the apex of the heart located closer to mid - line than found in the human anatomy.

Because of the laterally compressed thoracic confirmation of most dogs, cardiac contact with the chest wall without intervening lung was usually present on both sides of the thorax, and this allowed echocardiographic imaging from both the right and left intercostal locations. In dogs, as in humans, improved contact between the heart and chest wall enabling superior imaging was obtained by examination from the recumbent side of the thorax.

To achieve the best possible images of the dog thorax, the correct transducer frequency must be employed. The range of probes used for the cardiac scans in the present study were chosen for their depth of focus. It was found that a 5.0 MHz Pulsed Wave transducer provided adequate penetration and screen image resolution for chest scans amongst all the Beagle dogs when operating

in the right and left parasternal locations with the Interspec XL Scanner. Examination of the Greyhounds,with the larger and deeper chest configuration, required a 3.5 MHz Pulsed Wave transducer which gave the beam penetration needed to achieve successful imaging.

The arrival of the Interspec Apogee and Toshiba Scanners brought with them a 3.5 MHz Annular Phased Array transducer. As previously described in Chapter 4, this probe with its dynamic beam focusing allowed a degree of resolution and improved lateral resolution and penetration usually associated with frequencies higher than a non - annular system. The 3.5 MHz transducer was used on both breeds of dog in the parasternal and subcostal transducer location sites in the later stages of the study. There can be no doubt that the improvement of ultrasound transducers was responsible for the major advancement of ultrasonography in medical science to date.

One of the main aims of the present work was to help establish the basic principles and techniques for 2 - D and Doppler echocardiography. The preparation of the examination site by close clipping and shaving of all body hair, was proven essential in allowing maximum contact with the skin so as to provide optimum scanning results. The omission of the second stage shaving led to air being trapped in the close body hair, and inferior imaging resulted.

The acoustic physics and principles of ultrasound and Doppler along with the interpretation of the ultrasound images must be clearly understood in order that the operator fully appreciate their capabilities,and for this reason chapters 2 and 3 include the necessary information.

Correct interpretation of the ultrasound images as they appear on the screen is an important step in achieving accurate diagnosis. Once the basis of 2 - D and Pulsed Wave Doppler has been understood, the operator should then be aware of image artifacts. During the course of this study certain common artifacts occurred whilst scanning the dog thorax. Thus the appearance and the origins encountered in scanning the canine heart, including shadowing reverberation and outside interference along with aliasing in the Doppler

studies are discussed in Chapter 2 and 3. General information regarding the various features of the different ultrasound equipment (scanners and transducers) have been described in Chapter 4 (materials and methods). This information was required so as to enable the calibration of the various sector fields (Time Gain Compensation Curve) and thus provide the best possible images. The resulting images allow for the production of good quality photographs for teaching, clinical and research purposes. To record these images requires a knowledge of the use of hard copy instrumentation, including video tape and high density thermal copiers.

An efficient scanning discipline as explained in Chapter 4, is not only essential for achieving the optimum information, but also for the safety of the operator, the equipment and the dog. All the dogs scanned in this study were examined without the need of any sedation. The animals responded well to gentle handling and minimal restraint. However, it was recognised that in certain breeds with difficult temperaments, some mild sedation would be required to carry out the necessary imaging positions.

As previously stated, there are differences to be found in the basic anatomy of the heart in dog and man. The study of the gross anatomy of the canine heart was therefore essential before any echocardiography was carried out. In this study, the dog heart was first of all examined in the cadaver to verify its relative position in the thorax. The heart was then removed and sectioned through the various imaging planes so that the internal structures of the heart could be identified when compared to the ultrasound scan. The images observed of the heart on an ultrasound scan, even with prior gross anatomical study can prove to be confusing, so the immersion of a dog heart in a clear, water - filled plastic bag and then scanned with a transducer, allowed not only a visual appreciation of both the position of the probe in relation to the heart, but also gave a 2 - D image of the internal cardiac structures on the scanner screen.
This procedure made for easier recognition of the same structures on future examinations of the live dog. The scanning discipline, along with the location , orientation and detailed anatomy of the heart in Chapter 4, should help the examiner perform cardiac scans properly.

Once the basics of echocardiography have been understood the study of the heart can be carried out in detail. Complete examination of the left atrium, mitral valve, left ventricle, aortic valve and ascending aorta was possible in every dog using a combination of long and short axis views from the right and left parasternal views.

M - mode echocardiography was employed to examine clinical cardiac evaluation. This technique provided information about intracardiac anatomy, cavity dimensions and the motion patterns of the cardiac valves in a one - dimensional format. This format has been used extensively in calculating left ventricular function, and for the recognition of valvular defects. The results recorded in this study for left ventricular function compared favourably with those reported in previous studies. (O'Grady and others, 1986)

The formats of both 2D and M - mode ultrasound, were excellent in studying the internal and cross - sectional anatomy of the heart, but neither could examine cardiac bloodflow. Conventional M - mode echocardiography cannot visualise bloodflow directly, and can only detect abnormalities of flow when they are of sufficient magnitude to produce alterations in cardiac structure or function. PW Doppler proved to be a useful tool in providing direct haemodynamic data of bloodflow velocities through the heart chambers. The use of Doppler has been well documented but at the onset of the present study, only one published reference on Doppler echocardiography in animals was found. (Hagio, and others 1986) This report concentrated mainly on cardiac abnormalities and did not describe the normal bloodflow in any great detail.

To determine the normal heart valve signatures and to measure bloodflow velocities, all the cardiac valves were examined with a PW Doppler duplex scanner. This type of scanner made the Doppler examination much easier by allowing the rapid localisation of the sample volume in the examination site, particularly when mapping techniques, discussed later, were performed. Examinations of the MV and AV were achieved successfully from the right parasternal location with PW Doppler.
The bloodflow velocities through the TV were also recorded, but at times

imaging of the valve was occluded due to the encroachment of the lungs. Optimum bloodflow velocities of the TV were therefore carried out from the left parasternal location.

Mitral flow was examined first with the sample volume placed in the left atrium, just proximal to the valve. Sampling for mitral flow was generally carried out in the area of the mitral annulus to avoid the MV leaflets passing through the sample volume. Movement of the heart or accidental shifting of the transducer sometimes caused the sample volume to encroach upon the valve leaflets causing the leaflets to be displayed as highly resonate "clicks" in the Doppler spectrum. Examinations using PW Doppler, brought similar results to that obtained in man with regards to spectrum frequency shape. The twin peaked Doppler spectrum of mitral flow was identified as the two phases of flow. The first peak occurred early in diastole corresponding to the initial filling phase of the LA and namedthe E peak, with the second phase or A peak, illustrating the atrial systolic component of ventricle filling.

Although the dogs examined in the present study were all normal, the main advantage of PW Doppler is its ability to identify cardiac flow abnormalities. In the case of mitral regurgitation, Doppler evidence of retrograde flow disturbance detected in the left atrial side of the MV plane during systole, is a reliable indicator that mitral regurgitation is present. A regurgitant jet however can flow at any angle through the damaged valve and therefore a mapping procedure is required. This requires the tracking of the sample volume in a series of locations across the length of the left atrium to check for the occurrence of retrograde flow. This abnormal flow would be illustrated as a widespread spectrum away from the direction of normal flow (below the baseline) during systole.

Optimum MV outflow velocity was recorded in the left ventricle directly in line with the valve. Care had to be taken so as not to allow the sample volume to stray too near to the LVOT, as this produced recordings of lower velocity readings of bloodflow through the MV, due to the sample volume not being directly in line with the flow. This occurrence was recognised by the

appearance of aortic flow below the baseline, as bloodflow moved away from the transducer through the LVOT towards the AV.

The AV was examined using the same procedure as in the MV ; flow velocities were seen to increase rapidly with the opening of the AV and fell at a somewhat slower rate in the latter half of the ejection phase. The flow velocity pattern proximal to the AV in the LVOT was essentially the same as that found in the proximal aorta. The flow was illustrated as a single peaked flow, with a narrow - ranged frequency spectrum recorded below the baseline, indicating that unlike the MV, flow velocity was away from the transducer.

When the flow velocity was seen to exceed the maximal limit of the Doppler display, the excess fraction was displayed on the opposite side of the baseline. This phenomenon was recognised as "aliasing". Multiple aliasing, where equal portions of velocity were displayed on both sides of the baseline, (commonly found in aortic recordings) caused ambiguity in determining the true peak velocity. Also the true direction of flow, along with the establishment of the type of flow, either laminar (with blood cells moving at a relatively similar velocity and direction) or turbulent (with blood cells moving at various velocities and directions simultaneously) could not be determined.

Two ways of overcoming aliasing were identified ; the movement of the baseline to the top or bottom of the display to allow more of the spectrum to be displayed proved successful, but in the cases were this was not satisfactory, the increasing of the vertical scale, reduced the displayed size of the Doppler spectrum, and the complete trace was observed.

Viewing from the left parasternal window allowed detailed examination of all the heart chambers, although the apex of the heart could not be imaged due to the oblique viewing angle. PW Doppler velocity readings were achieved from both the MV and the AV. When compared to the results from the right parasternal location, it was found that the flow velocity was slightly lower in the left parasternal window due to the Doppler beam being more perpendicular to the velocity flow than was desirable to achieve quantitative results.

The left parasternal window was found to be ideal for detecting flow through the pulmonic and tricuspid valves. Unlike in the right parasternal view, the right heart chambers were clearly identifiable, with the RV to the top and the RA at the bottom of the image. Using PW Doppler, it was found best to start with a short axis view at the level of the aortic root, as this indicated that the Doppler signal directed at either the TV or PV was parallel with the direction of flow, resulting in a strong Doppler signal. Sample volumes were then positioned on either side of the valves, and the flow profiles found resembled the configuration of the left - sided valves, except that the velocities were slightly slower in nature. It was noted that this location would prove ideal for the study of regurgitation or valvular stenosis in the right heart valves.

The left parasternal view was also recognised to be of importance in the examination of the IVS for the detection of ventricular septal defects. Flow through a ventricular defect is generally parallel to the interrogating Doppler beam from this location. By moving the sample volume along the right ventricular side of the IVS, a ventricular septal defect would be located as a aliased signal if the defect was large enough to produce a high velocity flow. If the defect was small in nature, it would appear as a Doppler spectrum during ventricular systole.

The recording of optimum Doppler velocity as previously described, requires the Doppler beam to be directed as parallel to the flow as possible. For this reason the suprasternal and subcostal windows were employed. These windows however had a slight drawback, in that due to the depth that the ultrasound beam had to travel, they did not allow for the detailed imaging of the cardiac anatomy which was to be found in the left and right parasternal locations.

The suprasternal window did not permit the use of PW Doppler due to the narrowness of the thoracic outlet and therefore no 2D image was available and flow through the AV was recorded with CW Doppler only. This is a major difference from the human where the suprasternal window is a useful location for PW Doppler examination. The CW Doppler transducer gave optimum blood

velocities readings due to the continual updating of the Doppler signal back to the transducer. Placement of the CW transducer in the suprasternal notch allowed easy access to systolic flow toward (above the baseline) the transducer from the ascending aorta.

Both PW and CW Doppler examinations were carried out from the subcostal window, and this permitted the Doppler beam to be directed parallel to flow in the AV and MV. The PW Doppler allowed visual placing of the sample volume at the two valves and the recording of blood velocities. As in the suprasternal window, the optimum velocities were achieved with CW. PW Doppler also recorded blood velocity, but as the returning signal was pulsed and not continually updated the velocities recorded were lower than those of CW Doppler. The aortic flow unlike in the suprasternal location, was away from the probe and therefore appeared below the baseline.

There are important limitations to conventional PW Doppler. Firstly, its maximum detectable flow velocity is often below that present in stenotic jets, although this limitation, in certain cases, can be minimised by using CW Doppler. A second major limitation of either PW or CW Doppler, is that at any point and time, they can only detect Doppler frequency shifts along the one - dimensional path of the ultrasound beam. For PW Doppler systems, this is further limited to one isolated focus, defined by the sample volume. Flow disturbances are often isolated to relatively small areas and may not be detected in the regions where the sample volume is placed. Stenotic and regurgitant jets are often eccentric if the valve leaflets are deformed or stenotic, and this results in the PW Doppler missing or underestimating the severity of the flow disturbance. Septal defects pose similar problems if they are too small to be visualised and located by 2D echocardiography.

The introduction of colour flow mapping has been seen as a powerful ally to PW Doppler. The ability to convert bloodflow velocities into a spectrum of colour, makes detection of bloodflow abnormalities much simpler. Although in this study, only normal heart function was examined, once it was understood that bloodflow towards the transducer was depicted as red and flow away from

the probe as blue, the direction of flow through the cardiac valves and chambers was made more obvious.

The detection of regurgitation in the MV would be identified as a distinct blue colour from the mitral orifice into the left atrium during ventricular systole, as blood was leaked back through the valve from the left ventricle in the direction away from the transducer. Depending on the severity of the incompetence, a central mosaic area would represent turbulent flow, due to the scanners' colour converter translation of the high velocity flow.

Though colour flow mapping is a major asset in detecting bloodflow abnormalities, care must be taken in diagnosis, as there are sources of motion artifacts that may simulate abnormal flow states. The most common are signals arising from wall motion, generating red areas as the wall approaches the transducer and blue as it recedes. Similar signals are generated from valve motion and may simulate mild valvular incompetence. Although these artifacts must be recognised, colour aliasing can also prove to be a useful indication of abnormal flow patterns through a damaged valve. The recording of colour aliasing, (white or green spectrum in middle of normal colour) would indicate to the clinician that some defect was present in the valve or heart chamber being examined.

The present study found 2D, PW and CW Doppler to be powerful tools in both the study of cardiac anatomy and bloodflow analysis. In the past, definitive diagnosis of cardiac abnormalities required invasive studies, such as the injection of radio - opaque dyes, which incurred both patient stress and the exposure of the body tissues to radiation. The introduction of ultrasound has eliminated these hazards and offers non - invasive, real - time, two dimensional imaging of simultaneous intracardiac morphology and flow. Through the introduction of colour flow mapping, although expensive, and the continual development of transducers, echocardiography has been shown to be a useful diagnostic instrument in man.

The role of ultrasound in veterinary science is still in its infancy. There is an ever increasing popularity in the technique. Interest shown by under graduate students during the course of this study, indicated that the introduction of ultrasound into the teaching curriculum would enable a complete study of not only the heart, but also all other organs. The direct comparison of the ultrasound scan to radiographic plates and gross anatomical specimens, would be extremely beneficial to the student in their understanding of the domestic animal anatomy. In conclusion, it is hoped that ultrasound enjoys a similar role in the field of veterinary medicine that has already been established in human medicine.

BIBLIOGRAPHY.

ASHBERG, A., (1967). Ultrasonic Cinematography of the living heart. *Ultrasonics*, **6**, 564 - 565.

BAKER, D.W., RUBENSTEIN, S.A. and LORCH, G.S. (1977). Pulsed Doppler Echocardiography; principles and applications. *American Journal of Medicine.* **63**, 69 - 80.

BOMMER, W.J., and MILLER, L., (1982). Real - time, Two - dimensional, Colour - flow Doppler ; Enhanced Doppler flow in the diagnosis of cardiovascular disease. (abstract.). *American Journal of Cardiology.* **49**, 944 - 948.

BONAGURA, J.D., (1981). Electrical Alternans associated with Pericardial Effusion in the Dog. *Journal of the American Veterinary Medical Association.* **178**, 574 - 579.

BONAGURA, J.D., and PIPERS, F.S. (1981). Echocardiographic features of Pericardial Effusion in Dogs. *Journal of the American Veterinary Medical Association.* **179**, 49 - 56.

BONAGURA, J.D., and PIPERS, F.S., (1983a). Echocardiographic features of aortic valve endocarditis in a Dog, a Cow, and a Horse. *Journal of the American Veterinary Medical Association.* **182**(6), 595 - 599.

BONAGURA, J.D., and PIPERS, F.S., (1983b). Diagnosis of cardiac lesions by contrast echocardiography. *Journal of the American Veterinary Medical Association.* **182** (4), 396 - 402.

BROWN, T.G., (1960). Direct contact ultrasonic scanning technique for the visualisation of abdominal masses. *International Conference on Electronics.* C.H. Smyth, Illiffe and Sons Ltd., London. 358 - 366.

CALVERT, L.A., and BROWN, J., (1986). Use of M - mode echocardiography in the diagnosis of congestive cardiomyopathy in Doberman Pinchers. *Journal of the American Veterinary Medical Association.* **189**, (3) 293 - 297.

CROCKER, E.F., McLAUGHLIN, A.F., KOSSOF, G., and JELLINS, J., (1974). The Grey - scale echographic appearance of thyroid malignancy. *Journal of Clinical Ultrasound.* **2,** 305 - 306.

CURIE, J., CURIE, P., (1880). Development par pression de l'ectricite polaire dons les cristaux hemidres a faces inclinees. C.R. Acadamie of Science., Paris, **91**, 294 - 295.

DENNIS, M.O., NEALEIGH, R.C., PYLE, R.L., GILBERT Jr. S.H., LEE, A.C., and MILLER, C.W., (1978). Echocardiographic assessment of normal and abnormal valvular function in Beagle dogs. *American Journal of Veterinary Research.* **39** (10) 1591 - 1598.

DETWEILER, D.K., and PATTERSON, D.F., (1965). The prevalence and types of cardiovascular diseases in dogs. *New York Academy of Science.* **127**, 481.

DONALD, I. and BROWN, T.G., (1961). Demonstration of tissue interfaces within the body by ultrasonic echo sounding. *British Journal of Radiology.* **34**, 539 - 545.

DeMARIA, A., BOMMER, W., JOYE, J. and DEAN, D.T., (1980). Cross - sectional echocardiography ; Principles, Anatomical planes, Limitations and Pitfalls. *The American Journal of Cardiology.* **46**, 1097 - 1108.

DUSSIK, K.T., (1942). On the possibility of using ultrasound waves as a diagnostic aid. *Neurol., Psychiat.,* **174,** 153 - 168.

DUSSIK, K.T., DUSSIK, F. and WYT, L., (1947). Auf dem wege zur hyperphonographic des gehirnes. *Wein. Med. Wochenschr.* **97**, 425 - 429.

EDLER, I. and HERTZ, C.H., (1954a). The use of ultrasonic reflectoscope for the continuous recording of movements of the heart valves. *Kurgyl Fysiogr*, Sallsk (Lund) Forti. **24**, 1 - 19.

EDLER, I. and HERTZ, C.H., (1954b). The use of ultrasonic reflectoscope for the continuous recording of movements of heart walls. *Kurgyl Fysiogr,* Sallsk (Lund) Fordhandl. **25**, 5 - 40.

EDLER, I., (1955). The diagnostic uses of ultrasound in heart disease. *Medical Association of Scandanavia.* Suppl. **308**, 32 - 36.

FEIGENBAUM, H., ZAKY, A. and WALDHAUSEN, J.A., (1967). Use of reflected ultrasound in detecting pericardial effusion. *American Journal of Cardiology.* **19**, 84 - 90.

FEIGENBAUM, H. (1981). Echocardiography. 3rd. edition, Philadelphia : Lea and Febiger.

FRANKLIN, D.L., SCH W. and RUSHMER, R.F. (1961). Blood flow measured by Doppler frequency shift of back scattered ultrasound. *Science.* **134**, 564 - 565.

FRANKLIN Jr., T.D., WEYMAN, A.E. and EGENES, K.M. (1977). A closed chest model for cross - sectional echocardiographic study. *American Journal of Physiology.* **233**, 417 - 419.

FRAZIN, L.O., TALANO, V.L. and STEPHANIDES, L. (1976). Oesophageal Echocardiography. *Circulation.* **54**, 102 - 108.

GOODING, J.P., ROBINSON, W.F. and MEWS, G.C. (1986). The Echocardiographic assessment of left ventricular dimensions in clinically normal English Cocker Spaniels. *American Journal of Veterinary Research.* **47**, (2) 296 - 300.

GRIFFITH, J.M. and HENRY, W.L. (1973). A real - time system for two - dimensional echocardiography. *26th Annual Conference of Engineering in Medicine and Biology.* **15**, 422.

GUERET, P., MEERBAUM, S., WYATT, H.L., UCHIYAMA, T., LANG, T.W. and CORDAY, E. (1980). Two - dimensional echocardiographic quantitation of left ventricular volumes and ejection fraction. Importance of accounting for dyssynergy in short axis reconstruction models. *Circulation.* **62**, 1308 - 1318.

HAENDCHEN, R.V., POVZHITKOV, M. and MEERBAUM, S. (1982). Evaluation of changes in left ventricular end diastolic pressure by left atrial two dimensional echocardiography. *American Heart Journal.* **104**, 740 - 745.

HAGIO, M. and OTSUKA, H. (1985). Combined pulsed Doppler and two - dimensional echocardiography in canine and bovine heart diseases. In : *7th, International Veterinary Radiology Conference,* Dublin, Ireland.

HAGIO, M. and OTSUKA, H. (1987). Pulsed Doppler echocardiography in normal dogs and calves, and three cases of valvular regurgitation. *Japanese Journal of Veterinary Science.* **49**, 1113 - 1125.

HATLE, L. and ANGELSEN, B. (1985). Pulsed Doppler recording of intra - cardiac blood flow velocities : orientation and normal velocity patterns. *Doppler Ultrasound in Cardiology, Principles and Applications.,* 2nd edition Lea and Febiger, Philadelphia. 74 - 96.

HAWTHORNE, E.W. (1961). Instantaneous dimensional changes of the left ventricle in dogs. *Circulation Research.* **9**, 110 - 119.

HAZEL, L.M. and KLINE, E.A. (1959). Ultrasonic measurment of fatness in swine. *Journal of Animal Science.* **18**, 815.

HENRY, J.G., MUNDT, G.N. and HUGHES, W.F. (1956). Ultrasonics in ocular diagnosis. *American Journal of Opthalmology.* **41**, 488.

HENRY, W.L., MARON, B.J., GRIFFITH, J.M., REDWOOD, D.R. and EPSTEIN, S.E. (1975). Differential diagnosis of anomalies of the great arteries by Real - time two - dimensional echocardiography. *Circulation.* **51**, 283 - 291.

HENRY, W.L., DeMARIA, M.D., GRAMIAK, R.G., KING, D.L., KISSLO, J.A., POPP, R.L., SAHN, D.J., SCHILLER, N.B., TAJIK, A., TEICHHOLZ, L.E. and WEYMAN, A.E. (1980). Report of the American Society of Echocardiography Committe on Nomenclature and Standards in Two - dimensional Echocardiography. *Circulation.* **62**, 212 - 217.

HORWITZ, L.D., BISHOP, V.S. and STONE, H.L. (1968). Continuous measurement of internal left ventricular diameter. *Journal of Applied Physiology.* **24**, 738 - 740.

HOWRY, D.H. (1958). Development of an ultrasonic diagnostic instrument. *American Journal of Physical Medicine.* **37**, 234.

JACOBS, G., BOLTON, G.R. and WATROUS, B.J. (1983). Echocardiographic features of dilated coranary sinus in a dog with persistant left cranial vena cava. *Journal of the American Veterinary Medical Association.* **182**, (4) 407 - 408.

KALMANSON, D., VEYRAT, C., DERAI, C. and CHICHE, P. (1972). Diagnostic value of jugular venous flow velocity trace in right heart diseases. I*n Roberts, C. (edition) : Blood flow Measurement.* Sector Publishing Limited, London.

KERBER, R.E. and ABBOUD, F.M. (1973). Echocardiographic detection of regional myocardial infarction. An experimental study. *Circulation.* **47**, 997 - 1005.

KING, D.L. (1973). Real - time cross - sectional ultrasonic imaging of the heart using a linear and multi - element transducer. *Journal of Clinical Ultrasound.* **1**, 196 - 201.

KISSLO, J., VON RAMM, O.T. and THURSTONE, F.L. (1976). Cardiac imaging using a Phased Array Ultrasound System. : Clinical technique and application. *Circulation.* **53**, 262 - 267.

KITTLESON, M.D., EYESTER, G.E., KNOWLEN, G.G., BARI - OLIVER, N. and ANDERSON, L.K. (1984). Myocardial function in small dogs with chronic mitral regurgitation and severe congestive heart failure. *Journal of the American Veterinary Medical Association.* **184**, (4) 455 - 459.

KOSSOF, G., FRY, F.J. and EGGLETON, R.C. (1971). Application of digital computer to control ultrasonic visualisation equipment. *Ultrasonographica Medica.* J. Bock and K. Ossing, Verlag Weiner Med., Akad., **1**, 33 - 40.

KOSSOF, G. (1974). Display techniques in ultasound pulse investigations. : a review. *Journal of Clinical Ultrasound.* **2**, 61 - 72.

KOSTUCKI, W., VANDENBOSSCHE, J.L., FRIART, A. and ENGELERT, M. (1986). Pulsed Doppler flow patterns of normal valves. *American Journal of Cardiology.* **58**, 309 - 313.

KOTLER, M.N., MINTZ, G.S., SEGAL, B.L. and PARRY, W.R. (1980). Clinical uses of Two - dimensional Echocardiography. *American Journal of Cardiology.* **45**, 1061 - 1082.

LANGEVIN, P. (1924). De l'emploi des ondes ultrasonores pour le son. *Publ. Spec. Bureau Hydrogr. Internat.*, Monaco. **3**, 11.

LIGHT, H. (1969). Non - injurious ultrasonic technique for observing flow in the human aorta. *Nature.* **224**, 1119 - 1969.

LUDWIG, G.D. and STRUTHERS, F.W. (1949). Considerations underlying the use of ultrasound to detect gall stones and foreign bodies in the tissues. *United States Navy Medical Research Institute.* Report **4**, 1- 27.

MASHIRO, I., NELSON, R., COHN, J.N. and FRANCIOSA, J.A. (1976). Ventricular dimensions measured non - invasivley by echocardiography in the awake dog. *Journal of Applied Physiology.* **41**, 953 - 959.

McLEOD, F.D. (1967). Adirectional Doppler flowmeter. I*n Jacobson, b. (ed.), Digest of the 7th International Conference on Medical and Biological Engineering.* Almqvist and Wiskel Publishers, Stolkholm.

MILAN, J. (1972). Digital storage display of two - dimensional ultrasonic scans. *Journal of Physics and Medical Biology.* **17**, 440.

MILLER, C. W. and WINGFIELD, W.E. (1981). Applications of ultrasound to Veterinary diagnostics in a Veterinary Teaching Hospital. *Biomedical Scientific Instrumentation.* **17**, 85 - 90.

MIYATAKE, K., KINOSHITA, N., NAGATA, S., BEPPU, S., PARK, Y.D., SAKAKIBARA, H. and NIMURA, Y. (1980). Intra - cardiac flow pattern in mitral regurgitation studied with combined use of the ultrasound pulsed Doppler technique and cross - sectional echocardiography. *American Journal of Cardiology.* **45**, 155 - 162.

MIYATAKE, K., OKAMOTO, M., KINOSHITA, N., OHITA, M., KOZUKA, T., SAKAKAIBARA, H. and NIMURA, Y. (1982). Evaluation of tricuspid regurgitation by pulsed Doppler and two - dimensional echocardiography. *Circulation.* **66**, 777 - 784.

MIYATAKE, K., OKAMOTO, M., KINOSHITA, N., IZUMI, S., OWA, M. TAKAO, S., SAKAKIBARA, H. and NIMURA, Y. (1984). Clinical applications of a new type of real - time two - dimensional flow imaging system. *American Journal of Cardiology.* **54**, 857 - 868.

MYEROWITZ, P.D., GRIFFITH, A., ROBERTS, A.J., HARRISON, L.H., HENRY, W.L. and McINTOSH, C.L. (1974). Long term canine model for echocardiography. *American Journal of Cardiography.* **34**, 72 - 74.

NIMURA, Y. (1983). History of pulse and echo Doppler ultrasound in Japan. *In Spencer, M.P., (ed.) Cardiac Doppler Diagnosis.* Martimus Nijoff Publishers, Boston.

NORTHEVED, A., HOLM, H.H. and GAMMALGAARD, P.H. (1971). An improved ultrasonic scanning equipment with a new stage and display system for diagnosticuse. Electronic sector scanning with ultrasonic beams. *Ultrasonographica Medica., K. Ossoing, Verlag Weiner., Med., Akad.,* **1**, 44 - 50.

PARK, R.D., NYLAND, T.G., LATTIMER, J.C., MILLER, C.W. and LEBEL, J.L. (1981). B - Mode gray - scale ultrasound : Imaging artifacts and interpretation principles. *Veterinary Radiology,* **22**, 204 - 210.

O'GRADY, M.R., BONAGURA, J.D., POWERS, J.D. and HERRING, D.S. (1986). Quantitative cross - sectional echocardiography in the normal dog. *Veterinary Radiology.* **27**, (2) 34 - 49.

PIPERS, F.S. and HAMLIN, R.L. (1977). Echocardiography in the Horse. *Journal of the American Veterinary Medical Association.* **170**, 815 - 819.

PIPERS, F.S., MUIR III, W.W. and HAMLIN, R.L. (1978). Echocardiography in Swine. *American Journal of Veterinary Research.* **39**, 707 - 710.

PIPERS, F.S., RINGS, D.M. and HULL, B.L. (1978). Echocardiographic diagnosis in a Bull. *Journal of the American Veterinary Medical Association.* **172**, 1313 - 1316.

PIPERS, F.S., REEF, V. and HAMLIN, R.L. (1979). Echocardiography in the Domestic Cat. *American Journal of Veterinary Research.* **40**, 882 - 886.

PIPERS, F.S., REEF, V. and WILSON, J. (1985). Echocardiographic detection of ventricular septal defects in large animals. *Journal of American Veterinary Medical Association.* **187**, 810 - 816.

PIPERS, F.S., BONAGURA, J.D. HAMLIN, R.L. and KITTLESON, M. (1981). Echocardiographic abnormalities of the mitral valve associated with left sided heart diseases in the dog. *Journal of the American Veterinary Medical Association.* **179** (6), 580 - 586.

POPP, R.L., FOWLES, R., COLTART, J. and MARTIN, R. (1979). Cardiac anatomy viewed systemically with two - dimensional echocardiography. *Chest.* **75**, 579 - 585.

RANTANEN, N.W. and EWING III, B.S. (1981). Principles in ultrasound application in animals. *American Journal of Veterinary Radiology.* **22** (5), 196 - 203.

RICHARDSON, L.F. (1912a). Apparatus for warning a ship at sea of its nearness to large objects wholly or partly underwater. *British Patent No.* **1125.**

RICHARDSON, L.F. (1912b). Apparatus for warning a ship of its approach to large objects in fog. *British Patent No.* **9423.**

RUSHMER, B.F. CRYSTAL, D.K. and WAGNER, C. (1954). Continuous measurements of the left ventricular dimensions in intact, unanesthetized dogs. *Circulation Research.* **2**, 14 - 21.

RUSHMER, R.F., BAKER, D.W. JOHNSON, W.L. and STRANDNESS, D.E. (1967). Clinical applications of a transcutaneous ultrasonic flow detector. *Journal of the American Medical Association.* **199**, 104.

SAHN, D.J., WILLIAMS, D.E. and SHACKLETON, S. (1974). The validity of structure identification for cross - sectional echocardiography. *Journal of Clinical Ultrasound.* **2**, 201 - 216.

SALCEDO, E.E., GOCHOWSKI, K. and TARAZI, R.C. (1979). Left ventricular mass and wall thickness in hypertension. *American Journal of Cardiology.* **25**, 50 - 64.

SHIRLEY, I.M., BLACKWELL, R.J. CUSIK, G., FARMAN, D.J. and VICARY, F.R. (1978). A users guide to diagnostic ultrasound. Pitman Medical, Tunbridge Wells. ISBN 0 - 272 - 79419 -8.

SOKOLOV, S.Y. (1935). Ultrasonic methods of detecting internal flaws in metal articles. *Zavodskaya Laboratoriya.* **4**, 1468 - 1472.

SOMER, J.C. (1968). Electronic sector scanning for ultrasonic diagnosis. *Ultrasonics.* **6**, 153 - 159.

STEFAN, G. and BING, R.J. (1972). Echocardiographic findings in experimental myocardial infarction of the posterior left ventricular wall. *American Journal of Cardiology.* **30**, 629 - 639.

STEGALL, H.F., RUSHMER, R.F. and BAKER, D.W. (1966). A transcutaneous ultrasonic blood velocity meter. *Journal of Applied Physiology.* **21**, 707 - 711.

STEGALL, H.F., KARDON, M.B. and STONE, H.L. (1967). A portable simple sonomicrometer. *Journal of Applied Physiology.* **22**, 289 - 293.

SWITZER, D.D. and NAVIN, N.C. (1985). Doppler Color Flow Mapping. *Ultrasound in Medicine and Biology.* **11**, (3), 403 - 416.

TAJIK, A.J., SEWARD, J.B., HAGLER, D.J., MAIR, D.D. and LIE, J.T. (1978). Two - dimensional Real - Time Ultrasonic Imaging of the Heart and Great Vessels. *Mayo Clinic Proceedings.* **53**, 271 - 303.

TAYLOR, K.J.W., CARPENTER, D.A., HILL, C.R. and McREADY, V.R. (1976). Grey - scale ultrasound imaging. *Radiology,* **119**, 415 - 423.

TEMPLE, R.S., STONEAKER, N.N., HOWRY, D.H., POSUKANY, G. and HAZELUS, J. (1956). Ultrasonic and conductivity methods for estimating fat thickness in live cattle. *Proceedings of the American Society of Animal Products, West Section,* **7**, 477.

THOMAS, W.P. (1984). Two - dimensional, real - time echocardiography in the dog. Technique and anatomic validation. *Veterinary Radiology.* **25**, 50 - 64.

WALTON, S., UNDERWOOD, S.R. and HUNTER, G.J. (1989). A Colour Atlas of Diagnostic Investigation in Cardiology. Wolfe Medical Publications Ltd.,

WELLS, P.N.T. and ROSS, F.G.M. (1969). A time voltage analouge converter for ultrasonic cardiology. *Ultrasonics.* **7**, 171 - 176.

WELLS, P.N.T. (1969). A range - gated ultrasonic Doppler system. *Medical Biological Engineering.* **7**, 641.

WILD, J.J. (1950). The use of ultrasonic pulses for the measurement of biological tissues and the detection of density changes. *Surgery.* **27**, 183 - 188.

WINGFIELD, W.E., BOON, J. and MILLER, C.W. (1982). Echocardiographic assessment of mitral valve motion, cardiac structures and ventricular function in dogs with atrial fibrillation. *Journal of the American Medical Association.* **181** (1), 46 - 49.

WINGFIELD, W.E., BOON, J.A. and MILLER, C.W. (1983). Echocardiographic assessment of congenital aortic stenosis in dogs. *Journal of the American Veterinary Medical Association.* **183**, (6) 673 - 676.

WINGFIELD, W.E. and BOON, J.A. (1987). Echocardiography for the diagnosis of congenital heart defects in the dog. *Veterinary Clinic of North America (Small Animal Practice).* **17**, (3) 735 -753.

WYATT, H.L., HENG, M.K. and MEERBAUM, S. (1979). Cross - sectional echocardiography analysis of mathematic models for qualifying mass of the left ventricle in dogs. *Circulation.* **60**, 1104 - 1113.

YAMAGA, Y. and TOO, K. (1984). Diagnostic ultrasound imaging in domestic animals. : two - dimensional and M - mode echocardiography. *Nippon - Juigaku - Zasshi.* **46**, (4) 493 - 503.